



# Development of hydrogels and study the effect of their mechanical properties on podocyte behaviors

Maya Abdallah

## ► To cite this version:

Maya Abdallah. Development of hydrogels and study the effect of their mechanical properties on podocyte behaviors. Material chemistry. Université Montpellier, 2019. English. NNT : 2019MONT065 . tel-02887569

**HAL Id: tel-02887569**

**<https://theses.hal.science/tel-02887569>**

Submitted on 2 Jul 2020

**HAL** is a multi-disciplinary open access archive for the deposit and dissemination of scientific research documents, whether they are published or not. The documents may come from teaching and research institutions in France or abroad, or from public or private research centers.

L'archive ouverte pluridisciplinaire **HAL**, est destinée au dépôt et à la diffusion de documents scientifiques de niveau recherche, publiés ou non, émanant des établissements d'enseignement et de recherche français ou étrangers, des laboratoires publics ou privés.

# THÈSE POUR OBTENIR LE GRADE DE DOCTEUR DE L'UNIVERSITÉ DE MONTPELLIER

En Chimie et Physicochimie Des Matériaux

École doctorale SCIENCE CHIMIQUES BALARD (ED459)

Unité de recherche Institut Européen Des Membranes (UMR 5635, CNRS, UM, ENSCM)

## DEVELOPPER DES HYDROGELS ET ETUDIER LES EFFETS DES PROPRIETES MECANIQUES SUR LES ACTIVITES BIOLOGIQUES DES PODOCYTES

Présentée par Maya ABDALLAH

Le 10 Décembre 2019

Sous la direction de Sébastien BALME,  
La codirection de Maria BASSIL,  
L'encadrement de Mikhael BECHELANY

Devant le jury composé de

Mme Patricia BASSEREAU, Directrice de Recherche, CNRS, Institut Curie  
M. Hassane OUDADESSE, Professeur, Université de Rennes I  
M. Xavier GARRIC, Professeur, Université de Montpellier  
M. Michel BOISSIERE, Maître de Conférences, Université de Cergy-Pontoise  
Mme Maria BASSIL, Professeur, Université Libanaise  
M. Sébastien BALME, Maître de Conférences, Université de Montpellier  
M. Mikhael BECHELANY, Chargé de Recherches, CNRS

Rapporteur  
Rapporteur  
Examineur  
Examineur  
Co-Directeur  
Directeur  
Invité



UNIVERSITÉ  
DE MONTPELLIER



## **Acknowledgement**

*Thank you God for giving me the strength, the support, the opportunities and helping me to exceed all the difficulties and the barriers to pursue and complete the research work.*

*I would like to extend my deepest sincerest gratitude to all the people who helped me and have shared with me the knowledge to achieve this work.*

*My deepest appreciation belongs to Mr. Ramy Adwan, Mr. Anthony Awad and Ms. Sonia Abou Azar. You are the greatest and kindest people I have ever met. Thank you for your guidance and your valuable support. It was a great pleasure and honor to meet you.*

*I would like to acknowledge the attendance and the helpful suggestions from my committee members.*

*For my director “Dr. Sebastien Balme”: I would like to express my sincere gratitude for his continuous support, for his patience, his motivation, his enthusiasm and his immense knowledge. It was a great honor to work under his guidance. Thank you for teaching me the research methodology in order to present my work in a good way.*

*My deepest gratitude goes to my co-director “Dr. Maria Bassil” for helping me to pursue my PhD study in a very important and interesting field. Thank you for her continuous guidance, her expert advices and ideas that helped me to accomplish this research project.*

*I want to express my sincere gratitude to “Dr. Mikhael Bechelany”, my supervisor, for giving me the opportunity to work on my thesis within his research group and for providing me invaluable guidance during this period. His dynamism and motivation have deeply inspired me and I am really grateful for everything he offered to me. I would also thank him for his empathy and great sense of humor.*

*I would like to give my sincere gratitude to Dr. Frederic Cuisinier, Dr. Csilla Gergely, Dr. Marta Martin and Dr. Bela Varga for their expertise, their time, their suggestions and their encouragement. Thank you for allowing me to have an appropriate platform to work on the biological part and to get all the necessary information I need to make this thesis possible.*

*These acknowledgements would not complete without mentioning my research lab colleagues: “Thianji, Nicoletta, Socrates, Octavio, Habib and Amr”. It was a great pleasure*



*working with them and I appreciate their ideas, help and good humor. Special thanks goes to Saktivel for working together and sharing valuable ideas. Thank you my dearest Tunisian friends: “Zaineb, Soumaya, Ahmed and Wassim”. I really appreciate your true friendship, your guidance and your positive support. It was a great pleasure to meet you. I would like to express my sincere gratitude to my Lebanese friends: “Maryline, Loraine, Ghady, Ghenwa, Joelle, George, Marleine, and Petros” for having great time together within the same Institute. Thank you my special girls, my sisters “Sarah and Syrena” for having great moments, for spending the last working nights together and for providing such a great support. For my best friends, my supports, my sisters “Catherine and Rasha”, I would like to thank you for everything you have done for me. I love you so much!!*

*I would like to express my gratitude to my dearest friend, to my brother and to my love “Omar“, Thank you for your continuous support , your advices, your patience and your faith. You have always been encouraging me and caring throughout this period. I LOVE YOU.*

*Very special thanks to my lovely family and especially to my mother for their unconditional love, their continuous and spiritual support given to me throughout the time and their moral encouragement. I could not have done without them. I LOVE YOU. Thank Dr. Wissam for believing on me and helping me to start my PhD studies. You were always a great supporter for me and a big brother who I can count on. Thank you.*

### **Dedication**

*This humble piece of work is lovingly dedicated to my angel, to my FOTHER, who was my source of strength and my inspiration. You were always by my side.*

# Table of content

List of Figures .....	i
List of Tables.....	iii
List of Abbreviations.....	iv
General Introduction.....	1
Chapter I: Literature Review .....	7
I. Introduction .....	9
II. Hydrogels .....	10
1. Definition .....	10
2. Hydrogels as scaffolding materials: .....	12
3. Natural and Synthetic Hydrogels.....	13
4. Preparation methods of hydrogels .....	23
5. Hydrogels propertie .....	30
6. Hydrogels For Tissue Engineering Applications .....	36
III. Cell-ECM interaction .....	37
1. Mechanotransduction .....	37
2. Effect of stiffness on tissue functions .....	41
IV. Podocytes .....	44
1. Definition .....	44
2. Podocyte Slit Diaphragm .....	46
V. Conclusion .....	50
VI. Thesis Objectives .....	51
VII. References .....	53
Chapter II: Materials and Methods .....	67
I. Materials.....	69
1. Fabrication of Hydrolyzed Polyacrylamide Hydrogels.....	69
2. Synthesis of Gelatin Methacrylamide(GelMA) .....	71
3. Preparation of GelMA-AAm hydrogels.....	72
4. Swelling Measurement .....	72
5. Cell Culture .....	72
6. Immunocytochemical characterization .....	73

7. Cell Proliferation Assay .....	74
8. Western Blot .....	74
<b>II. Experimental Methods .....</b>	<b>75</b>
1. Conventional Scanning Electron Microscopy (CSEM) .....	75
2. Environmental Scanning Electron Microscopy (ESEM).....	76
3. Atomic Force Microscopy (AFM) .....	77
4. Fluorescence Microscopy and Immunocytochemical characterization.....	81
5. Multiphoton Microscopy (MPM).....	84
6. Rheology .....	86
7. Differential Scanning Calorimetry (DSC) .....	88
8. Infrared Spectroscopy .....	89
9. Statistical Analysis.....	90
<b>III. Conclusion.....</b>	<b>91</b>
<b>IV. References .....</b>	<b>92</b>
<b>Chapter III: Influence of hydrolyzed polyacrylamide hydrogel stiffness on podocyte morphology, phenotype and mechanical properties .....</b>	<b>95</b>
<b>I. Abstract .....</b>	<b>97</b>
<b>II. Introduction .....</b>	<b>99</b>
<b>III. Materials and Methods .....</b>	<b>102</b>
1. Fabrication of Hydrolyzed Polyacrylamide Hydrogels.....	102
2. Swelling Measurement .....	103
3. Rheology of PAAm Hydrogel .....	103
4. Differential Scanning Calorimetry (DSC) .....	104
5. Scanning Electron Microscopy (SEM) .....	104
6. Atomic Force Microscopy (AFM) .....	104
7. Cell Culture .....	105
8. Immunocytochemical characterization.....	106
9. Multiphoton Microscopy (MPM).....	106
10. Cell Proliferation Assay .....	107
11. Statistical Analysis.....	107
<b>IV. Results and Discussion.....</b>	<b>108</b>
1. PAAm hydrogels properties .....	108
2. Influence of the scaffold mechanical properties on podocyte cells.....	114

V. Conclusion.....	122
VI. References .....	124
<b>Chapter IV: Enhancement of Podocyte Attachment on Polyacrylamide Hydrogel with Gelatin-based polymers.....</b>	
	130
I. Introduction .....	131
II. Materials and Methods .....	133
1. Synthesis of GelMA.....	133
2. Preparation of GelMA-PAAm hydrogels .....	134
3. Swelling Measurements.....	134
4. Fourier Transform Infrared Spectroscopy (FT-IR).....	135
5. Mechanical Characterization .....	135
6. Cell culture.....	136
III. Results.....	137
1. H-NMR of Gelatin Methacrylamide .....	137
2. FT-IR of hydrogel material .....	138
3. Swelling Characterization .....	139
4. Mechanical Properties .....	142
5. Podocytes Cells Culture.....	145
6. Cells Elasticity .....	147
IV. Conclusion .....	149
V. References.....	151
<b>General Conclusion .....</b>	<b>156</b>



## List of Figures:

### Chapter I:

Figure 1: Picture of swelled polyacrylamide hydrogel .....	11
Figure 2: (a) Collagen Triple-Helix Structure (b) Ball-and-stick image of a segment of collagen triple helix .....	15
Figure 3: Basic Chemical Structure of Gelatin .....	17
Figure 4: Gelatin methacrylate (GelMA) synthesis scheme .....	18
Figure 5: Polyacrylamide Matrix Structure .....	19
Figure 6: (a) The heterobifunctional photoreactive reagent sulfo-SANPAH. (b) A scheme is shown for ECM protein conjugation using sulfo-SANPAH. ....	20
Figure 7: Hydrolyzed PAAm hydrogels functionalized with EDC and NHS. ....	22
Figure 8: Types of crosslinking: Physical and Chemical Hydrogels.....	24
Figure 9: Representative reactions during the photocrosslinking of GelMA to form hydrogel networks. ....	26
Figure 10: (a) Addition of radical to acrylamide monomer. (b) Propagation of PAAm polymerization. ....	27
Figure 11: Hydrogel network formation due to intermolecular H-bonding in CMC at low pH.....	28
Figure 12: Ionotropic gelation by interaction between anionic groups on alginate (COO-) with divalent metal ions (Ca <sup>2+</sup> ) .....	29
Figure 13: Swelling of hydrophilic polymers.....	32
Figure 14: Cells are tuned to the materials properties of their matrix.....	33
Figure 15: Sensation of, and responses to, matrix-generated mechanical signals .....	40
Figure 16: Effect of matrix mechanics on cell behavior. Schematic of general changes in cell behavior observed as matrix stiffness increases .....	40
Figure 17: Podocytes Imaging.....	46
Figure 18: The glomerulus and slit diaphragm .....	49

### Chapter II:

Figure 1: PAAm hydrogels polymerization.....	70
Figure 2: Reversible network swelling and shrinking with solvent.....	71
Figure 3: Synthesis of GelMA .....	71
Figure 4: Conventional Scanning Electron Microscopy .....	76
Figure 5: Environmental Scanning Electron Microscopy .....	77
Figure 6: Tip (A) and cantilever (B) schematics of the MLCT tips (noted as C and D) used in our work (© Bruker AFM Probe).....	78
Figure 7: Principle of the AFM imaging modes .....	78
Figure 8: Typical force-curve as a function of sample indentation showing the contact point between the tip and the sample and the fit performed to calculate the Young's modulus. ....	79
Figure 9: Energy diagram describing the excitation and emission states.....	83
Figure 10: Epi- fluorescence microscope set-up .....	84
Figure 11: Mechanisms of two-photon excited fluorescence (Fluo-2P). ....	85
Figure 12: Confinement of the 2P excitation to a point like volume (© Cornell University).....	85
Figure 13: Basic modular components of the multiphoton microscope. ....	86
Figure 14: Infrared spectrometer .....	90

## Chapter III:

Figure 1: (A) Representative curve of swelling degree as a function of Bis-acrylamide concentrations (0.5, 1, 2, 5, 10 and 30 $\mu$ l). (B) Scanning Electron Microscopy images of dehydrated PAAm hydrogels.....	109
Figure 2: DSC curves for PAAm hydrogels having different concentrations of crosslinker. Curve (1) corresponds to 1 $\mu$ l of Bis-acrylamide and curve (2) corresponds to 30 $\mu$ l of Bis-acrylamide.....	111
Figure 3: (A) Polyacrylamide hydrogels Young's modulus maps measured by AFM.....	113
Figure 4: A) Human Podocyte Cells Line cultured on PAAm hydrogels substrates having different properties (2 and 10 $\mu$ l Bis-acrylamide respectively). (B) Podocyte proliferation: % of podocytes cover surface as a function of substrate's elastic modulus.....	115
Figure 5: Immortalized podocytes showed an arborized morphology and interdigitating foot processes with adjacent cells (yellow arrow). These images were taken using multiphoton microscopy (A) and environmental SEM (B) for substrate of 2.1 kPa .....	116
Figure 6: (A) (B) Representative immunofluorescence images of podocytes cultured on PAAm substrates with an elasticity ranging from 0.6 to 44 kPa .....	119
Figure 7: Western Blot for the detection of podocin expression on PAAm hydrogels with various elasticity .....	120
Figure 8: Elasticity of podocytes cultured on PAAm membranes.(B) AFM elasticity distribution indicating podocyte elasticity for cells cultured on different samples. (C) Evolution of the cells' Young's modulus (E) as a function of hydrogel stiffness.....	121

## Chapitre IV:

Figure 1: Synthesis of GelMA .....	134
Figure 2: $^1\text{H}$ -NMR of gelatin and modified gelatin (methacrylamide gelatin GelMA).....	138
Figure 3: FT-IR of pure gelatin and GelMA-AAm interpenetrated polymer network .....	139
Figure 4: Representative histogram of swelling degree as a function of acrylamide and GelMA concentrations .....	140
Figure 5: Schematic simplified view of GELMA-PAAm sequences: (a) GELMA-GELMA macromolecules; (b) GELMA-AAm; (c) AAm-AAm .....	141
Figure 6: Scanning Electron Microscopy for GelMA-AAm based hydrogel having different polymers concentrations .....	142
Figure 7: (A) Elasticity distribution of GelMA-PAAm hydrogels swelled in cell medium. Young's moduli were fitted with Gaussian distributions. (B) Evolution of the Young's modulus "E" as a function of GelMA and AAm concentrations.....	143
Figure 8: The storage modulus of GelMA-PAAm membranes fully swelled in water was determined as function GelMA and AAm concentrations .....	144
Figure 9: (A) Podocyte cells stained with calcein for the determination of cells viability. (B) Representative immunofluorescence images of podocytes cultured on GelMA-PAAm substrates having various mechanical properties .....	147
Figure 10: Evolution of the Young's modulus (E) as a function of AMM and GelMA concentrations .....	149

## List of Tables:

Table 1: Properties of hydrogels as biomaterials .....	13
Table 2: List of natural and synthetic hydrogels.....	14
Table 3: The characteristics of: Collagen, Gelatin and PAAm .....	23
Table 4: Physical and chemical hydrogels properties.....	30
Table 5: Hydrogels: Preparation and Mechanical Properties .....	35
Table 6: Design criteria for hydrogels as scaffolds for tissue engineering .....	37



## **List of Abbreviations:**

**CKD: Chronic Kidney Disease**

**GFB: Glomerular Filtration barrier**

**GBM: Glomerular Basement Membrane**

**ECM: Extracellular Matrix**

**AAM: Acrylamide**

**PAAm: Polyacrylamide**

**GelMA: Gelatin Methacrylate**

**TEMED: Tetramethylethylenediamine**

**APS: Ammonium Persulfate**

**ESRD: End Stage Renal Disease**

**ERIC: Extracellular Signal Regulated Kinase**

# General Introduction



Regenerative medicine and tissue engineering are defined as an expanding interdisciplinary field implicated in the restriction of donor shortage and immunological rejection evaluated as a major public health issue. The concept of tissue engineering consists to develop a functional scaffold in order to regenerate and enhance the functions of damaged or diseased tissues and organs. The strategies of tissue engineering requires the following factors: (1) the isolation of cells from target tissue, (2) the design of biomaterial scaffold providing an appropriate mechanical environment for cell functions in order to mimic the extracellular matrix, (3) the use of molecules such as proteins and growth factors for cells survival. Nowadays, hydrogels have shown a great advancement and progression as scaffolding materials in tissue engineering. They are defined as three-dimensional hydrophilic polymers network and characterized by their high water content. Various natural and synthetic polymers have been employed to generate physical and chemical crosslinked hydrogels. These hydrogels provide mechanical and physical support similar to the natural extracellular matrix microenvironment of targeted tissue and allow the cell growth and tissue regeneration. The main question is how to design a suitable hydrogel scaffold for tissue engineering. The design of these scaffolds requires various criteria such as biocompatibility, mechanical strength and biofunctionality indispensable in the regulation of cellular behaviors. The purpose of this manuscript is focused on the synthesis of two polymers based hydrogels: Hydrolyzed polyacrylamide as a synthetic hydrogel and GelMA-AAm as a natural/synthetic hydrogel able to: (i) promote the cell adhesion, (ii) ensure the transport of nutrients and growth factors for cell survival and proliferation, (iii) have a negligible immune response and toxicity, (iv) deliver the seeded cells towards the desired damaged site and (v) control and regulate the structure and functions of engineered tissue. Chronic kidney disease (CKD) affects 10% of the population worldwide. CKD is the consequence of

glomerular filtration barrier (GFB) dysfunction. The GFB is composed of endothelial cells which are involved in the maintenance of the filtration barrier. Podocyte provide a barrier composed of filtration slits between foot processes that prevent the passage of plasma proteins into the urinary filtrate. The progression of glomerulopathies is the consequence of podocyte injury. These scaffolds materials were developed to mimic the kidney glomerular basement membrane in order to restore the main function of the glomerulus kidney.

This thesis manuscript is composed of four chapters:

1. The first chapter is an overview of various categories of hydrogels, the preparation methods and the main properties of hydrogels. The application of hydrogels as a scaffold in tissue engineering and the criteria implicated in the development of efficient hydrogel scaffold were studied. Moreover, since the extracellular matrix (ECM) provides mechanical and biological environment involved in the regulation of cells behaviors such as proliferation and differentiation, the mechanisms of ECM-cells interaction were developed to better understand the effect of polymer substrates on cells. Furthermore, the characteristics of the *in vivo* kidney podocytes and their role on maintaining the glomerular filtration barrier were investigated as the work consists to develop a scaffold material having properties similar to the physiological glomerular basement membrane of the kidney.
2. The second chapter will describe on details the materials and the methods used to synthesize the hydrogels scaffolds and to characterize their properties such as the swelling and the mechanical properties. Furthermore, the effect of substrate mechanical properties on the podocyte behaviors was investigated by evaluating the morphology, the proliferation rate, the cytoskeleton organization and the differentiation of these cells.

3. The third chapter will focus on the development of hydrolyzed PAAm hydrogel as a new scaffolding material which is a key step toward the development of adaptive implant materials. First, hydrolyzed PAAm hydrogels were synthesized and covalently crosslinked with various concentrations of Bis-acrylamide that contribute to obtain various crosslinking polymer network densities and mechanical strengths. The influence of hydrolyzed PAAm hydrogels mechanical properties on podocyte morphology, cytoskeleton organization, differentiation and mechanical properties was also evaluated. The hydrolyzed PAAm substrates, on which the physiological activities of podocytes were preserved, were determined. These substrates have shown elasticity within the range of the physiological stiffness.
4. The fourth chapter will present a novel stable hybrid hydrogels based scaffold composed of gelatin methacrylate and acrylamide (GelMA-AAm). The combination of biological and synthetic materials imitates the heterogeneity of native ECM due to the presence of bioactive cell-binding domain and tunable mechanical properties. The properties of GelMA-AAm hydrogels and the effect of scaffolds mechanical properties on the podocyte behaviors were investigated.

Finally, the conclusion part will summarize the main findings of this thesis. Moreover, perspectives will be proposed as possible for future work.



# Chapter I: Literature Review





# Hydrogels: Promising Scaffold for Tissue Engineering

## I. Introduction:

Extracellular matrix (ECM) is a complex and organized network having a wide variety of macromolecules. Therefore, each tissue is characterized by their specific ECM structure and composition which are altered by the diseases. The major components of ECMs are proteins including laminin, fibronectin, elastin and collagen. These proteins present specific binding sites that recognize and interact with cell surface receptors and matrix constituents that form a three dimensional network. ECM regulates the cells behaviors and promotes the main biological activities such as tissue homeostasis, cellular growth, survival and differentiation<sup>1,2,3</sup>. The regulation of cells functions is maintained by ECM signals transmitted to the cells. Cells sense the signals, interpret and respond to the different parameters such as ECM structure, components and mechanical properties as stiffness and viscoelasticity<sup>4,5</sup>. The loss of ECM functions characterized by the modification of its composition and physical properties induce an alteration of ECM-cells interactions and thus create a microenvironment leading to the development and progression of several diseases<sup>5</sup>. Among these diseases, autoimmune and inflammatory diseases have shown the presence of a modified ECM. However, the understanding of ECM properties and characteristics helps to develop and optimize an *in vitro* cell culture environment to generate a three-dimensional (3D) model such as biomaterials having requirements close to the *in vivo* milieu. The 3D *in vitro* system can be applied in various biomedical applications such as drug delivery system and tissue engineering helping to elaborate a new therapeutic target for disease treatment. Nowadays, tissue engineering strategies consist to develop *in vitro* biological or synthetic materials mimicking the native ECM and able to replace and recover the functions of injured

tissues or organs. Tissue engineering should follow different criteria to be achieved. In fact, a functional engineered tissue should be characterized by appropriateness mechanical properties of native tissues and should be incorporated within the physiological environment. The concept of tissue engineering aims to comprehend the *in vivo* mechanical properties of tissues and to study the biophysical environment of cells. The characterization of ECM properties has permitted the advancement and the progression of substrate used as an engineered construct. In this chapter, the development of hydrogels study and the comprehension of ECM mechanical properties and their influence on cells behaviour such as cell proliferation and differentiation will be discussed and developed. The first part of this chapter consists to define the concept of hydrogels and to develop their preparation methods and their properties. Moreover, the application of hydrogels in tissue engineering field will be elaborated. Then, the chapter will be based on the mechanisms of cells - ECM interactions and the effect of ECM mechanical properties on the cellular behaviors. The third part of this chapter will be focused on introducing the podocyte kidney cells. This work will lead to establish a biomaterial based hydrogel to study the effect of kidney glomerulus extracellular matrix on podocyte behaviors.

## **II. Hydrogels:**

### **1. Definition:**

Gels are defined as semi-solid material composed of hydrophilic polymers and dispersed in a large quantity of fluid. Different types of gels have been identified and classified depending on the type of the swelling factor employed such as hydrogels, organogels and xerogels. In this work, hydrogels are the gels of study. They are characterized by their three-dimensional

crosslinked hydrophilic polymer network holding a large amount of water within their network without dissolving (Fig.1). Recently, hydrogels have been progressed and advanced as biomaterials in biomedical engineering such as tissue engineering and drug delivery.

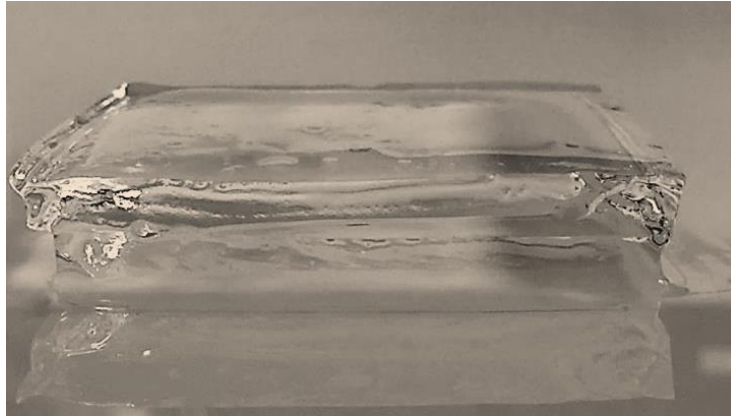


**Figure 1: Picture of swelled polyacrylamide hydrogel.**

“Hydrogel” term was started since 1894 and was previously widely used in many researches papers, according to Lee, Kwon and Park<sup>6</sup>. In 1960, polyhydroxyethylmethacrylate (PHEMA) was considered as a first material crosslinked network having a high water affinity and the development of this material has been used in many research projects of permanent contact lens production. “Hydrogel” was considered as a soft material advanced to be used in vivo as a biomaterial. The history classification of hydrogels was identified by Buwalda *et al.*<sup>7</sup>:

- Hydrogel history was started by the development of materials having a high swelling degree and tunable mechanical properties. These materials were characterized by random crosslinking polymer network using initiators to induce the chemical modifications.
- Then, these materials were developed and optimized to respond to the variations of specific stimuli such as temperature, pH and polymers concentrations. These stimuli

were utilized to induce specific phenomenon including the polymer polymerization and the drug delivery systems<sup>7</sup>.

- Finally, the researchers were focused on the development of stereo-complexed materials such as PEG-PLA interactions<sup>8</sup> and this category of hydrogels has shown a promising advancement.

## **2. Hydrogels as scaffolding materials:**

Research studies have investigated the role and the effect of substrate stiffness on cells behaviour. Generally, the study of cellular processes is directed on non-physiological support as polystyrene which exhibit a high stiffness (1GPa)<sup>9,10</sup>. With such environment, unconventional cells behaviors were developed corresponding to a loss of phenotype differentiation. Thus, these traditional cell culture techniques fail to ensure a milieu to recapitulate the functional characteristics of cells<sup>11</sup>. Recently, experiment researches have exhibited the significant role of cell's microenvironment mechanical properties on cellular behaviors<sup>12,13,14</sup>. Then, new *in vitro* culture systems were advanced and progressed in order to establish an appropriate microenvironment for cells and so to mimic a functional unit of human living organ in *vitro* environment. Biomaterials, and particularly hydrogels, have recently shown a great potential in several biomedical fields such as drug delivery applications and tissue engineering<sup>15,16</sup>. Moreover, since the mechanical properties have exhibited a great impact on cells behaviour, these polymer materials have permitted to develop 3D *in vitro* cell culture model with tunable elasticity in order to study the effect of the substrate stiffness on cells<sup>17</sup>.

Hydrogels materials are viscoelastic crosslinked polymer networks. They are characterized by their hydrophilic structure which allows the absorption of high amount of water and

biological fluid, their biocompatibility and their robust mechanical properties similar to living tissues<sup>15,18,19</sup>. These hydrogels characteristics permit to imitate the properties of native ECM and then to act as an artificial ECM. Therefore, these materials are considered as a promising candidate for tissue engineering due to the similarities of native ECM structure and composition<sup>20</sup>. Since each tissue requires specific necessities, hydrogels properties can be modified and adjusted in order to match the features of an organ for tissue engineering applications. Over the past decade, hydrogels used as biomaterials have been progressed and have been applied in several applications. Table 1 shows the main properties of hydrogels as biomaterials.

**Table 1: Properties of hydrogels as biomaterials<sup>21</sup>**

Properties
<ul style="list-style-type: none"> <li>• Biocompatible</li> <li>• Ease of handling</li> <li>• Injectable</li> <li>• High water content</li> <li>• Mechanical strength</li> <li>• Chemical modification (e.g. having attached cell adhesion ligand)</li> <li>• Addition of cells/drugs</li> </ul>

The following sections will be focused on a detailed description of some hydrogels widely used in tissue engineering. Afterward, the methods of preparation and the properties of hydrogels will be talked over.

### **3. Natural and Synthetic Hydrogels:**

Hydrogels were classified into natural and synthetic categories depending on polymer network nature<sup>22,23,24</sup> (Table 2).

Table 2: List of natural and synthetic hydrogels<sup>21</sup>

Natural Polymers	Synthetic Hydrogels
<ul style="list-style-type: none"> <li>• Collagen</li> <li>• Gelatin</li> <li>• Alginate</li> <li>• Hyaluronic acid</li> <li>• Fibrin</li> </ul>	<ul style="list-style-type: none"> <li>• Poly(ethylene glycol)</li> <li>• Poly(acrylamide)</li> <li>• Poly(vinyl alcohol)</li> <li>• Poly(acrylic acid)</li> <li>• Poly(hydroxyethyl methacrylate)</li> </ul>

Natural polymers are biological systems characterized by their intrinsic biocompatibility, their biodegradability and their specific interactions with the cells due to their bioactive properties. However, these hydrogels present many disadvantages such as the difficulty of purification, the immunogenicity and the pathogen transmission. Collagen, gelatin, chitosan, fibrin and alginate are considered as natural hydrogels and they represent the most essential components of the extracellular matrix *in vivo*<sup>25</sup>. The reproducibility of the structure and the mechanical properties of this category remains a problem poorly understood<sup>26,27</sup>. These drawbacks can be limited and controlled by using hydrogels based on synthetic polymers. The synthetic hydrogels including polyethylene glycol (PEG), polyacrylamide (PAA) and polyvinyl Alcohol (PVA) are more reproducible and can be controlled and modified for tuning the desired mechanical properties. However, many important factors are investigated as polymer composition, biocompatibility and mechanical properties to design a material suitable to be applied in tissue engineering<sup>23,26</sup>.

Natural hydrogels such as collagen and gelatin and synthetic hydrogels such as polyacrylamide will be described in this section. In this thesis, these hydrogels will be studied and investigated as scaffold materials for cell culture.

### a. Collagen:

Type I collagen is the most abundant protein present in human connective tissues accompanied by a significant amount of collagen type II, III and IV. The structure of native collagen structure is characterized by its triple-helical  $\alpha 1$ -  $\alpha 2$  chains having a molecular weight of 300kDa<sup>28</sup>. Glycine, proline and hydroxylproline constitute the major amino acid sequences of collagen involved in the establishment of triple helix (Fig.2). Collagen protein plays a crucial role in performing numerous biological activities. These proteins provide physical anchorage sites inducing the cells attachment and the cell signalling pathway through the cell-surface receptors such as integrin<sup>29</sup>.

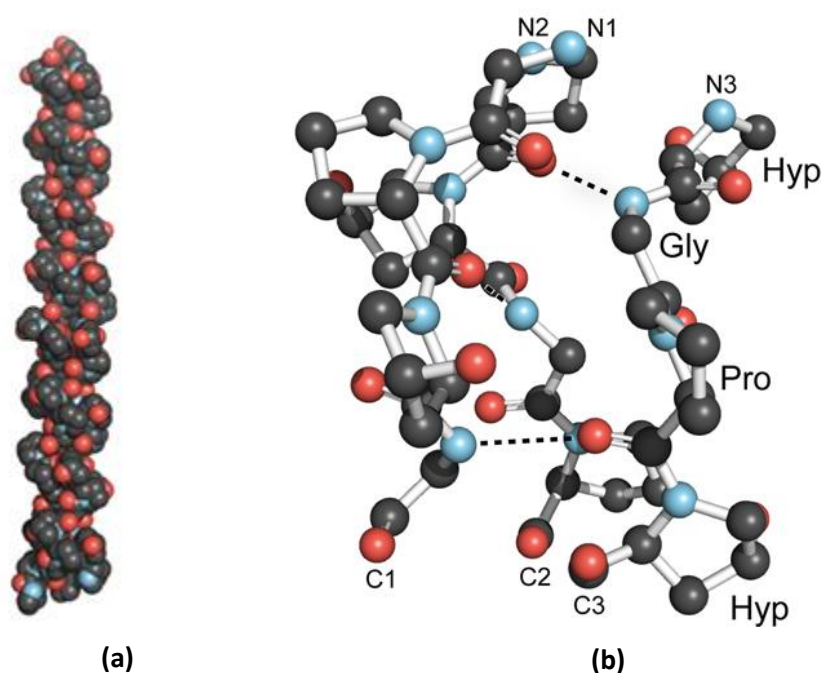


Figure 2: (a) Collagen Triple-Helix Structure (b) Ball-and-stick image of a segment of collagen triple helix  
Collagen Structure and Stability<sup>28</sup>.

Collagen is considered as a natural polymer widely studied for the development of hydrogels scaffolds. Collagen based hydrogels have been used to mimic the extracellular matrix and have shown advancement as three-dimensional scaffold for cell culture and tissue



engineering due to their biomimetic properties such as biocompatibility and similarity to native extracellular matrix<sup>30</sup>. Collagen scaffold have been used as biomaterials for numerous applications such as wound cover dressings, osteogenic and bone filling materials<sup>31,32</sup>. However, one of the main inconveniences of using hydrogels based on collagen type I as a substrate for tissue engineering is the difficulty to optimize the properties of these materials. Therefore, the ability to reproduce a scaffold having properties similar to physiological tissues and thus to establish physiological factors for cell regulation remain a problem. This problem depends on the variability of collagen I hydrogel origin. Moreover, collagen type I hydrogels are characterized by their low mechanical strength and low stability. It has been shown that in the absence of chemical crosslinker agent which may damage the collagen structure, there is a difficulty to generate a collagen scaffold with high stiffness ( $> 1 \text{ kPa}$ )<sup>11</sup>. Collagen type I hydrogels have been used in several applications use for regenerative medicine. Eric Hess *et al.* have studied the influence of collagen derived hydrogel on Bone Marrow Stromal Cells behaviors. It has been shown the ability of these cells to migrate and to proliferate on these hydrogels. In addition, the osteogenic differentiation was detected on these biomaterials and this study was elaborated to develop a novel bone graft based on collagen type I hydrogels. Moreover, Wong *et al.* have investigated the collagen based scaffolds properties for brain tissue engineering. Researchers have shown the potential role of collagen in repairing and regenerating the injured brain by providing a supportive matrix for cells<sup>33</sup>.

#### **b. Gelatin:**

Gelatin is a natural denatured form of collagen while maintaining the bioactive properties such as RGD sequences (Arg-Gly-Asp). Gelatin is the result of collagen hydrolysis and is

considered as a reversible gel dissolving at body temperature. Figure 3 represents the basic chemical structure of gelatin.

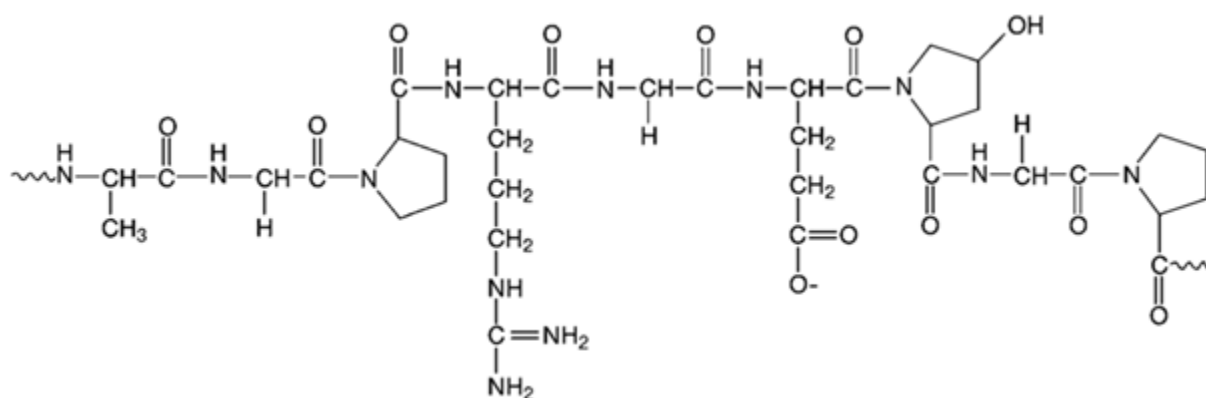


Figure 3: Basic Chemical Structure of Gelatin<sup>34</sup>.

Gelatin hydrogels have been widely used and applied as suitable scaffolding biomaterials in tissue engineering such as cardiovascular, bone and hepatic tissue engineering due to their significant characteristics such as biocompatibility, biodegradability and poor immunogenicity and cytotoxicity<sup>35</sup>. Nevertheless, gelatin hydrogels represent many disadvantages recognized by the mechanical properties and their unstable structure which lead to a quick enzymatic degradation. These drawbacks contribute to restrict the gelatin hydrogel applications in tissue engineering field. To improve the mechanical properties and the stability of these hydrogels, gelatin based hydrogels can be covalently crosslinked with carbodiimide and glutaraldehyde<sup>36,37</sup>. However, these chemical crosslinking agents are cytotoxic and elicit immunological responses. Gelatin methacrylate (GelMA), derivative form of gelatin, has shown a potential attention as implantable materials in tissue engineering applications. The preparation of GelMA is based on the reaction of methacrylic anhydride with the hydroxyl and the amino groups presenting on the side chains of gelatin. This reaction is carried out in the phosphate buffer at 50°C (Fig. 4).

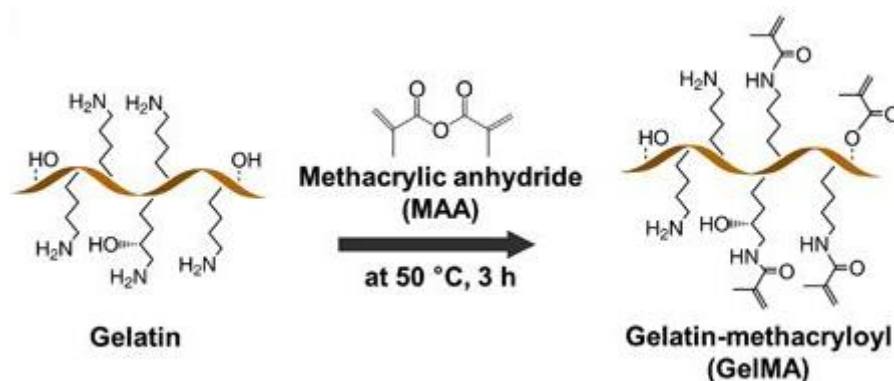


Figure 4: Gelatin methacrylate (GelMA) synthesis scheme<sup>38</sup>

The polymerization of GelMA is performed by UV irradiation using a water soluble photoinitiator such as Irgacure 2959<sup>39</sup>. The photopolymerization reaction contributes to the development of a covalently crosslinked GelMA polymer network. The photocrosslinked GelMA hydrogels are characterized by their biocompatibility, their inherent biological activity due to the presence of cell-attachment sequence and their tunable mechanical properties. These characteristics provide a platform to study the cellular behaviors and therefore GelMA hydrogels will be the choice of study as they represent good candidates to mimic the native extracellular matrix for cell culture<sup>40,41</sup>.

### c. Polyacrylamide:

Polyacrylamide (PAAm) hydrogel is a synthetic covalently crosslinked polymer network. PAA hydrogels have been used as a biomaterial for cell culture and have shown a wide progression in this field due to their several important advantages. These materials have formed an important platform to study the cell-substrate interactions depending on material stiffness. The preparation of PAAm hydrogels is simple and inexpensive. PAAm hydrogels are biocompatible and non-biodegradable polymers and can be exposed with broad range of elasticity (0.3 kPa-300 kPa) by changing the acrylamide and bis-acrylamide relative concentrations. The stiffness variations contribute to study and to more understand the

influence of substrate stiffness on cellular behaviors such as cell morphology, motility and differentiation<sup>42</sup>. PAAm hydrogels are synthesized by mixing various concentrations of acrylamide and bis-acrylamide crosslinker. This reaction is initiated and catalyzed using Ammonium Persulfate (APS) and *N, N, N', N'* Tetramethylethylenediamine respectively (Fig.5). APS serves as an inducer of a free radical polymerization<sup>43</sup>.

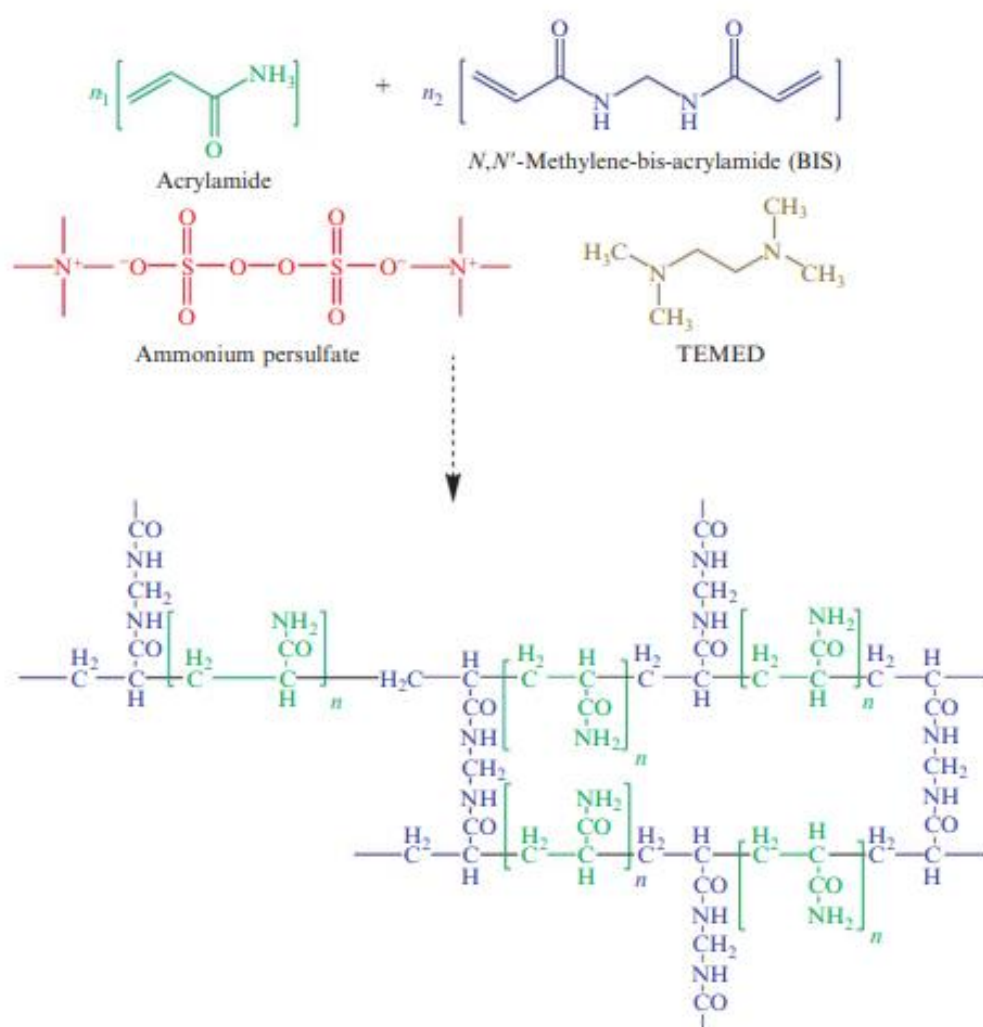


Figure 5: Polyacrylamide Matrix Structure<sup>44</sup>

Furthermore, ECM proteins comprising laminin, fibronectin and collagen type I, IV are covalently conjugated to PAAm hydrogels surface which serve as ligands for cell attachment. Sulfosuccinimidyl 6-(40-azido-20-nitrophenylamino) hexanoate, known as Sulfo-SANPAH, is a

photoactivatable heterobifunctional reagent holding two functional groups: Sulfosuccinimidyl group reacts constitutively with the primary amine groups of proteins and phenylazide group forms a non-specific binding with polymerized PAAm hydrogel during the photoactivation. Thus, ECM proteins - PAAm hydrogels surface interactions is covalent using sulfo-SANPAH (Fig. 6).

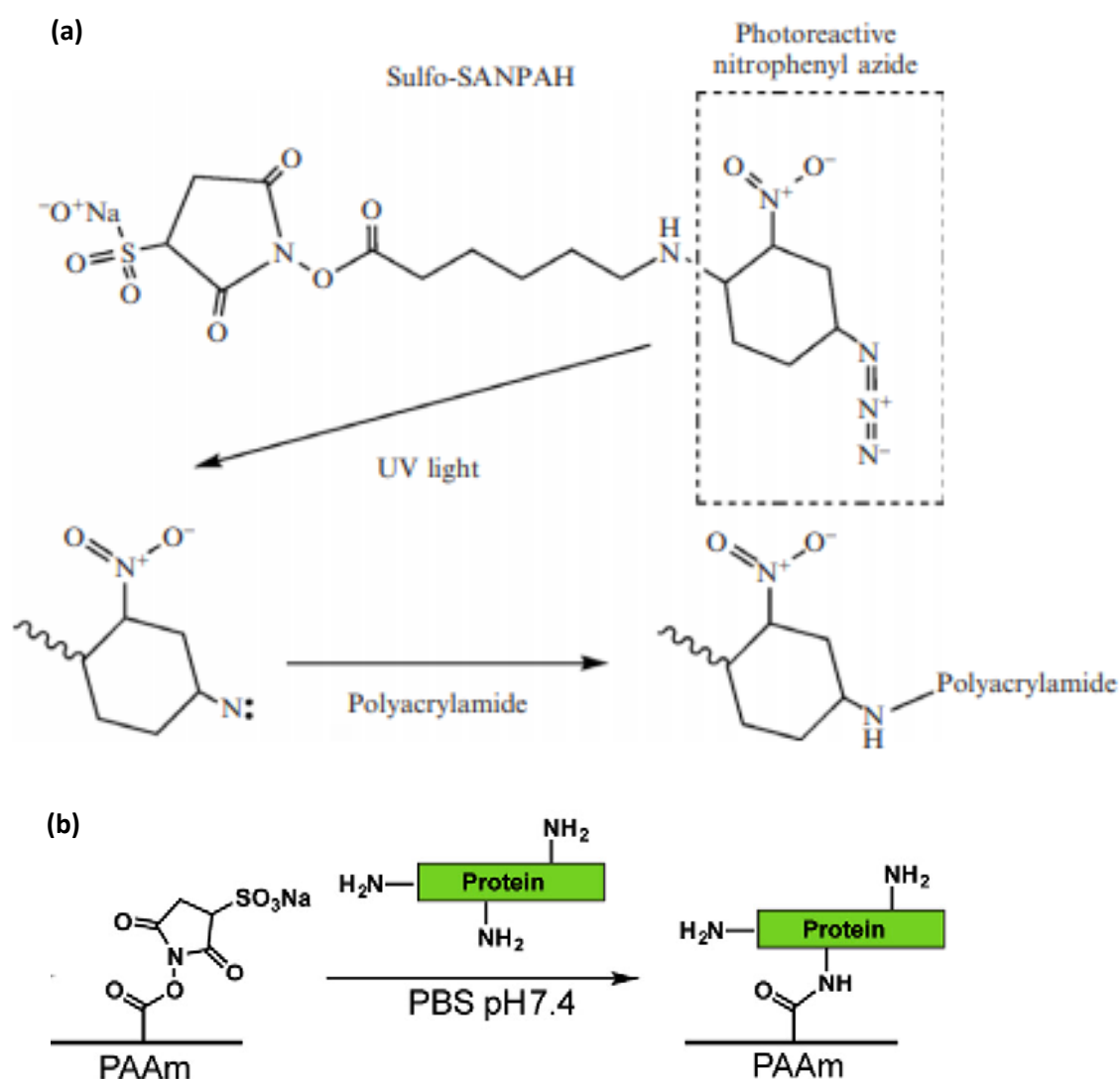
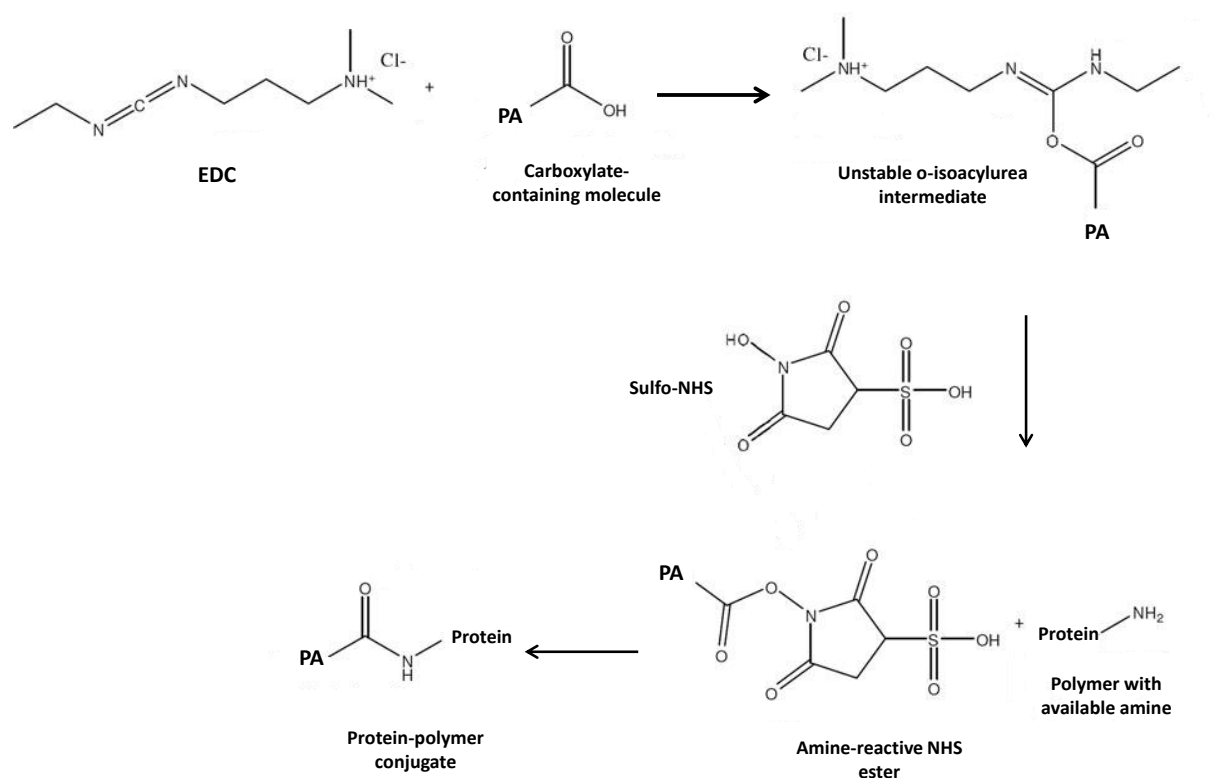


Figure 6: (a) The heterobifunctional photoreactive reagent sulfo-SANPAH<sup>44</sup>. (b) A scheme is shown for ECM protein conjugation using sulfo-SANPAH<sup>45</sup>.

Since PAAm hydrogels furnish for cell culture a physiological environment, Yeung *et al.* have worked on PAAm substrates and have studied the effect of substrate stiffness on cells fate. They have concluded that the surface stiffness has an impact on cells morphology and proteins expression by showing that the morphology of fibroblast and endothelial cells, seeded on substrate having elasticity higher than 2kPa, is more spread and promotes the development of actin stress fibers. Furthermore, the regulation of cell locomotion has been studied on PAAm hydrogel with variable elasticity. Researchers have observed that the migration rate of fibroblasts is high on soft substrates comparing to stiff substrates. In addition, it has been shown that the epithelial cells on these substrates present a highly lamellipodial protrusion which is the consequence of destabilized adhesion<sup>46</sup>. Despite these advantages, PAAm hydrogels have a limited capacity to interact with the physiological environment and the presence of unreacted acrylamide within the PAAm hydrogels which is toxic for the cells will be remained<sup>44</sup>. Once placed in a basic solution, the PAAm hydrogel will turn into hydrolyzed PAAm form. The hydrolyzed PAAm hydrogel are defined as biocompatible polyelectrolyte holding a large amount of water and biological fluids within its interstitial space. During the swelling process, the unpolymerized acrylamide will be washed out from the polymer matrix. Hydrolyzed PAAm hydrogel are capable to exhibit morphological changes in response to the external stimuli such as pH, electrical fields and ionic strength<sup>47</sup>. In this thesis, hydrolyzed polyacrylamide hydrogel is investigated as a new scaffolding material which is an important step toward the development of adaptive implant materials.

The hydrolyzed PAAm hydrogel surface is functionalized with (3-dimethylaminopropyl) carbodiimide-HCL (EDC). EDC reacts with the carboxyl groups of hydrolyzed PAAm hydrogel and induce the appearance of an amino-reactive intermediate which contributes to the

protein conjugation. EDC is used in combination with N-hydroxysuccinimide (NHS) or sulfo-NHS in order to create a more stable intermediate by increasing the coupling efficiency<sup>48</sup>(Fig. 7).



**Figure 7: Hydrolyzed PAAm hydrogels functionalized with EDC and NHS<sup>48</sup>.**

Table 3 shows a summary of the main characteristics of the hydrogels mentioned above.

**Table 3: The characteristics of: Collagen, Gelatin and PAAm.**

	<b>Collagen</b>	<b>Gelatin</b>	<b>PAAm</b>
<b>Nature</b>	Natural	Natural	Synthetic
<b>Bonding</b>	Physical	Physical	Chemical
<b>Preparation Methods</b>	Protein Self-Assembly	Protein Self-Assembly	Free Radical Polymerization
<b>Advantages</b>	Biocompatible (Biological properties) Biodegradable	Biocompatible (Biological properties) Biodegradable Poor immunogenicity	Tunable mechanical properties Durable and storage stability Possibility of control
<b>Disadvantages</b>	Weak mechanical properties Limited long term stability Batch-to-batch variability	Weak mechanical properties Non-stable	Toxicity of unreacted monomers
<b>Tested on</b>	Cartilage Bone Tendons	Cartilage Bone	Podocyte Brain Fibroblast

#### 4. Preparation methods of hydrogels:

The preparation methods of polymers based hydrogels are processed in different ways according to their applications. Depending on crosslinking types, hydrogels can be classified into two categories: physical and chemical crosslinked hydrogels. Chemical hydrogels require the development of covalent crosslinked polymer network. Different methods are applied to synthesize chemically crosslinked permanent hydrogels including photopolymerization and chemical polymerization. The crosslinking mechanisms are based on the chemical reaction of polymer having functional groups as OH, COOH and NH<sub>2</sub> with the crosslinking agent. Physical hydrogels do not require the use of crosslinker and are considered as reversible polymer network. The forces implicated in the development of physical hydrogels are hydrogen bonding, ionic bonding and hydrophobic interactions. These interactions can be disrupted with changes in the physical conditions<sup>49,50</sup>. These chemical and physical methods are discussed and summarized below (Fig.1).



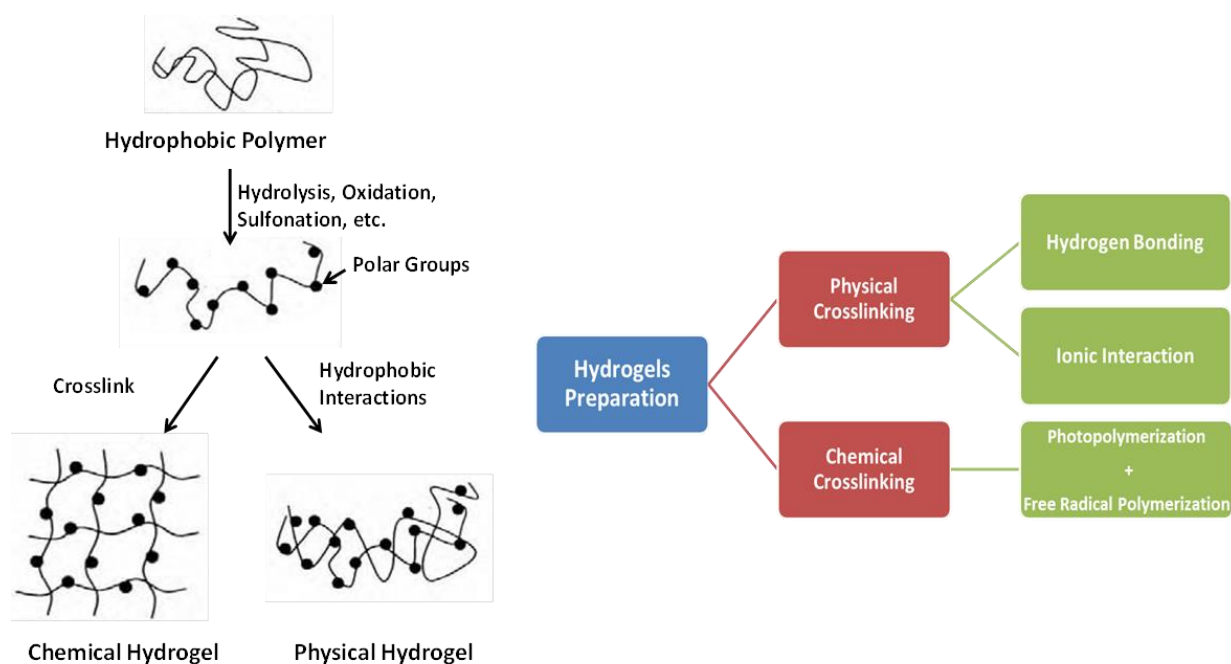


Figure 8: Types of crosslinking: Physical and Chemical Hydrogels<sup>51</sup>

#### a. Chemical crosslinked hydrogels:

Chemical crosslinked hydrogels are characterized by the presence of covalent interaction bonds. The polymerization of end-functional group in polymers chain is the common method to establish covalently crosslinked polymer network. The photochemical and chemical polymerization will be described below in details.

##### i. Photochemical polymerization:

Photoinitiated polymerization process is considered as an efficient method for hydrogels synthesis. This technique provides many advantages during the hydrogels preparation such as no need to use catalysts or additives to initiate the polymerization, the crosslinking density of the polymer network chain can be controlled by changing the irradiation dose and the presence of contamination will be eliminated. The photopolymerization method has been widely used for many biomedical applications due these benefits. Photopolymerization, known also as free radical polymerization technique, is based on the

presence of monomers holding appropriate photosensitive functional groups. Photopolymerization process follows up the subsequent steps: initiation, propagation and termination. The initiation step is activated by the use of a photoinitiator involved in free radical generation. These radicals initiate the polymerization by interacting with the monomer reagent in order to turn it into an active form. Then, the propagation step goes on to get a polymer radical chain. The termination step is thus accomplished through radical combination leading to the development of connected polymer network chain<sup>20</sup>. As example, many research studies have worked on the photopolymerization of PEG by using UV irradiations with specific photoinitiator in order to generate radicals which induce the polymerization. PEG photopolymerization contributes to the development of PEG hydrogels used as a scaffold for cells delivery involved in tissue regeneration. For example, PEG hydrogels have been used as a matrix for osteoblasts encapsulation to evaluate their applicability in promoting bone tissue engineering<sup>52,53,54</sup>. Moreover, GelMA based hydrogels have been widely used in biomedical research field due to their suitable biological properties and tunable mechanical characteristics. The photopolymerization is the method of GelMA hydrogels preparation. The initiation of GelMA polymerization is induced by the presence of free radicals generated by the photoinitiator. The propagation of GelMA chain is performed between the methacryloyl groups. Eventually, the termination step will be occurred between two propagating chains or between one propagating chain and a second radical<sup>55</sup>(Fig. 9).

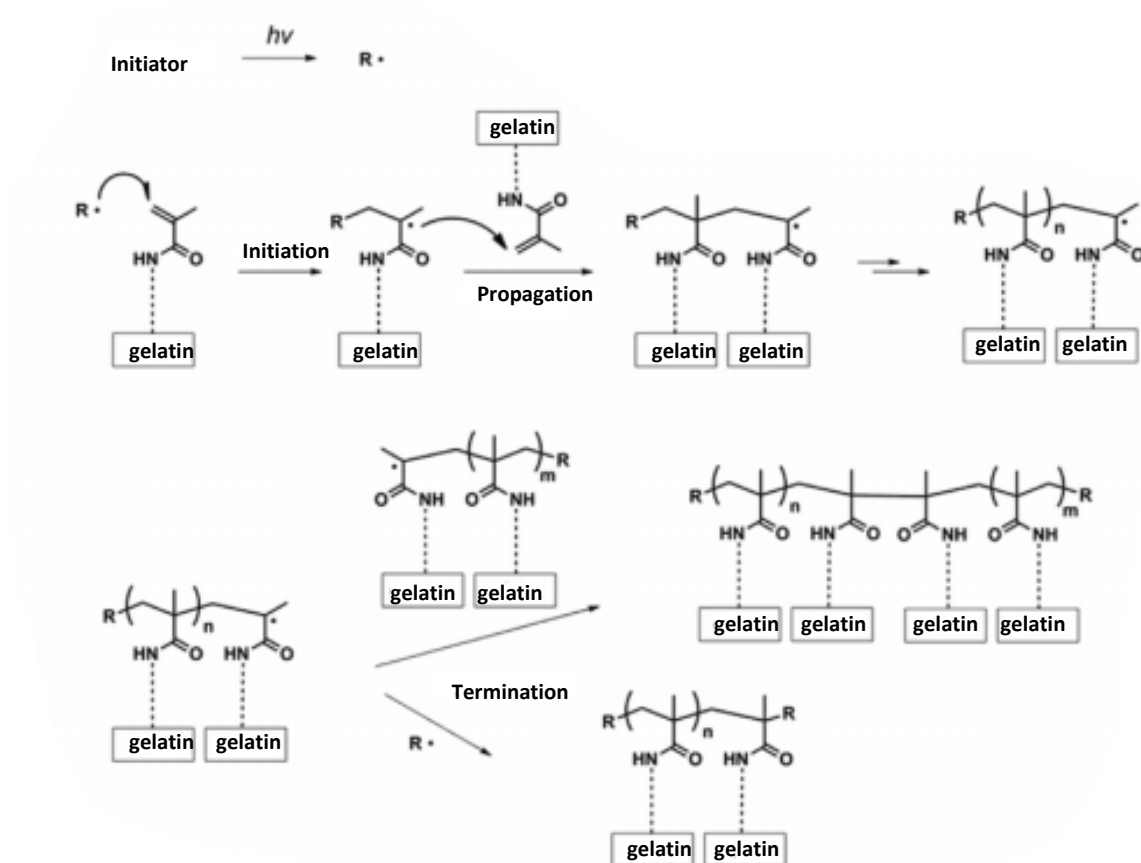


Figure 9: Representative reactions during the photocrosslinking of GelMA to form hydrogel networks<sup>55</sup>.

## ii. Chemical polymerization:

Chemical polymerization is considered as one of the main polymerization techniques for the development of natural and synthetic hydrophilic polymers based hydrogels. This technique is based on chemical reaction of bi-functional crosslinking agent with a hydrophilic polymer holding appropriate functional group such as  $\text{COOH}$ ,  $\text{OH}$  and  $\text{NH}_2$ <sup>20</sup>. This technique has been widely utilized to form various chitosan-based hydrogels. These hydrogels are covalently crosslinked polymer hydrogels and involved in many applications such as drug delivery systems by releasing bioactive materials and can be used as a scaffold for cell culture due to their biocompatibility<sup>56</sup>. For instance, gelatin and albumin based hydrogels were prepared using dialdehyde or formaldehyde as crosslinking agents. In this thesis, polyacrylamide

hydrogels are synthesized using acrylamide monomer and bis-acrylamide as crosslinking agent. This polymerization technique requires the use of Ammonium Persulfate (APS) and *N, N', N'* Tetramethylethylenediamine (TEMED) to induce and initiate the polymerization reaction of polyacrylamide. In fact, the following steps are involved in the synthesis of polyacrylamide: (1) The initiation of polyacrylamide polymerization is induced by the presence of free radicals generated and accelerated by APS and TEMED respectively; (2) The free radicals provoke the activation of the acrylamide monomers by converting them into acrylamide free radicals. The activated acrylamide monomers react with the unactivated one and induce the elongation of polymer chain. Meanwhile, the polyacrylamide chain is also covalently crosslinked with bis-acrylamide; (3) The termination of polyacrylamide propagation is achieved when the activated acrylamide monomers are totally consumed<sup>57</sup> (Fig. 10).

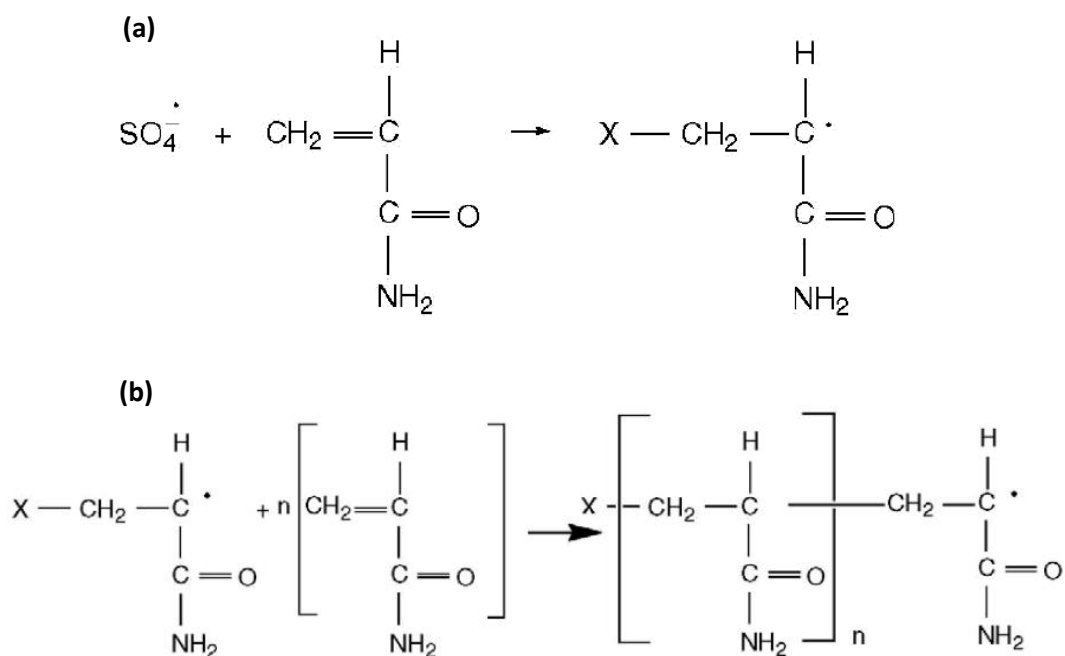


Figure 10: (a) Addition of radical to acrylamide monomer. (b) Propagation of PAAm polymerization.

### b. Physical crosslinked hydrogels:

The physical crosslinking of polymers represents a common technique for hydrogel synthesis. For instance, the physical interactions corresponding to hydrogen bonding and ionic interactions will be developed. These techniques are generally processed under mild conditions.

#### i. Hydrogen Bonding:

Hydrogen bonds mechanism contributes to obtain physically cross-linked hydrogels. H-bonded hydrogel is obtained with the presence of polymers containing carboxyl groups in a low pH solution as carboxymethyl cellulose (CMC) in HCl solution. The substitution of CMC sodium with hydrogen of acidic solution promotes the creation of hydrogen bonds within the polymer. These hydrogen bonds decrease the solubility of CMC in water which contribute to the development of an elastic physical hydrogel<sup>58</sup>(Fig. 11).

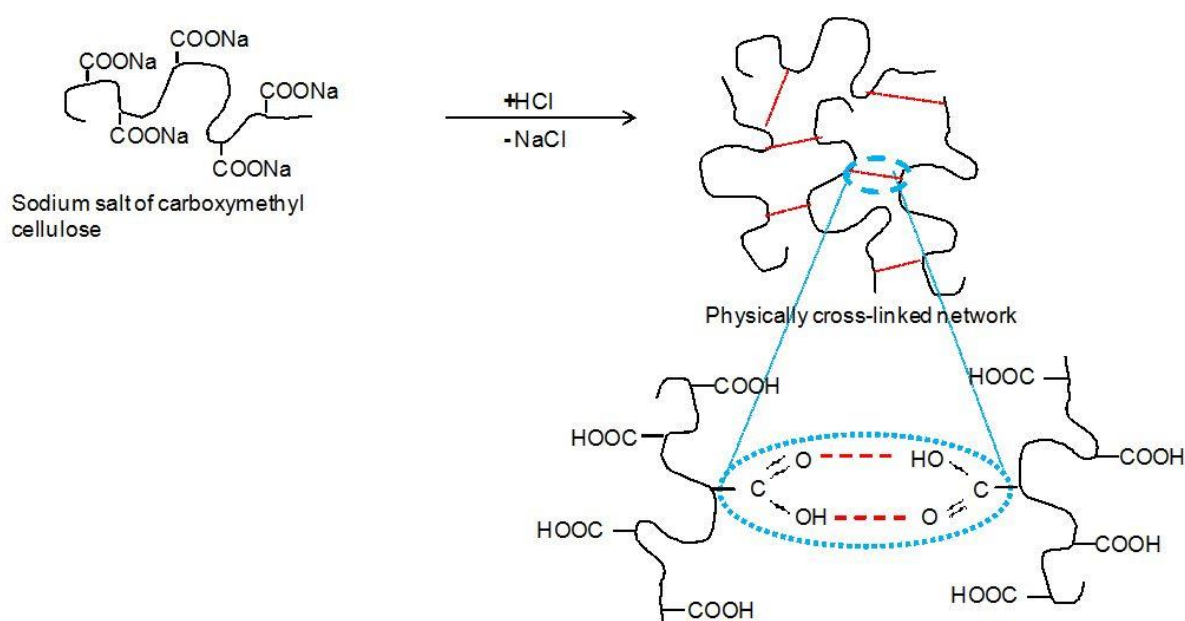


Figure 11: Hydrogel network formation due to intermolecular H-bonding in CMC at low pH<sup>59</sup>.

## ii. Ionic Interaction:

Physical hydrogels can be developed as well through ionic interactions under physiological conditions. Alginate, a naturally derived polymer, is a linear polysaccharide copolymer composed of  $\beta$ -D-mannuronic acid and  $\alpha$ -L-guluronic acid. Alginate hydrogel, used as a matrix for protein release and living cells incorporation, is formed in the presence of divalent cations such as calcium  $\text{Ca}^{2+}$  which interact with the carboxylic groups of alginate polymer chain (Fig.12). The mechanical strength of these ionic crosslinked hydrogels was shown a variation over time due to the exchange of  $\text{Ca}^{2+}$  ions with monovalent ions in surrounding solutions and thus this procedure is considered uncontrollable<sup>60</sup>. Likewise, chitosan polymer network is ionically crosslinked and mainly used for drug delivery<sup>56</sup>.

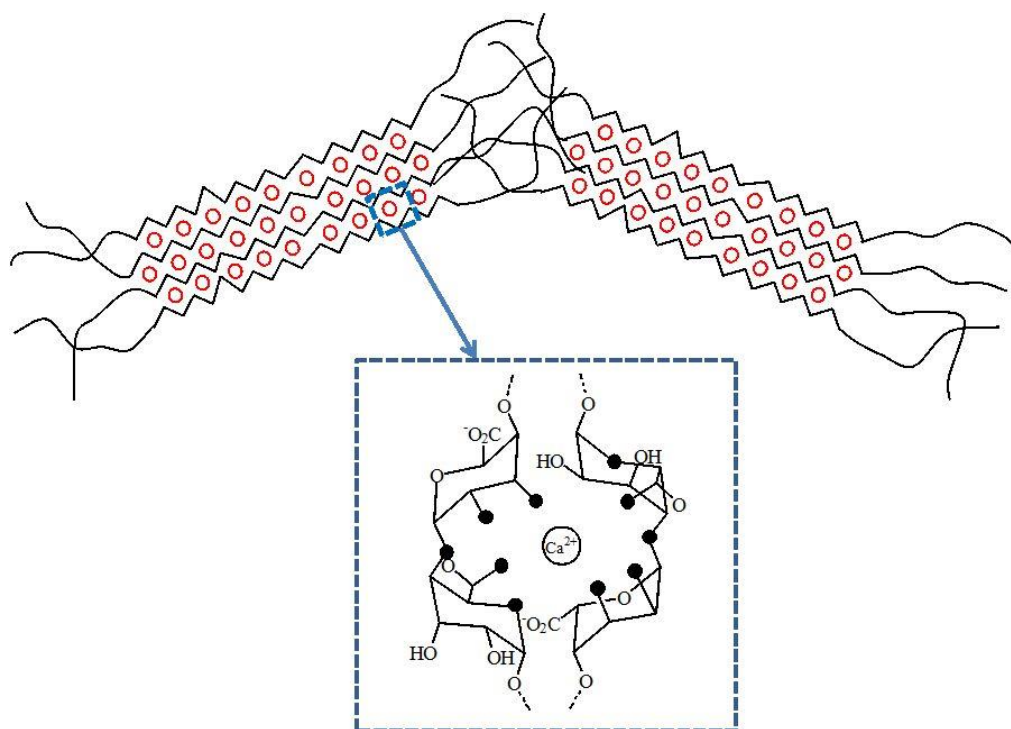


Figure 12: Ionotropic gelation by interaction between anionic groups on alginate ( $\text{COO}^-$ ) with divalent metal ions ( $\text{Ca}^{2+}$ )<sup>59</sup>.

Table 4 shows the characteristics and properties of physical and chemical crosslinking hydrogels<sup>61</sup>.

**Table 4: Physical and chemical hydrogels properties**

Physical Hydrogels	Chemical Hydrogels
<ul style="list-style-type: none"> <li>• Non-permanent but sufficient to get hydrogels insoluble in aqueous milieu</li> <li>• Reversible</li> <li>• Water absorbance but network defects or inhomogeneities may produce due to the chain loops and free chain ends</li> </ul>	<ul style="list-style-type: none"> <li>• Permanent</li> <li>• Non reversible</li> <li>• Ability to absorb high amount of water</li> </ul>

In our study, the chemical polymerization was focused on to synthesize the hydrogels scaffolds.

## 5. Hydrogels properties:

Hydrogels are characterized by numerous properties such as swelling, mechanical strength and biocompatibility. For a perfect scaffolding material, these physical properties should be as similar as *in vivo* for specific tissue engineering. These properties depend on hydrogel structure that can be controlled by modifying the synthesis mechanisms and the chemical compositions<sup>62</sup>. The characterization of these properties permits to understand their abilities to affect cells behaviors and therefore their influence on cells mechanotransduction.

### a. Swelling:

Swelling property is the capacity of hydrogels, in an aqueous environment, to uptake a large amount of water without dissolution since hydrogels are defined as hydrophilic polymers and characterized by their high water affinity due to the presence of hydrophilic groups within the polymer network chains such as -OH, -COOH<sup>63,64</sup>. The water molecules are attracted toward these hydrophilic and polar groups and form primary bound water. The hydrophobic moieties also interact with the water molecules and form secondary bound

water. Moreover, additional water will be absorbed by the hydrogels under the influence of an osmotic driving force opposed to the network elastic force based on the polymer network crosslinks. This imbibed water, called free water, contributes to reach the equilibrium swelling of hydrogels. A balance between the osmotic pressure and the elastic force will be occurred at the equilibrium swelling. This concept is explained by the Flory-Huggens theory<sup>65</sup>. Swelling phenomenon is based on osmotic pressure due to the presence of unequal ions distribution in the polymer network and the aqueous environment<sup>20</sup>. Once hydrogels are placed in water, the osmotic pressure promotes the expansion of polymer network and the hydrogels start to be swelled. The equilibrium swelling degree will be reached when the osmotic forces and the elastic forces of polymer chains are balanced. Swelling ratio indicates the hydrophilicity and the crosslinking degree of polymer network. It was shown that the swelling ratio of hydrogels decreases with increasing the crosslinking density of polymer chains because the polymer structure will become more compacted limiting the network extent<sup>57,63</sup>. Moreover, Vishal *et al.* have studied the effect of the ionic strength on hydrogel swelling capacity. They have shown that hydrogels placed in a swelling medium, containing  $\text{Na}^+$  and  $\text{Cl}^-$  ions, contributes to decrease the osmotic pressure and thus the swelling degree due to the presence of counter ions<sup>66</sup>. The water swelling capacity of polyacrylamide hydrogel is lower than the hydrolyzed form of polyacrylamide because of the electrostatic repulsion induced by the resultant anionic carboxyl groups. To obtain a hydrolyzed form, PAAm hydrogel is placed in a basic solution of sodium hydroxide (NaOH). The hydrolysis process induces the conversion of amine moieties ( $\text{R-NH}_2$ ) of PAAm network chain into carboxylate ( $-\text{COO}^-$ ) moieties having a high water affinity. Furthermore,  $\text{Na}^+$  ions present in NaOH solution are attracted toward the  $\text{COO}^-$  entrapped into the PAAm polymer chain. Afterwards, the hydrolyzed PAAm hydrogel is placed in deionized water. A counterion



osmotic pressure will be occurred since the concentration of  $\text{Na}^+$  free ions present into the polymer chain is not equivalent to the ions in the swelling solution.  $\text{Na}^+$  ions start to diffuse to the outer solution in order to decrease the concentration gradient and thus the swelling phenomenon of the PAAm hydrogel is occurred. The equilibrium state of water swelling degree becomes established where the osmotic pressure and the network elastic forces are balanced<sup>63</sup>. Experimentally, the swelling ratio is determined as the ratio of wet weight ( $W_s$ ) to dry weight ( $W_d$ ) and is expressed using this following equation:

$$S = \frac{W_s - W_d}{W_d}$$

Where  $W_s$  is obtained by measuring the weight of a fully swollen hydrogels (in equilibrium with water and cell media) and  $W_d$  is the measurement of a dehydrated hydrogel weight<sup>67</sup> (Fig.13).

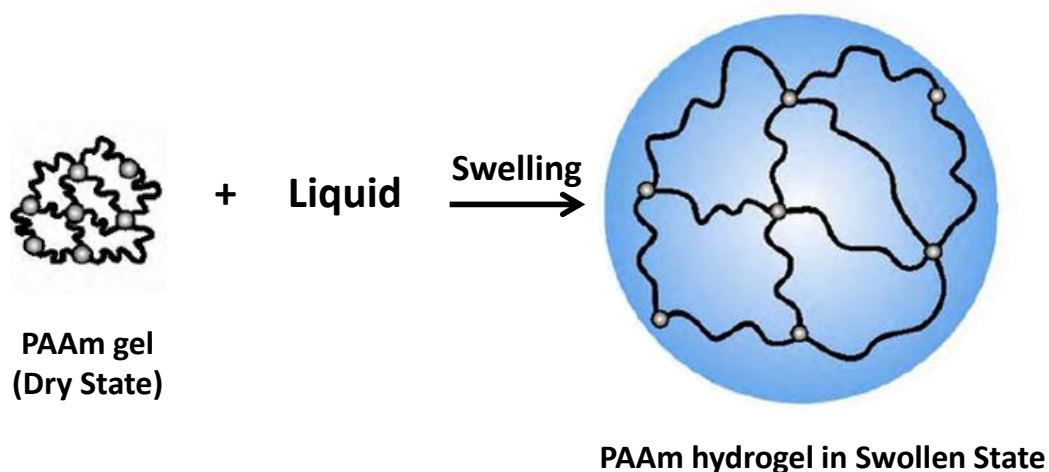
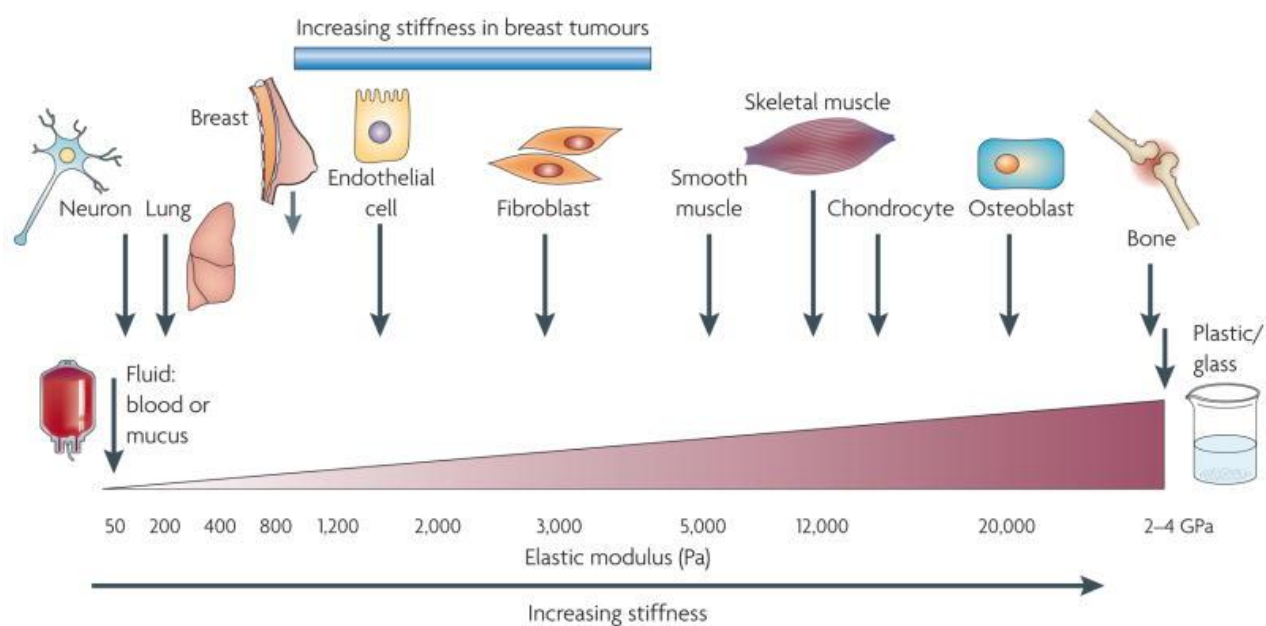


Figure 13: Swelling of hydrophilic polymers<sup>68</sup>.

#### b. Mechanical properties:

The mechanical properties, characteristics of cell microenvironment, have been shown critical role in the regulation and maintenance of cell behaviour. Matrix stiffness represents

a fundamental physical property and affects the cells by modifying their shape, size and cytoskeleton organization<sup>46</sup>. Cell-extracellular matrix (ECM) interactions induce the cells to respond to the physical properties of the membrane and to react by applying a force in order to control the cellular functions through actin dynamics and actomyosin contractility. The tension of this force applied depends on the matrix stiffness. Therefore, each type of cell has a specific mechanical microenvironment (Fig.14).



**Figure 14: Cells are tuned to the materials properties of their matrix<sup>69</sup>.**

Recent studies have shown that the mechanical properties of the substrate and particularly the stiffness have a great impact on cells functions including cells migration<sup>70,71</sup>, proliferation and differentiation<sup>72,73</sup>. Numerous studies have worked on various density of crosslinking hydrogel in order to clarify the effects of mechanotransduction on cells behaviors. Substrate stiffness can be assessed by measuring the Young's Modulus defined as material resistance to deformation using different characterization methods such atomic force microscopy (AFM), dynamic mechanical analysis (DMA) and rheology by applying force on a definite material zone. Researches have used AFM to measure the hydrogels surface elasticity and

thus to evaluate the network crosslinking density<sup>10,74</sup>. Actually, the Young's Modulus of a substrate increases with increasing the concentration of crosslinker and therefore the substrate is considered as a stiff material. Hydrogels, with tunable elastic properties, were developed so as to create *in vitro* cell culture model mimicking the extracellular environment. Notably, polyacrylamide hydrogels have been widely used as biomaterials for tissue engineering as they present a wide range of adjustable elasticity imitating several tissues stiffness as neurons ( $\sim 0.5\text{kPa}$ )<sup>75</sup>, fibroblast ( $\sim 10\text{kPa}$ )<sup>76</sup> and osteoblast ( $>20\text{kPa}$ )<sup>77</sup> stiffness and this stiffness variation depends on polymer network crosslinking density. Most studies have worked on the stiffness effect on mesenchymal stem cells (MSCs) differentiation. They have shown that MSCs upregulate the expression of neuronal markers on soft substrate having an elasticity close to brain tissue whereas these cells express myogenic and osteogenic markers on stiff substrate with elasticity similar to muscle and collagenous bone, respectively<sup>14</sup>. Moreover, the GelMA hydrogels have shown a great interest as scaffold materials for biomedical applications due to their widely biological properties and their tunable mechanical properties. Wang *et al.* have shown that the degree of methacrylation has a significant effect on the GelMA mechanical properties. The high methacrylation degree increases the stiffness of GelMA hydrogels due to the increase of methacrylic substitutions that induces the network crosslinking<sup>78</sup>. According to the mechanical property, hydrogels were used recently for several biomedical applications such as drug delivery, wound dressing and tissue engineering.

Table 5 includes different type of hydrogels using as scaffold materials in biomedical applications. The preparation methods and the mechanical properties of these hydrogels are also determined.

Table 5: Hydrogels: Preparation and Mechanical Properties

Hydrogels	Method of Synthesis	Method of Characterization	Elasticity	References
Gelatin-mTG	Chemical Polymerization	Rheology	0,6 kPa – 13 kPa	Mufeng Hu <i>et al.</i> <sup>79</sup>
Gelatin-EDC	Chemical Polymerization	Rheology Tensile Stress	2 kPa 196 kPa	Qi Xing <i>et al.</i> <sup>80</sup>
Polyacrylamide	Chemical Polymerization	Atomic Force Microscopy	2 kPa – 10 kPa	Jérôme Solon <i>et al.</i> <sup>10</sup>
	Photopolymerization	Atomic Force Microscopy	1 kPa – 240 kPa	Raimon Sunyer <i>et al.</i> <sup>81</sup>
	Chemical Polymerization	Rheology	0,18 kPa – 16 kPa	Tony Yeung <i>et al.</i> <sup>76</sup>
PEG-GelMA	Photopolymerization	Tensile Stress	0.2 MPa – 0.6 MPa	Jia Liang <i>et al.</i> <sup>82</sup>
PEGMA-PEGDMA	Photopolymerization	Rheology	10 <sup>6</sup> Pa – 10 <sup>8</sup> Pa	Ji Won Hwang <i>et al.</i> <sup>83</sup>
PEG-PLLA-DA	Photopolymerization	Compression Test	1 kPa – 13 kPa	Yu-Chieh Chiu <i>et al.</i> <sup>84</sup>
GelMA	Photopolymerization	Compression Test	1 kPa – 34 kPa	Yupeng Sun <i>et al.</i>

### c. Biocompatibility:

Tissue engineering concept requires the development of an appropriate biomaterial able to restore the main tissue functions and to obstruct the immune system by inhibiting the macrophage response which knocks down the functional properties of implantable materials. Biocompatibility is defined as the material ability to interact within the physiological environment without damaging the host tissues. Many studies have suggested the usage of appropriate extracellular matrix based polymer for cells transplantation. Therefore, biocompatibility is a main property in making polymer based hydrogels for tissue engineering applications<sup>85</sup>. Researchers have studied the central nervous system (CNS) properties to develop biocompatible hydrogels for neural tissue engineering. It was proved that the non-biocompatibility of hydrogels with neural tissue induces the neuroimmune

system to react toward the implanted polymer and thus damages will be produced. Recently, the development of biocompatible hydrogels for neural tissue engineering has advanced and has shown that neural cells transplantation encased within a hydrogel might be protected from acute inflammatory response and thus enhances the cells survival<sup>86</sup>.

The evaluation of biological responses allows characterizing the materials biocompatibility. Inflammation diseases, mechanical damages and immunological rejections are assessed as side effects of synthetic materials. The toxicity of synthetic hydrogels remains a drawback for tissue engineering due to the initiators and organic solvents used and due to the presence of unreacted monomers during hydrogel polymerization which are harmful for tissue cells. Nowadays, researches start to focus on the development of advanced biomaterials by controlling their efficacy in order to reduce their side effects.

According to these properties, hydrogel has been used as a promising candidate in tissue engineering. The application of hydrogels as a scaffold for tissue engineering requires various main functions including the cell adhesion, the nutrients and growth factors transport ensuring the cell survival, the delivery of seeded cells toward the desired site and the absence of toxicity. Therefore, the concept of tissue engineering using hydrogels as matrix will be elaborated.

## **6. Hydrogels For Tissue Engineering Applications:**

Tissue engineering is a promising process to regenerate and replace damaged tissues or organs. Tissue engineering concept was suggested by Langer et al. in 1990s as “the application of engineering and the life sciences principles toward the fundamental understanding of structure-function relationships in normal and pathological mammalian tissues and the development of biological substitutes that restore, maintain or improve tissue function”. Tissue engineering strategy consists to develop and design an appropriate

scaffold material serving as an extracellular matrix for appropriate tissue cells without inducing immune responses reactions. Biomaterials such as hydrogels are used as functional scaffolds for tissue engineering as they provide mechanical support for cells and suitable biophysical and biochemical signals implicated in the regulation of cell behaviour and function. Selection and design of the appropriate hydrogel scaffold material for tissue engineering requires fundamental characteristics such as hydrogels biocompatibility, mechanical strength and biofunctionality essential in the regulation of cellular behaviors. Table 6 shows the main characteristics of hydrogel to be designed as a scaffold material for tissue engineering.

**Table 6: Design criteria for hydrogels as scaffolds for tissue engineering**

Hydrogels design criteria
<ul style="list-style-type: none"> <li>• Gel synthesis mechanisms</li> <li>• Appropriate mechanical properties</li> <li>• Appropriate diffusion of nutrients and metabolites</li> <li>• Biological properties</li> <li>• Biocompatibility</li> <li>• Promotion of cell adhesion, proliferation and differentiation</li> </ul>

The following section will be focused on the mechanisms of interaction between the extracellular matrix and the cells and on the study of the effect of hydrogels mechanical properties on tissue functions.

### **III. Cell-ECM interaction:**

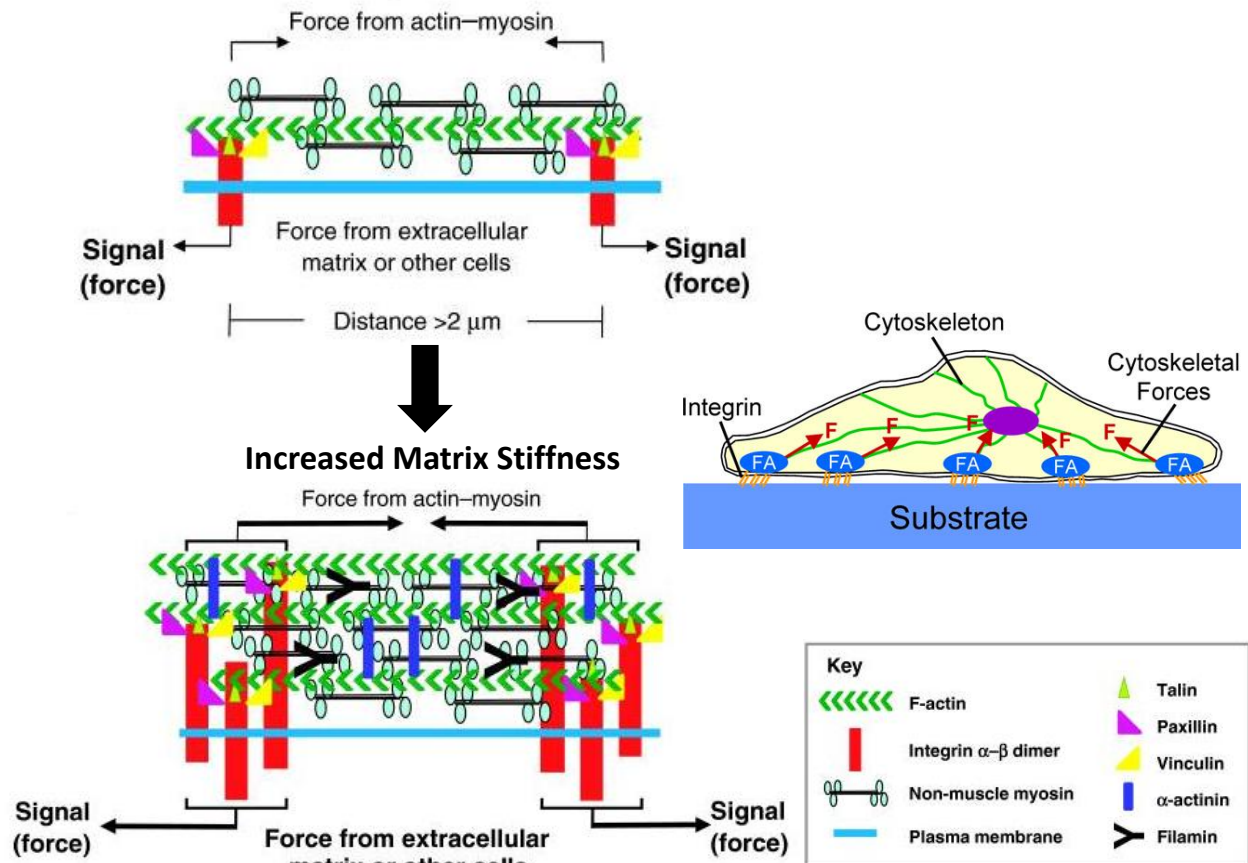
#### **1. Mechanotransduction:**

The ECM mechanical characteristics have an important role in the regulation of cell fate and cell behaviour. Cells sense, integrate and interpret the physical and chemical signals of extracellular environment. Thus, cells feel the topography<sup>87,88</sup> and the rigidity<sup>12,14</sup> of ECM and therefore produce appropriate physiological responses regulating the cellular activities

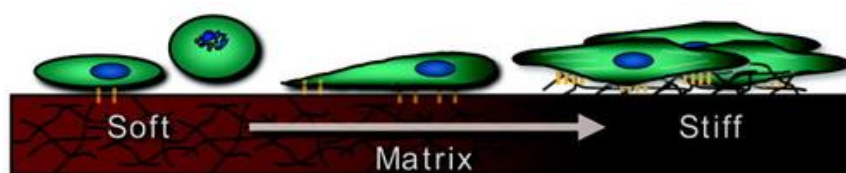
such as proliferation, migration, differentiation and apoptosis<sup>89</sup>. Accordingly, every living tissue is determined by a specific elasticity. Previous studies have shown the significant role of ECM mechanical properties in the progression of breast cancer disease. They have proved that the stiffness of healthy mammary glands is approximately 150 Pa, while the breast tumor exhibits a high stiffness of 4 kPa. Moreover, the morphology and the growth rate of mammary epithelial cells have showed a significant difference depending on stiffness environment<sup>90</sup>. Regarding the liver tissue, the stiffness of healthy liver is around 300 - 600 kPa while the stiffness of liver diseases such as fibrosis and cirrhosis increases over 20 kPa<sup>91</sup>. Cellular adhesion machinery is composed of specialized transmembrane receptors associated via the cytoplasmic domain with the actin cytoskeleton. These sites enhance the ECM – cells and cells - cells interactions in a way to maintain the specific form and mechanical properties of tissues. Through these active sites, cells recognize the physical cues which are defined by the mechanical forces applied to cellular membrane. Several studies have investigated the importance of microenvironment mechanical properties in the regulation of cellular behaviors<sup>92,93,94,95</sup>. In fact, cells sense and respond to the mechanical properties generated by ECM through integrin. Integrin is a transmembrane cell adhesion protein characterized by the presence of two domains: an intracellular domain in interaction with the cell cytoskeleton and an extracellular domain binding to the substrate<sup>96,97</sup>. ECM mechanical signals will be transduced into intracellular signals and affect the cells properties as cells morphology, migration, cytoskeleton organization, differentiation and cells stiffness. This is called a mechanosensing phenomenon. The mechanosensing definition is the capability of a tissue or cell to detect the microenvironment applied forces such as contractile forces<sup>5,93</sup>. The transduction of ECM mechanical signals is established through focal adhesion complex characterized by the binding of ECM molecules to a group of

integrins. Integrins serve as a linker and reinforce the connection of ECM to cells actin fibers<sup>98</sup>. Moreover, the focal adhesion complex is also characterized by the presence of non-muscle myosin and proteins cluster such as talin<sup>99</sup> and vinculin<sup>100</sup>. In fact, the force generated by actin polymerization contributes to the requirement of these proteins group which are able to assemble and to link the integrin to actin fibers and to non-muscle myosin. These non-muscle myosin proteins are actin-binding proteins that play an important role in multiple cellular processes such as cell adhesion and migration<sup>101</sup>. They are characterized by their contractile functions and produce an additional force to match the encountered mechanical environment (Fig.15). Actually, cells feel the variation of ECM stiffness and react in a different process. For instance, cells sense the ECM high stiffness which contributes to the loss of cells ability to respond and to contract against the matrix. Thus, cells produce additional forces and the number of focal adhesion and so the number of actin fibers connected to non-muscle myosin will be increased leading to an increase in cell stiffness in order to go with matrix stiffness. Contrariwise, the cells on a matrix with low stiffness generate a small force and show a few number of focal adhesion complex and thus actin fibers. In conclusion, cell responds and reacts to the variation of substrate stiffness which contributes to regulate the organization of actin cytoskeleton<sup>102</sup>.





Substrate stiffness constitutes as well an essential element to act on cell morphology. In fact, several studies have investigated the effect of substrate stiffness on cell morphology behaviour. It was shown that cells on low substrate stiffness exhibit a round shapes whereas this morphology becomes more spread when the cells sense a substrate having a high stiffness (Fig.16).



Yeung *et al.* have worked on fibroblast and endothelial cells and have studied the effect of substrate stiffness on cells morphology and cytoskeletal structure. As they concluded, cells are characterized by spread morphology and the presence of actin stress fibers on PAA substrates elasticity greater than 2 kPa<sup>76</sup>. As mentioned previously, ECM mechanical properties control the differentiation of mesenchymal stem cells (MSCs). Park *et al.* have reported the effect of matrix stiffness on MSCs differentiation into a variety of cell lineage including smooth muscle cells (SMCs) and adipocytes. They have shown that MSCs seeded on soft substrate differentiate into chondrogenic and adipogenic lineage while the stiff substrate permits the differentiation of MSCs into SMC lineage. These observations are comparative with the *in vivo* environment<sup>104</sup>.

## **2. Effect of stiffness on tissue functions:**

The extracellular and intracellular microenvironment mechanical properties present the main feature of tissues and cells. These elastic properties control the cells fate and behaviour including cells morphology and functions. To mention that the intracellular elastic properties are defined by the cells ability to develop an internal force depending on matrix stiffness. This force affects the quantity of polymerized actin, the cytoskeleton organization and the generation of adhesion complexes. The disturbance of the mechanical environment disrupts the tissue functions and acts on the progression of several diseases including malignancy<sup>5</sup>.

- Numerous *in vitro* researches have shown the effect of substrate stiffness on cells behavior such as cells shape and differentiation. Soft tissues as liver, lung, breast and kidney are considered as part of viscoelastic materials having an elasticity varying from 0.2 to 4 kPa<sup>90</sup>. It was shown that the control of tissue stiffness permits to maintain the

specific cells differentiation. Engler *et al.* have proved that the differentiation of mesenchymal stem cells (MSCs) depends on substrate elasticity. MSCs cultured on soft substrate, having a range of elasticity similar to brain stiffness (0.1 – 1 kPa), differentiate into neuronal cells. Whereas, MSCs differentiate into myocyte-like cells and osteoblast-like cells on substrates with stiffness corresponding to muscle stiffness ranged from 8 to 17 kPa, and on stiffest substrates (25 – 40 kPa) respectively<sup>105</sup>. Moreover, several studies have shown that neurons growth is more selective when brain cortical cells are seeded on soft substrates having a standard elasticity of normal brain (0.15 – 0.30 kPa). Whereas, these cells grown on stiff substrates (2 kPa) permit the activation and the proliferation of glial cells such as astrocytes. It has been shown that astrocytes cultured on soft substrates are less spread and the actin filaments are not well organized comparing to astrocytes on stiff substrates<sup>106</sup>.

- Breast cancer is considered one of the most common cancers among women worldwide. Levental *et al.* have shown that breast tissue represents a soft material with elasticity of 0.2 kPa. In case of breast tumor, this stiffness exhibits a significant increase and the breast tissue will become stiffer than healthy breast (>4 kPa)<sup>90</sup>. Several researches have studied the effect of matrix stiffness on breast tissue behavior. They have proved that an increase on matrix elasticity promote the progression of breast cancer accompanied by the loss of epithelial cells morphology, the development of acini which constitutes a malignant phenotype and the increase of Rho and extracellular-signal-regulated kinase (ERK) activities. These features contribute to the development of breast cancer<sup>107</sup>.
- Kidney glomerulus has specific mechanical properties which permit to maintain the fundamental kidney functions and specifically the differentiated state of podocytes glomerular cells. It has been suggested that glomerular disease is associated with the

alterations of biophysical mechanical properties. The stiffness of normal healthy kidney glomerulus has been defined in the order of 2.5kPa. Tandon and colleagues have worked on HIV-associated nephropathy (HIVAN) mice models to study whether the glomerular mechanical properties were modified. According to HIVAN disease, they have demonstrated that glomerular elasticity decreases and therefore the kidney glomerular become significantly softer with a reduction of 30% comparing to healthy kidney state<sup>108,109</sup>.

- Liver disease has been investigated to point out the key role of liver mechanical properties on cellular behaviors. As tissues are specified by their proper mechanical characteristics, the stiffness of healthy liver tissue is approximatively 0.5kPa. Whereas, liver injury or fibrosis conditions show a significant increase of tissue elasticity reaching a value of 15kPa<sup>91,110</sup>. As mentioned previously concerning the effect of matrix stiffness on cells differentiation, Li *et al.* have proved that liver cells such as hepatocyte, portal fibroblasts and stellate cells fail to maintain the differentiated phenotype and the division of these cells will become uncontrollable as a result of matrix elasticity increasing<sup>111</sup>.

In summary, extracellular matrix provides mechanical support system for cell attachment and migration. Furthermore, ECM provides biochemical and biomechanical signals affecting the activities of cells including phenotypic modulation, survival and differentiation. Mechanobiology is defined by how cells sense and respond to the ECM mechanical signals and how cells exert force and control the mechanical properties of the surrounding environment.

Kidney diseases are a worldwide public health problem. Renal failure follows several disease stages including acute and chronic kidney symptoms. Current treatment options are limited

to dialysis and kidney transplantation; however, problems such as shortage in kidney donors, graft rejection and other numerous complications remain a concern. To address this issue, cell based approaches using tissue engineering may provide attractive approaches to replace the damaged kidney cells with functional renal specific cells; leading to restoration of normal kidney functions. The objective of this work was focused on the study of the effect of mechanical properties of polymers based hydrogels on kidney podocyte behavior in order to develop a membrane mimicking the glomerular basement membrane (GBM) to restore the kidney functions. The following part will describe the morphology and the function of GBM and podocyte kidney cells.

#### **IV. Podocytes:**

##### **1. Definition:**

Glomerulonephritis is a chronic kidney disease characterized by the inflammation of the glomeruli which is responsible for the filtration of waste products from blood. The glomerular filtration barrier (GFB) is formed by capillary endothelial cells and podocytes separated by a glomerular basement membrane (GBM). GBM is the extracellular matrix of kidney glomerulus. GBM functions as a selective barrier helping to restrict the macromolecules passage and therefore GBM is involved in the development and maintenance of the proper functions of the glomerular filtration barrier (GFB). GFB permits the blood filtration by selecting molecules according to their size and charge. The electrolytes, cationic molecules and small solutes will be filtered through the slit diaphragm in order to form urine, while the macromolecules and the anionic molecules will be retained such as plasma proteins<sup>112</sup>. The research studies have shown that the development of

kidney glomerular disease is associated with the alteration of GBM composition and mechanical properties. Genetic and physiological studies have proved that the mutations of GBM genes (as collagen IV  $\alpha 3$  or  $\alpha 5$  chain and podocyte-specific proteins that alter cell-cell junctions), affecting the GBM and the cytoskeleton of glomerular cells, cause the development of glomerular diseases. Moreover, the mechanical environment is considered as fundamental factor that determine the cellular behaviors during a healthy and diseased state. GBM physical properties have shown a significant role in maintaining the differentiated form of podocyte glomerular cells which maintain the main function of kidney glomerulus. A healthy kidney GBM is characterized by specific mechanical characteristics with an elastic modulus of 2.5 kPa. An increase of GBM elasticity has shown a loss of organ functions in the late stages of disease<sup>109,113</sup>.

Podocytes are the most differentiated renal epithelial cells of the kidney glomerulus and represent the essential component for the formation and maintenance of the glomerular filtration barrier. The complexity of podocytes structure is characterized by cytoplasmic projections localized and attached on the glomerular capillary basement membrane external surface known as “foot processes”. These foot processes interdigitate with each other and form slits diaphragm of specific proteins leading to establish a porous filtration barrier<sup>114</sup> (Fig. 17). Moreover, podocytes foot processes are coated by negative charges due to the presence of glycocalyx which is composed of several sialoglycoproteins including podocalyxin. Podocalyxin acts to maintain the podocytes cytoarchitecture by generating an electronic repulsion between the neighboring podocytes foot processes contributing to control the glomerular filtration barrier<sup>115</sup>.

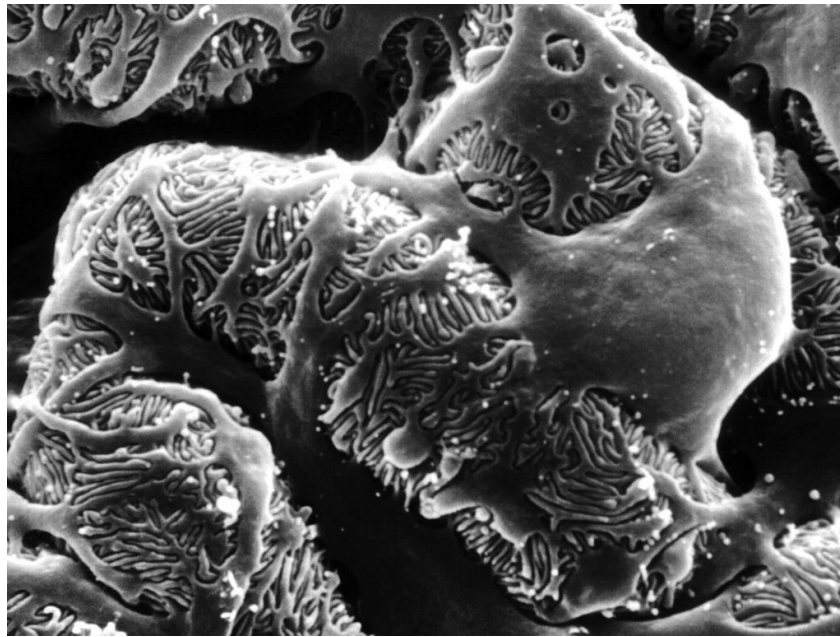


Figure 17: Podocytes Imaging<sup>116</sup>

Podocytes, a functional element for filtering blood in the glomerulus, are influenced by different signals such as mechanical and chemical signal from GBM. These signals control the maintenance of slit diaphragm and thus the main podocytes activity. Once podocytes are damaged or podocytes-GBM interaction is altered, the podocytes connectivity will be modified and the foot processes will become flattened and fused. This phenomenon is called foot process effacement which will contribute to lose the slit diaphragm and thus the filtration barrier. Proteinuria also called albuminuria is the sign of early kidney disease; it is the result of a massive proteins leakage into the urine during the blood filtration due to the glomerular filtration barrier dysfunction<sup>79</sup>.

## 2. Podocyte Slit Diaphragm:

The maturation of podocytes is determined by their unique architecture, characterized by foot processes, and by the expression of specific protein markers which are involved in the development of podocyte slit diaphragm. These proteins such as Nephrin, Podocin, CD2AP,

WT-1 and Synaptopodin are able to maintain the slit diaphragm integrity and hence the glomerular filtration functions (Fig. 18). In case of gene mutation or inactivation, the barrier filtration will be disrupted and causes proteinuria<sup>117</sup>.

- Nephrin, regulated by NPHS1 gene, is associated with the maturation of podocyte during the development of kidney glomerulus<sup>118</sup>. Many studies have shown that the progression of glomerular diseases, such as diabetic nephropathy and HIV-associated nephropathy, is correlated to the downregulation and expression of nephrin<sup>119,120</sup>. Nephrin protein is composed of three domains: extracellular, transmembrane and intracellular domains. Nephrin, a signaling protein phosphorylated by Src family kinase, such as Src<sup>121</sup> and Fyn<sup>121,122,123</sup>, develop a network of cytoplasmic binding proteins which affect podocyte functions as cell survival and actin organization. The loss of nephrin phosphorylation activity contributes to the development of podocyte foot process effacement<sup>124</sup>.
- Podocin, regulated by NPHS2 gene, have a main role in the glomerular filtration and permeability. The development of nephrotic syndrome was shown mutations in NPHS2 genes<sup>125</sup>. Podocin is an integral membrane protein with a short membrane domain having a hairpin structure with C- and N- terminal domains localized in the cytosol<sup>126</sup>. Podocin interacts with the intracellular domains of slit diaphragm proteins such as nephrin and P-cadherin. Podocin maintains the integrity of glomerular filtration barrier and connects the slit diaphragm components to the actin cytoskeleton<sup>126</sup>.
- CD2-associated protein (CD2AP), regulated by CD2AP gene, is an adaptor molecule which interacts with the intracellular domain of nephrin. CD2AP-nephrin interactions are implicated in the maintaining of slit diaphragm functions. Researchers have proved that the CD2AP deficiency contributes to congenital nephrotic syndrome progression associated with foot process effacement<sup>127</sup>. Moreover, recent studies have reported that



CD2AP is involved in the repression of apoptosis signaling induced by Transforming growth factor (TGF- $\beta$ ) in podocyte cells. In fact, albuminuria disease is associated with increasing TGF- $\beta$  expression due to the absence of CD2AP proteins<sup>128</sup>.

- Podocytes are also specified by the presence of specific protein markers involved in kidney development procedure such as WT-1 and synaptopodin regulated by WT-1 and SYNPO genes respectively. WT-1 protein acts as a transcription factor, affects cell growth and apoptosis and interacts with nephrin protein to regulate it and hence to protect the filtration barrier integrity. WT-1 mutation has been noted a reduction of nephrin expression and so a low renal development. Synaptopodin is implicated in the cytoskeleton regulation by controlling RhoA activity, necessary for podocyte foot processing.

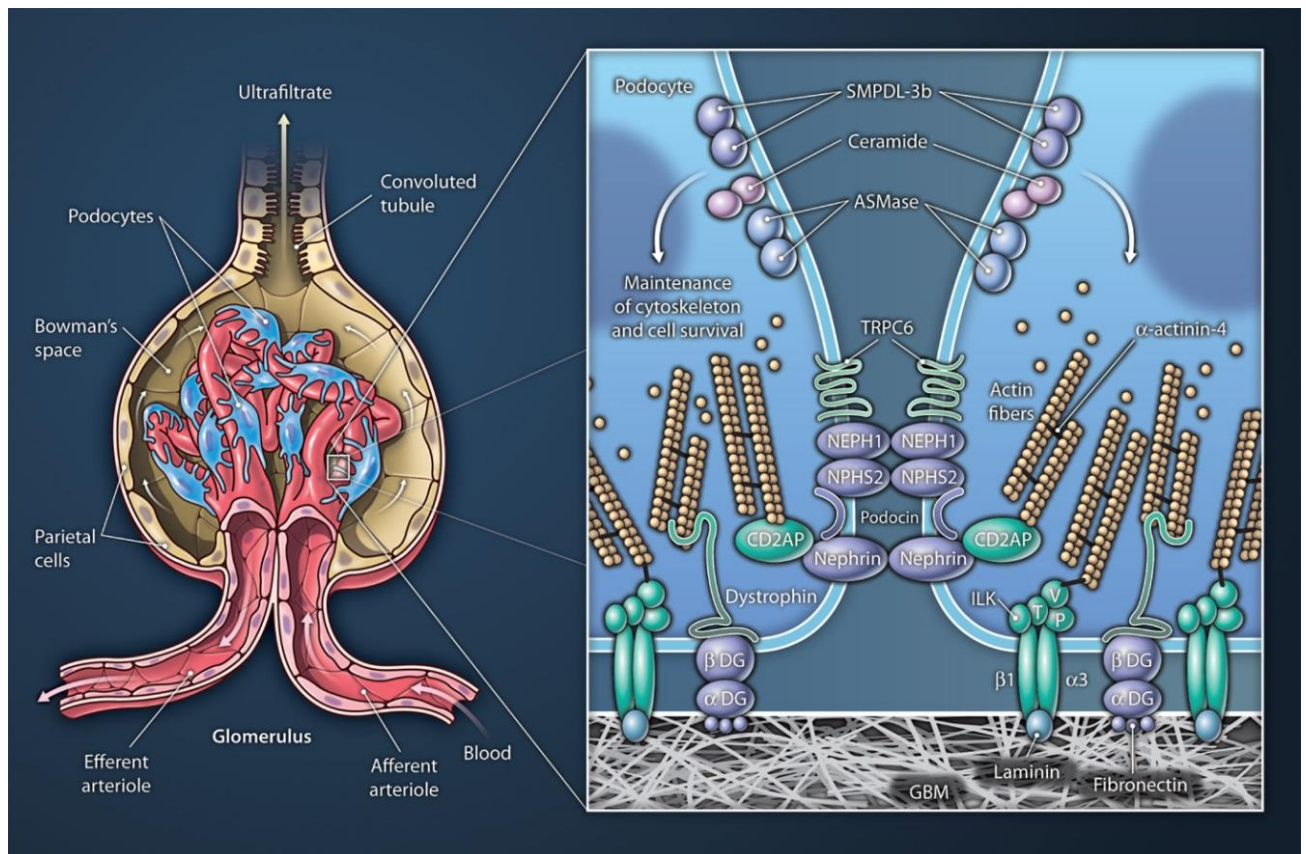


Figure 18: The glomerulus and slit diaphragm<sup>129</sup>

Podocytes maintain the integrity and the function of the glomerular filtration barrier. The damaging of podocytes slit diaphragm represents the hallmark of the development of many glomerular diseases such as proteinuric kidney disease. Recently, kidney tissue engineering using hydrogels as scaffolding materials in interaction with podocytes cells has shown a great advancement in the regeneration of kidney functions. Many researches have been worked on the development of hydrogels based scaffolds system having similar mechanical properties of the physiological kidney glomerulus and acting as substitute for glomerular basement membrane (ECM)<sup>130</sup>. Moreover, these scaffolds materials have been developed to study the effect of their mechanical properties on the podocytes cells including cell migration, proliferation and differentiation<sup>79</sup>. Mufeng Hu *et al.* have developed of a stable biomimetic gelatin-mTG substrates based on natural enzyme microbial transglutaminase

crosslinked with gelatin. They have considered various scaffolds stiffness and investigated their effect on the regulation of podocytes spreading, migration and differentiation. A high expression of differentiated podocytes markers was shown on the gelatin-mTG substrates having elasticity close to the *in vivo* glomerular basement membrane (GBM). Therefore, gelatin-mTG is considered as a great platform as an *in vitro* system to mimic the mechanical properties of targeted tissue due to their wide range of elasticity<sup>79</sup>. Moreover, Addie Embry *et al.* have also investigated the podocytes behaviors using polyacrylamide as scaffold material having various mechanical properties. They have shown that podocytes on substrates with a range of elasticity close to the GBM physiological stiffness exhibit an *in vivo* phenotype. Furthermore, they have studied the effect of renal ischemia and ischemia-reperfusion injury on the glomerular elastic modulus and have detected a decrease of the glomerular basement membrane elasticity. Therefore, the glomerular injury is a sign of GBM elasticity reduction<sup>131</sup>.

## **V. Conclusion:**

Hydrogels have received a great attention as scaffold materials in tissue engineering applications due to their composition, biocompatibility and desirable mechanical properties similar to the native extracellular matrix of target tissues. This chapter was focused on the characterization of the various origins of polymers including natural and synthetic polymers and on the synthesis of these polymers via chemical or physical crosslinking. Furthermore, the main properties such as swelling capacity, mechanical properties and biocompatibility indispensable in the development of an appropriate scaffold for tissue engineering were elaborated. Since the behaviors of cells such as proliferation, migration and differentiation

are regulated by the surrounding mechanical environment, the study of the mechanisms of the interaction between the cells and the extracellular matrix known as mechanotransduction were developed contributing to understand the effect of mechanical properties such as stiffness on tissue dysfunction. Finally, the kidney cells and specially the podocytes structure and function were developed as the aim of the work is to establish a suitable hydrogels mimicking the characteristic of glomerular basement membrane in order to restore the kidney functions.

## **VI. Thesis Objectives:**

Chronic kidney disease (CKD) is characterized by a reduced kidney function that will inevitably progress to end-stage renal disease (ESRD). Podocytes are highly specialized glomerular epithelial cells which form with the glomerular basement membrane and capillary endothelium the glomerular filtration barrier (GFB). Podocytes adhere to and cover the outer urinary side of the glomerular basement membrane. Podocytes foot processes interdigitate in a zipper-like structure to form sophisticated filtration slits (slit diaphragm) that act as a selective molecular sieve against many components of the blood. Slit diaphragm structure is maintained by expressing podocytes-specific markers including Nephlin (NPHS1), synaptopodin (SYN) and podocin (NPHS2). Damage to the basement membrane or loss of podocyte markers will lead to a defective GFB encountered in CKD. The aim of this study was to control the function and the fate of podocyte cells by controlling the physical properties of the extracellular matrix (ECM) to which podocyte adhere. First, the design of polymers based hydrogel scaffolds were investigated due to their potential use as a construct to engineer a functional in vitro glomerular-like filtration barrier. Their most important

properties relevant to biomedical applications are identified and studied. Simultaneously, glomerular podocytes were cultured on these polymers based hydrogels and different methods were evaluated in order to know how podocyte cells sense signals from their biophysical environment and respond to these signals at the molecular level. Finally, these hydrogel-based cell culture systems will allow investigating podocyte – extracellular matrix (ECM) interactions that mimic in vivo setting. This study will allow us: (1) Gaining a robust fundamental understanding of podocyte cells attachment and proliferation behaviour when interfacing with scaffolds having various mechanical properties, (2) Modelling the kidney filtration barrier by an artificial composite layer composed of cells on gel matrix, (3) Uncovering much needed data on podocyte biology in an environment similar to the in vivo setting and (4) Establishing in vitro model that mimics in vivo setting in the kidney glomerulus, this will help in gaining further molecular knowledge on podocyte cellular behaviour during health and disease states.

## VII. References:

- (1) Frantz, C.; Stewart, K. M.; Weaver, V. M. The Extracellular Matrix at a Glance. *J. Cell Sci.* **2010**, *123* (24), 4195–4200.
- (2) Clause, K. C.; Barker, T. H. Extracellular Matrix Signaling in Morphogenesis and Repair. *Curr. Opin. Biotechnol.* **2013**, *24* (5), 830–833.
- (3) BROWN, B. N.; BADYLAK, S. F. Extracellular Matrix as an Inductive Scaffold for Functional Tissue Reconstruction. *Transl. Res. J. Lab. Clin. Med.* **2014**, *163* (4), 268–285.
- (4) Bauer, A. L.; Jackson, T. L.; Jiang, Y. Topography of Extracellular Matrix Mediates Vascular Morphogenesis and Migration Speeds in Angiogenesis. *PLoS Comput. Biol.* **2009**, *5* (7), e1000445.
- (5) Janmey, P. A.; Miller, R. T. Mechanisms of Mechanical Signaling in Development and Disease. *J. Cell Sci.* **2011**, *124* (Pt 1), 9–18.
- (6) Mishra, S.; Rani, P.; Sen, G.; Dey, K. P. Preparation, Properties and Application of Hydrogels: A Review. In *Hydrogels: Recent Advances*; Thakur, V. K., Thakur, M. K., Eds.; Gels Horizons: From Science to Smart Materials; Springer Singapore: Singapore, 2018; pp 145–173.
- (7) Buwalda, S. J.; Boere, K. W. M.; Dijkstra, P. J.; Feijen, J.; Vermonden, T.; Hennink, W. E. Hydrogels in a Historical Perspective: From Simple Networks to Smart Materials. *J. Control. Release Off. J. Control. Release Soc.* **2014**, *190*, 254–273.
- (8) Yom-Tov, O.; Neufeld, L.; Seliktar, D.; Bianco-Peled, H. A Novel Design of Injectable Porous Hydrogels with in Situ Pore Formation. *Acta Biomater.* **2014**, *10* (10), 4236–4246.
- (9) Syed, S.; Karadaghy, A.; Zustiak, S. Simple Polyacrylamide-Based Multiwell Stiffness Assay for the Study of Stiffness-Dependent Cell Responses. *J. Vis. Exp. JoVE* **2015**, No. 97.
- (10) Solon, J.; Levental, I.; Sengupta, K.; Georges, P. C.; Janmey, P. A. Fibroblast Adaptation and Stiffness Matching to Soft Elastic Substrates. *Biophys. J.* **2007**, *93* (12), 4453–4461.
- (11) Caliri, S. R.; Burdick, J. A. A Practical Guide to Hydrogels for Cell Culture. *Nat. Methods* **2016**, *13* (5), 405–414.

- (12) Discher, D. E.; Janmey, P.; Wang, Y.-L. Tissue Cells Feel and Respond to the Stiffness of Their Substrate. *Science* **2005**, *310* (5751), 1139–1143.
- (13) Pelham, R. J.; Wang, Y. Cell Locomotion and Focal Adhesions Are Regulated by Substrate Flexibility. *Proc. Natl. Acad. Sci. U. S. A.* **1997**, *94* (25), 13661–13665.
- (14) Engler, A. J.; Sen, S.; Sweeney, H. L.; Discher, D. E. Matrix Elasticity Directs Stem Cell Lineage Specification. *Cell* **2006**, *126* (4), 677–689.
- (15) Chai, Q.; Jiao, Y.; Yu, X. Hydrogels for Biomedical Applications: Their Characteristics and the Mechanisms behind Them. *Gels* **2017**, *3* (1), 6.
- (16) Yahia, Lh.; Chirani, N.; Gritsch, L.; Motta, F. L.; SoumiaChirani; Fare, S. History and Applications of Hydrogels. *J. Biomed. Sci.* **2015**, *4* (2).
- (17) Tibbitt, M. W.; Anseth, K. S. Hydrogels as Extracellular Matrix Mimics for 3D Cell Culture. *Biotechnol. Bioeng.* **2009**, *103* (4), 655–663.
- (18) Ahmed, E. M. Hydrogel: Preparation, Characterization, and Applications: A Review. *J. Adv. Res.* **2015**, *6* (2), 105–121.
- (19) Williams, D. F. On the Mechanisms of Biocompatibility. *Biomaterials* **2008**, *29* (20), 2941–2953.
- (20) El-Sherbiny, I. M.; Yacoub, M. H. Hydrogel Scaffolds for Tissue Engineering: Progress and Challenges. *Glob. Cardiol. Sci. Pract.* **2013**, *2013* (3), 316–342.
- (21) Burdick, J. A.; Stevens, M. M. 11 - Biomedical Hydrogels. In *Biomaterials, Artificial Organs and Tissue Engineering*; Hench, L. L., Jones, J. R., Eds.; Woodhead Publishing Series in Biomaterials; Woodhead Publishing, 2005; pp 107–115.
- (22) Lee, K. Y.; Mooney, D. J. Hydrogels for Tissue Engineering. *Chem. Rev.* **2001**, *101* (7), 1869–1879.
- (23) Drury, J. L.; Mooney, D. J. Hydrogels for Tissue Engineering: Scaffold Design Variables and Applications. *Biomaterials* **2003**, *24* (24), 4337–4351.
- (24) Traphagen, S.; Yelick, P. C. Reclaiming a Natural Beauty: Whole-Organ Engineering with Natural Extracellular Materials. *Regen. Med.* **2009**, *4* (5), 747–758.

- (25) Zhu, J.; Marchant, R. E. Design Properties of Hydrogel Tissue-Engineering Scaffolds. *Expert Rev. Med. Devices* **2011**, *8* (5), 607–626.
- (26) Zhu, J. Bioactive Modification of Poly(ethylene Glycol) Hydrogels for Tissue Engineering. *Biomaterials* **2010**, *31* (17), 4639–4656.
- (27) Orban, J. M.; Wilson, L. B.; Kofroth, J. A.; El-Kurdi, M. S.; Maul, T. M.; Vorp, D. A. Crosslinking of Collagen Gels by Transglutaminase. *J. Biomed. Mater. Res. A* **2004**, *68* (4), 756–762.
- (28) Shoulders, M. D.; Raines, R. T. Collagen Structure and Stability. *Annu. Rev. Biochem.* **2009**, *78*, 929–958.
- (29) Levental, K. R.; Yu, H.; Kass, L.; Lakins, J. N.; Egeblad, M.; Erler, J. T.; Fong, S. F. T.; Csiszar, K.; Giaccia, A.; Weninger, W.; et al. Matrix Crosslinking Forces Tumor Progression by Enhancing Integrin Signaling. *Cell* **2009**, *139* (5), 891–906.
- (30) Antoine, E. E.; Vlachos, P. P.; Rylander, M. N. Review of Collagen I Hydrogels for Bioengineered Tissue Microenvironments: Characterization of Mechanics, Structure, and Transport. *Tissue Eng. Part B Rev.* **2014**, *20* (6), 683–696.
- (31) Khan, R.; Khan, M. H. Use of Collagen as a Biomaterial: An Update. *J. Indian Soc. Periodontol.* **2013**, *17* (4), 539–542.
- (32) Muthukumar, T.; Sreekumar, G.; Sastry, T. P.; Chamundeeswari, M. Collagen as a Potential Biomaterial in Biomedical Applications. *Rev. Adv. Mater. Sci.* **2018**, *53* (1), 29–39.
- (33) Wong, F. S.; Lo, A. C.-Y. Collagen-Based Scaffolds for Cell Therapies in the Injured Brain; 2015.
- (34) Kommareddy, S.; Shenoy, D. B.; Amiji, M. M. Gelatin Nanoparticles and Their Biofunctionalization. In *Nanotechnologies for the Life Sciences*; American Cancer Society, 2007.
- (35) Nikkhah, M.; Akbari, M.; Paul, A.; Memic, A.; Dolatshahi-Pirouz, A.; Khademhosseini, A. Gelatin-Based Biomaterials For Tissue Engineering And Stem Cell Bioengineering. In *Biomaterials from Nature for Advanced Devices and Therapies*; John Wiley & Sons, Ltd, 2016; pp 37–62.



- (36) Kuijpers, A. J.; Engbers, G. H.; Krijgsveld, J.; Zaat, S. A.; Dankert, J.; Feijen, J. Cross-Linking and Characterisation of Gelatin Matrices for Biomedical Applications. *J. Biomater. Sci. Polym. Ed.* **2000**, *11* (3), 225–243.
- (37) Bigi, A.; Cojazzi, G.; Panzavolta, S.; Rubini, K.; Roveri, N. Mechanical and Thermal Properties of Gelatin Films at Different Degrees of Glutaraldehyde Crosslinking. *Biomaterials* **2001**, *22* (8), 763–768.
- (38) Lee, B. H.; Shirahama, H.; Kim, M. H.; Lee, J. H.; Cho, N.-J.; Tan, L. P. Colloidal Templating of Highly Ordered Gelatin Methacryloyl-Based Hydrogel Platforms for Three-Dimensional Tissue Analogues. *NPG Asia Mater.* **2017**, *9* (7), e412–e412.
- (39) Van Den Bulcke, A. I.; Bogdanov, B.; De Rooze, N.; Schacht, E. H.; Cornelissen, M.; Berghmans, H. Structural and Rheological Properties of Methacrylamide Modified Gelatin Hydrogels. *Biomacromolecules* **2000**, *1* (1), 31–38.
- (40) Xiao, S.; Zhao, T.; Wang, J.; Wang, C.; Du, J.; Ying, L.; Lin, J.; Zhang, C.; Hu, W.; Wang, L.; et al. Gelatin Methacrylate (GelMA)-Based Hydrogels for Cell Transplantation: An Effective Strategy for Tissue Engineering. *Stem Cell Rev. Rep.* **2019**, *15* (5), 664–679.
- (41) Sun, M.; Sun, X.; Wang, Z.; Guo, S.; Yu, G.; Yang, H. Synthesis and Properties of Gelatin Methacryloyl (GelMA) Hydrogels and Their Recent Applications in Load-Bearing Tissue. *Polymers* **2018**, *10* (11).
- (42) Wen, J. H.; Vincent, L. G.; Fuhrmann, A.; Choi, Y. S.; Hribar, K. C.; Taylor-Weiner, H.; Chen, S.; Engler, A. J. Interplay of Matrix Stiffness and Protein Tethering in Stem Cell Differentiation. *Nat. Mater.* **2014**, *13* (10), 979–987.
- (43) Tse, J. R.; Engler, A. J. Preparation of Hydrogel Substrates with Tunable Mechanical Properties. *Curr. Protoc. Cell Biol.* **2010**, Chapter 10, Unit 10.16.
- (44) Kandow, C. E.; Georges, P. C.; Janmey, P. A.; Beningo, K. A. Polyacrylamide Hydrogels for Cell Mechanics: Steps Toward Optimization and Alternative Uses. In *Methods in Cell Biology*; Cell Mechanics; Academic Press, 2007; Vol. 83, pp 29–46.

- (45) Lee, J. P.; Kassianidou, E.; MacDonald, J. I.; Francis, M. B.; Kumar, S. N-Terminal Specific Conjugation of Extracellular Matrix Proteins to 2-Pyridinecarboxaldehyde Functionalized Polyacrylamide Hydrogels. *Biomaterials* **2016**, *102*, 268–276.
- (46) Yeung, T.; Georges, P. C.; Flanagan, L. A.; Marg, B.; Ortiz, M.; Funaki, M.; Zahir, N.; Ming, W.; Weaver, V.; Janmey, P. A. Effects of Substrate Stiffness on Cell Morphology, Cytoskeletal Structure, and Adhesion. *Cell Motil. Cytoskeleton* **2005**, *60* (1), 24–34.
- (47) Bassil, M.; Davenas, J.; EL Tahchi, M. Electrochemical Properties and Actuation Mechanisms of Polyacrylamide Hydrogel for Artificial Muscle Application. *Sens. Actuators B Chem.* **2008**, *134* (2), 496–501.
- (48) Zustiak, S. P.; Wei, Y.; Leach, J. B. Protein-Hydrogel Interactions in Tissue Engineering: Mechanisms and Applications. *Tissue Eng. Part B Rev.* **2013**, *19* (2), 160–171.
- (49) Hennink, W. E.; van Nostrum, C. F. Novel Crosslinking Methods to Design Hydrogels. *Adv. Drug Deliv. Rev.* **2002**, *54* (1), 13–36.
- (50) Parhi, R. Cross-Linked Hydrogel for Pharmaceutical Applications: A Review. *Adv. Pharm. Bull.* **2017**, *7* (4), 515.
- (51) Yahia, Lh.; Chirani, N.; Gritsch, L.; Motta, F. L.; SoumiaChirani; Fare, S. History and Applications of Hydrogels. *J. Biomed. Sci.* **2015**, *4* (2).
- (52) Fairbanks, B. D.; Schwartz, M. P.; Bowman, C. N.; Anseth, K. S. Photoinitiated Polymerization of PEG-Diacrylate with Lithium Phenyl-2,4,6-Trimethylbenzoylphosphinate: Polymerization Rate and Cytocompatibility. *Biomaterials* **2009**, *30* (35), 6702–6707.
- (53) Burdick, J. A.; Anseth, K. S. Photoencapsulation of Osteoblasts in Injectable RGD-Modified PEG Hydrogels for Bone Tissue Engineering. *Biomaterials* **2002**, *23* (22), 4315–4323.
- (54) Elisseeff, J.; Anseth, K.; Sims, D.; McIntosh, W.; Randolph, M.; Yaremchuk, M.; Langer, R. Transdermal Photopolymerization of Poly(ethylene Oxide)-Based Injectable Hydrogels for Tissue-Engineered Cartilage. *Plast. Reconstr. Surg.* **1999**, *104* (4), 1014–1022.

- (55) Yue, K.; Santiago, G. T.; Alvarez, M. M.; Tamayol, A.; Annabi, N.; Khademhosseini, A. Synthesis, Properties, and Biomedical Applications of Gelatin Methacryloyl (GelMA) Hydrogels. *Biomaterials* **2015**, *73*, 254–271.
- (56) Berger, J.; Reist, M.; Mayer, J. M.; Felt, O.; Peppas, N. A.; Gurny, R. Structure and Interactions in Covalently and Ionically Crosslinked Chitosan Hydrogels for Biomedical Applications. *Eur. J. Pharm. Biopharm. Off. J. Arbeitsgemeinschaft Pharm. Verfahrenstechnik EV* **2004**, *57* (1), 19–34.
- (57) Saini, K. Preparation Method, Properties and Crosslinking of Hydrogel: A Review; 2017.
- (58) Preparation and properties of CMC gel | M. Takigami | Request PDF  
[https://www.researchgate.net/publication/285474681\\_Preparation\\_and\\_properties\\_of\\_CMC\\_gel](https://www.researchgate.net/publication/285474681_Preparation_and_properties_of_CMC_gel) (accessed Jul 11, 2019).
- (59) (PDF) Hydrogels: Methods of Preparation, Characterisation and Applications  
[https://www.researchgate.net/publication/221914137\\_Hydrogels\\_Methods\\_of\\_Preparation\\_Characterisation\\_and\\_Applications](https://www.researchgate.net/publication/221914137_Hydrogels_Methods_of_Preparation_Characterisation_and_Applications) (accessed Sep 22, 2019).
- (60) Lee, K. Y.; Mooney, D. J. Alginate: Properties and Biomedical Applications. *Prog. Polym. Sci.* **2012**, *37* (1), 106–126.
- (61) (PDF) Cross-linking in hydrogels - a review  
[https://www.researchgate.net/publication/303025587\\_Cross-linking\\_in\\_hydrogels\\_-\\_a\\_review](https://www.researchgate.net/publication/303025587_Cross-linking_in_hydrogels_-_a_review) (accessed Sep 15, 2019).
- (62) Serrano-Aroca, Á. Enhancement of Hydrogels' Properties for Biomedical Applications: Latest Achievements. *Hydrogels* **2018**.
- (63) Bhadani, R.; Mitra, U. K. Synthesis and Studies on Water Swelling Behaviour of Polyacrylamide Hydrogels. *Macromol. Symp.* **2016**, *369* (1), 30–34.
- (64) Mittal, H. S.; Kaith, B. S.; Jindal, R. Synthesis, Characterization and Swelling Behaviour of Poly(acrylamide-Comethacrylicacid) Grafted Gum Ghatti Based Superabsorbent Hydrogels; 2010.

- (65) Rizwan, M.; Yahya, R.; Hassan, A.; Yar, M.; Azzahari, A. D.; Selvanathan, V.; Sonsudin, F.; Abouloula, C. N. pH Sensitive Hydrogels in Drug Delivery: Brief History, Properties, Swelling, and Release Mechanism, Material Selection and Applications. *Polymers* **2017**, *9* (4).
- (66) Gupta, N. V.; Shivakumar, H. G. Investigation of Swelling Behavior and Mechanical Properties of a pH-Sensitive Superporous Hydrogel Composite. *Iran. J. Pharm. Res. IJPR* **2012**, *11* (2), 481–493.
- (67) Tang, C.; Yin, L.; Yu, J.; Yin, C.; Pei, Y. Swelling Behavior and Biocompatibility of Carbopol-Containing Superporous Hydrogel Composites. *J. Appl. Polym. Sci.* **2007**, *104* (5), 2785–2791.
- (68) (PDF) WATER-SWELLABLE MATERIALS—APPLICATION IN SELF-HEALING SEALING SYSTEMS [https://www.researchgate.net/publication/228427543\\_WATER-SWELLABLE\\_MATERIALS-APPLICATION\\_IN\\_SELF-HEALING\\_SEALING\\_SYSTEMS](https://www.researchgate.net/publication/228427543_WATER-SWELLABLE_MATERIALS-APPLICATION_IN_SELF-HEALING_SEALING_SYSTEMS) (accessed Sep 15, 2019).
- (69) Butcher, D. T.; Alliston, T.; Weaver, V. M. A Tense Situation: Forcing Tumour Progression. *Nat. Rev. Cancer* **2009**, *9* (2), 108–122.
- (70) Canver, A. C.; Ngo, O.; Urbano, R. L.; Clyne, A. M. Endothelial Directed Collective Migration Depends on Substrate Stiffness via Localized Myosin Contractility and Cell-Matrix Interactions. *J. Biomech.* **2016**, *49* (8), 1369–1380.
- (71) Shukla, V. C.; Higueta-Castro, N.; Nana-Sinkam, P.; Ghadiali, S. N. Substrate Stiffness Modulates Lung Cancer Cell Migration but Not Epithelial to Mesenchymal Transition. *J. Biomed. Mater. Res. A* **2016**, *104* (5), 1182–1193.
- (72) Mao, A. S.; Shin, J.-W.; Mooney, D. J. Effects of Substrate Stiffness and Cell-Cell Contact on Mesenchymal Stem Cell Differentiation. *Biomaterials* **2016**, *98*, 184–191.
- (73) Moazzem Hossain, M.; Wang, X.; Bergan, R. C.; Jin, J.-P. Diminished Expression of h2-Calponin in Prostate Cancer Cells Promotes Cell Proliferation, Migration and the Dependence of Cell Adhesion on Substrate Stiffness. *FEBS Open Bio* **2014**, *4*, 627–636.

- (74) Kloxin, A.; Kloxin, C.; Bowman, C.; Anseth, K. Mechanical Properties of Cellularly Responsive Hydrogels and Their Experimental Determination. *Adv. Mater. Deerfield Beach Fla* **2010**, *22* (31), 3484–3494.
- (75) Flanagan, L. A.; Ju, Y.-E.; Marg, B.; Osterfield, M.; Janmey, P. A. Neurite Branching on Deformable Substrates. *Neuroreport* **2002**, *13* (18), 2411–2415.
- (76) Yeung, T.; Georges, P. C.; Flanagan, L. A.; Marg, B.; Ortiz, M.; Funaki, M.; Zahir, N.; Ming, W.; Weaver, V.; Janmey, P. A. Effects of Substrate Stiffness on Cell Morphology, Cytoskeletal Structure, and Adhesion. *Cell Motil.* **2005**, *60* (1), 24–34.
- (77) Zhang, T.; Lin, S.; Shao, X.; Zhang, Q.; Xue, C.; Zhang, S.; Lin, Y.; Zhu, B.; Cai, X. Effect of Matrix Stiffness on Osteoblast Functionalization. *Cell Prolif.* **2017**, *50* (3).
- (78) Wang, Z.; Tian, Z.; Menard, F.; Kim, K. Comparative Study of Gelatin Methacrylate Hydrogels from Different Sources for Biofabrication Applications. *Biofabrication* **2017**, *9* (4), 044101.
- (79) Hu, M.; Azeloglu, E. U.; Ron, A.; Tran-Ba, K.-H.; Calizo, R. C.; Tavassoly, I.; Bhattacharya, S.; Jayaraman, G.; Chen, Y.; Rabinovich, V.; et al. A Biomimetic Gelatin-Based Platform Elicits a pro-Differentiation Effect on Podocytes through Mechanotransduction. *Sci. Rep.* **2017**, *7*, 43934.
- (80) Increasing Mechanical Strength of Gelatin Hydrogels by Divalent Metal Ion Removal <https://www.ncbi.nlm.nih.gov/pmc/articles/PMC3988488/> (accessed Sep 22, 2019).
- (81) Fabrication of Hydrogels with Steep Stiffness Gradients for Studying Cell Mechanical Response <https://journals.plos.org/plosone/article?id=10.1371/journal.pone.0046107> (accessed Sep 22, 2019).
- (82) Liang, J.; Guo, Z.; Timmerman, A.; Grijpma, D.; Poot, A. Enhanced Mechanical and Cell Adhesive Properties of Photo-Crosslinked PEG Hydrogels by Incorporation of Gelatin in the Networks. *Biomed. Mater. Bristol Engl.* **2019**, *14* (2), 024102.
- (83) Hwang, J. W.; Noh, S. M.; Kim, B.; Jung, H. W. Gelation and Crosslinking Characteristics of Photopolymerized Poly(ethylene Glycol) Hydrogels. *J. Appl. Polym. Sci.* **2015**, *132* (22).

- (84) Evaluation of Physical and Mechanical Properties of Porous Poly (Ethylene Glycol)-co-(L-Lactic Acid) Hydrogels during Degradation  
<https://www.ncbi.nlm.nih.gov/pmc/articles/PMC3621899/> (accessed Sep 22, 2019).
- (85) Naahidi, S.; Jafari, M.; Logan, M.; Wang, Y.; Yuan, Y.; Bae, H.; Dixon, B.; Chen, P. Biocompatibility of Hydrogel-Based Scaffolds for Tissue Engineering Applications. *Biotechnol. Adv.* **2017**, *35* (5), 530–544.
- (86) Aurand, E. R.; Wagner, J.; Lanning, C.; Bjugstad, K. B. Building Biocompatible Hydrogels for Tissue Engineering of the Brain and Spinal Cord. *J. Funct. Biomater.* **2012**, *3* (4), 839–863.
- (87) Curtis, A.; Riehle, M. Tissue Engineering: The Biophysical Background. *Phys. Med. Biol.* **2001**, *46* (4), R47–R65.
- (88) Spatz, J. P.; Geiger, B. Molecular Engineering of Cellular Environments: Cell Adhesion to Nano-Digital Surfaces. In *Methods in Cell Biology*; Cell Mechanics; Academic Press, 2007; Vol. 83, pp 89–111.
- (89) Geiger, B.; Spatz, J. P.; Bershadsky, A. D. Environmental Sensing through Focal Adhesions. *Nat. Rev. Mol. Cell Biol.* **2009**, *10* (1), 21–33.
- (90) Levental, I.; Georges, P. C.; Janmey, P. A. Soft Biological Materials and Their Impact on Cell Function. *Soft Matter* **2007**, *3* (3), 299–306.
- (91) Georges, P. C.; Hui, J.-J.; Gombos, Z.; McCormick, M. E.; Wang, A. Y.; Uemura, M.; Mick, R.; Janmey, P. A.; Furth, E. E.; Wells, R. G. Increased Stiffness of the Rat Liver Precedes Matrix Deposition: Implications for Fibrosis. *Am. J. Physiol. Gastrointest. Liver Physiol.* **2007**, *293* (6), G1147–G1154.
- (92) Orr, A. W.; Helmke, B. P.; Blackman, B. R.; Schwartz, M. A. Mechanisms of Mechanotransduction. *Dev. Cell* **2006**, *10* (1), 11–20.
- (93) Janmey, P. A.; Weitz, D. A. Dealing with Mechanics: Mechanisms of Force Transduction in Cells. *Trends Biochem. Sci.* **2004**, *29* (7), 364–370.
- (94) Bershadsky, A. D.; Balaban, N. Q.; Geiger, B. Adhesion-Dependent Cell Mechanosensitivity. *Annu. Rev. Cell Dev. Biol.* **2003**, *19*, 677–695.

- (95) Bershadsky, A.; Kozlov, M.; Geiger, B. Adhesion-Mediated Mechanosensitivity: A Time to Experiment, and a Time to Theorize. *Curr. Opin. Cell Biol.* **2006**, *18* (5), 472–481.
- (96) Lo, S. H. Focal Adhesions: What's New inside. *Dev. Biol.* **2006**, *294* (2), 280–291.
- (97) Geiger, B.; Bershadsky, A.; Pankov, R.; Yamada, K. M. Transmembrane Crosstalk between the Extracellular Matrix--Cytoskeleton Crosstalk. *Nat. Rev. Mol. Cell Biol.* **2001**, *2* (11), 793–805.
- (98) Alberts, B.; Johnson, A.; Lewis, J.; Raff, M.; Roberts, K.; Walter, P. Integrins. *Mol. Biol. Cell 4th Ed.* **2002**.
- (99) Yao, M.; Goult, B. T.; Chen, H.; Cong, P.; Sheetz, M. P.; Yan, J. Mechanical Activation of Vinculin Binding to Talin Locks Talin in an Unfolded Conformation. *Sci. Rep.* **2014**, *4*, 4610.
- (100) Grashoff, C.; Hoffman, B. D.; Brenner, M. D.; Zhou, R.; Parsons, M.; Yang, M. H. T.; Mclean, M. A.; Sligar, S. G.; Chen, C. S.; Ha, T.; et al. Measuring Mechanical Tension across Vinculin Reveals Regulation of Focal Adhesion Dynamics. In *Nature*; 2010.
- (101) Vicente-Manzanares, M.; Ma, X.; Adelstein, R. S.; Horwitz, A. R. Non-Muscle Myosin II Takes Centre Stage in Cell Adhesion and Migration. *Nat. Rev. Mol. Cell Biol.* **2009**, *10* (11), 778–790.
- (102) Janmey, P. A.; Miller, R. T. Mechanisms of Mechanical Signaling in Development and Disease. *J Cell Sci* **2011**, *124* (1), 9–18.
- (103) Wells, R. G. The Role of Matrix Stiffness in Regulating Cell Behavior. *Hepatology* **2008**, *47* (4), 1394–1400.
- (104) Park, J. S.; Chu, J. S.; Tsou, A. D.; Diop, R.; Tang, Z.; Wang, A.; Li, S. The Effect of Matrix Stiffness on the Differentiation of Mesenchymal Stem Cells in Response to TGF- $\beta$ . *Biomaterials* **2011**, *32* (16), 3921–3930.
- (105) Engler, A. J.; Sweeney, H. L.; Discher, D. E.; Schwarzbauer, J. E. Extracellular Matrix Elasticity Directs Stem Cell Differentiation. *J. Musculoskelet. Neuronal Interact.* **2007**, *7* (4), 335.

- (106) Georges, P. C.; Miller, W. J.; Meaney, D. F.; Sawyer, E. S.; Janmey, P. A. Matrices with Compliance Comparable to that of Brain Tissue Select Neuronal over Glial Growth in Mixed Cortical Cultures. *Biophys. J.* **2006**, *90* (8), 3012–3018.
- (107) Paszek, M. J.; Zahir, N.; Johnson, K. R.; Lakins, J. N.; Rozenberg, G. I.; Gefen, A.; Reinhart-King, C. A.; Margulies, S. S.; Dembo, M.; Boettiger, D.; et al. Tensional Homeostasis and the Malignant Phenotype. *Cancer Cell* **2005**, *8* (3), 241–254.
- (108) Tandon, R.; Levental, I.; Huang, C.; Byfield, F. J.; Ziembicki, J.; Schelling, J. R.; Bruggeman, L. A.; Sedor, J. R.; Janmey, P. A.; Miller, R. T. HIV Infection Changes Glomerular Podocyte Cytoskeletal Composition and Results in Distinct Cellular Mechanical Properties. *Am. J. Physiol.-Ren. Physiol.* **2007**, *292* (2), F701–F710.
- (109) Wyss, H. M.; Henderson, J. M.; Byfield, F. J.; Bruggeman, L. A.; Ding, Y.; Huang, C.; Suh, J. H.; Franke, T.; Mele, E.; Pollak, M. R.; et al. Biophysical Properties of Normal and Diseased Renal Glomeruli. *Am. J. Physiol. - Cell Physiol.* **2011**, *300* (3), C397–C405.
- (110) The role of matrix stiffness in regulating cell behavior. - PubMed - NCBI  
<https://www.ncbi.nlm.nih.gov/pubmed/18307210> (accessed Mar 8, 2019).
- (111) Li, Z.; Dranoff, J. A.; Chan, E. P.; Uemura, M.; Sévigny, J.; Wells, R. G. Transforming Growth Factor-Beta and Substrate Stiffness Regulate Portal Fibroblast Activation in Culture. *Hepatology. Baltim. Md* **2007**, *46* (4), 1246–1256.
- (112) Miner, J. H. Glomerular Basement Membrane Composition and the Filtration Barrier. *Pediatr. Nephrol. Berl. Ger.* **2011**, *26* (9), 1413–1417.
- (113) Pozzi, A. Diseased Renal Glomeruli Are Getting Soft. Focus on “Biophysical Properties of Normal and Diseased Renal Glomeruli.” *Am. J. Physiol. - Cell Physiol.* **2011**, *300* (3), C394–C396.
- (114) Pavenstädt, H.; Kriz, W.; Kretzler, M. Cell Biology of the Glomerular Podocyte. *Physiol. Rev.* **2003**, *83* (1), 253–307.
- (115) Nielsen, J. S.; McNagny, K. M. The Role of Podocalyxin in Health and Disease. *J. Am. Soc. Nephrol.* **2009**, *20* (8), 1669–1676.
- (116) 3D CO-CULTURE OF PODOCYTES & ENDOTHELIAL CELLS. *Knowledgeshare*.



- (117) Miner, J. H. Focusing on the Glomerular Slit Diaphragm. *Am. J. Pathol.* **2002**, *160* (1), 3–5.
- (118) Doné, S. C.; Takemoto, M.; He, L.; Sun, Y.; Hultenby, K.; Betsholtz, C.; Tryggvason, K. Nephric Is Involved in Podocyte Maturation but Not Survival during Glomerular Development. *Kidney Int.* **2008**, *73* (6), 697–704.
- (119) Li, X.; He, J. C. An Update: The Role of Nephric inside and Outside the Kidney. *Sci. China Life Sci.* **2015**, *58* (7), 649–657.
- (120) Cooper, M. E.; Mundel, P.; Boner, G. Role of Nephric in Renal Disease Including Diabetic Nephropathy. *Semin. Nephrol.* **2002**, *22* (5), 393–398.
- (121) Lahdenperä, J.; Kilpeläinen, P.; Liu, X. L.; Pikkariainen, T.; Reponen, P.; Ruotsalainen, V.; Tryggvason, K. Clustering-Induced Tyrosine Phosphorylation of Nephric by Src Family Kinases. *Kidney Int.* **2003**, *64* (2), 404–413.
- (122) Verma, R.; Wharram, B.; Kovari, I.; Kunkel, R.; Nihalani, D.; Wary, K. K.; Wiggins, R. C.; Killen, P.; Holzman, L. B. Fyn Binds to and Phosphorylates the Kidney Slit Diaphragm Component Nephric. *J. Biol. Chem.* **2003**, *278* (23), 20716–20723.
- (123) Li, H.; Lemay, S.; Aoudjit, L.; Kawachi, H.; Takano, T. SRC-Family Kinase Fyn Phosphorylates the Cytoplasmic Domain of Nephric and Modulates Its Interaction with Podocin. *J. Am. Soc. Nephrol. JASN* **2004**, *15* (12), 3006–3015.
- (124) Martin, C. E.; Jones, N. Nephric Signaling in the Podocyte: An Updated View of Signal Regulation at the Slit Diaphragm and Beyond. *Front. Endocrinol.* **2018**, *9*.
- (125) Boute, N.; Gribouval, O.; Roselli, S.; Benessy, F.; Lee, H.; Fuchshuber, A.; Dahan, K.; Gubler, M. C.; Niaudet, P.; Antignac, C. NPHS2, Encoding the Glomerular Protein Podocin, Is Mutated in Autosomal Recessive Steroid-Resistant Nephrotic Syndrome. *Nat. Genet.* **2000**, *24* (4), 349–354.
- (126) Roselli, S.; Gribouval, O.; Boute, N.; Sich, M.; Benessy, F.; Attié, T.; Gubler, M.-C.; Antignac, C. Podocin Localizes in the Kidney to the Slit Diaphragm Area. *Am. J. Pathol.* **2002**, *160* (1), 131–139.

- (127) Li, C.; Ruotsalainen, V.; Tryggvason, K.; Shaw, A. S.; Miner, J. H. CD2AP Is Expressed with Nephrin in Developing Podocytes and Is Found Widely in Mature Kidney and Elsewhere. *Am. J. Physiol. Renal Physiol.* **2000**, *279* (4), F785–F792.
- (128) Schiffer, M.; Mundel, P.; Shaw, A. S.; Böttinger, E. P. A Novel Role for the Adaptor Molecule CD2-Associated Protein in Transforming Growth Factor- $\beta$ -Induced Apoptosis. *J. Biol. Chem.* **2004**, *279* (35), 37004–37012.
- (129) Chan, A. C. Rituximab's New Therapeutic Target: The Podocyte Actin Cytoskeleton. *Sci. Transl. Med.* **2011**, *3* (85), 85ps21–ps85ps21.
- (130) Jansen, K.; Schuurmans, C. C. L.; Jansen, J.; Masereeuw, R.; Vermonden, T. Hydrogel-Based Cell Therapies for Kidney Regeneration: Current Trends in <sup>[[L]]</sup><sub>SEP</sub> Biofabrication and In Vivo Repair. *Curr. Pharm. Des.* **2017**, *23* (26), 3845–3857.
- (131) Embry, A. E.; Mohammadi, H.; Niu, X.; Liu, L.; Moe, B.; Miller-Little, W. A.; Lu, C. Y.; Bruggeman, L. A.; McCulloch, C. A.; Janmey, P. A.; et al. Biochemical and Cellular Determinants of Renal Glomerular Elasticity. *PLOS ONE* **2016**, *11* (12), e0167924.



## Chapter II: Materials and Methods



This chapter is devoted to the presentation of the materials and the experimental methods used in this research study.

## **I. Materials:**

Since the aim of this thesis is to investigate the effect of polymers based hydrogels on cells behaviors such as cells adhesion, proliferation and differentiation, the materials used to study the mechanical and biological properties of the hydrogels and the cells respectively will be represented.

### **1. Fabrication of Hydrolyzed Polyacrylamide Hydrogels:**

#### **a. Fabrication of Polyacrylamide Gels:**

Acrylamide monomer (AAM, Sigma Aldrich, A8887, 79-06-1, purity >99%) and *N, N'*-Methylenbisacrylamide crosslinker (Bis-acrylamide, Sigma Aldrich, M7279, 110-26-9 purity >99.5%) aqueous solutions having concentrations of 30 wt % and 2 wt % respectively were prepared and used. The free radical polymerization reaction is initiated by Ammonium Persulfate (APS, 25 wt %, Sigma Aldrich, 248614, 7727-54-0, purity >98%) and catalyzed by *N, N, N', N'* Tetramethylethylenediamine (TEMED, Sigma Aldrich, T7024, 110-18-9) (Fig.1).

Six PAAm gels having different crosslinking densities were prepared by mixing 1 ml of AAM, 1  $\mu$ l of APS and 1  $\mu$ l TEMED to different Bis-acrylamide concentrations (0.5, 1, 2, 5, 10 and 30  $\mu$ l). After mixing, the gel solution was poured into a rectangular rubbery mold (6 cm x 2 cm x 0.8 cm) sandwiched between 2 glass slides and left for 3 hours at room temperature to achieve polymerization.

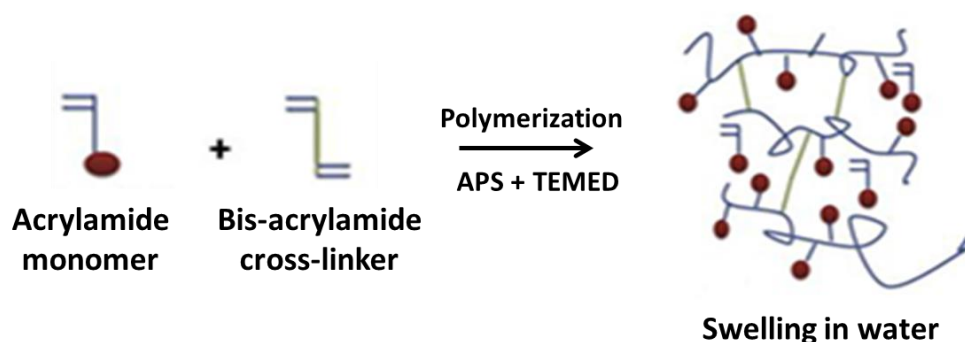


Figure 1: PAAm hydrogels polymerization

### b. From Gel to Hydrogel: Hydrolysis and Swelling:

After complete polymerization, PAAm gel layers were gently removed from the mold and soaked overnight in a basic solution of sodium hydroxide (1 M) (NaOH, Sigma Aldrich, S8045, 1310-73-2, purity > 98 %) to hydrolyze the PAAm gel. The hydrolysis reaction converts the amine moieties ( $\text{R-NH}_2$ ) of the PAAm network chains into carboxylate ( $-\text{COO}^-$ ) moieties that are characterized by their high affinity for water. The hydrolyzed gel layers were then placed in deionized water (DW, MilliQ, conductivity higher than 18 M $\Omega$ ) that was repeatedly changed for seven days until the equilibrium swelling was reached (Fig.2). The resulting fully swelled hydrogel layers were gently removed and placed in an excessive amount of complete cell medium that was repeatedly changed until reaching a new equilibrium.

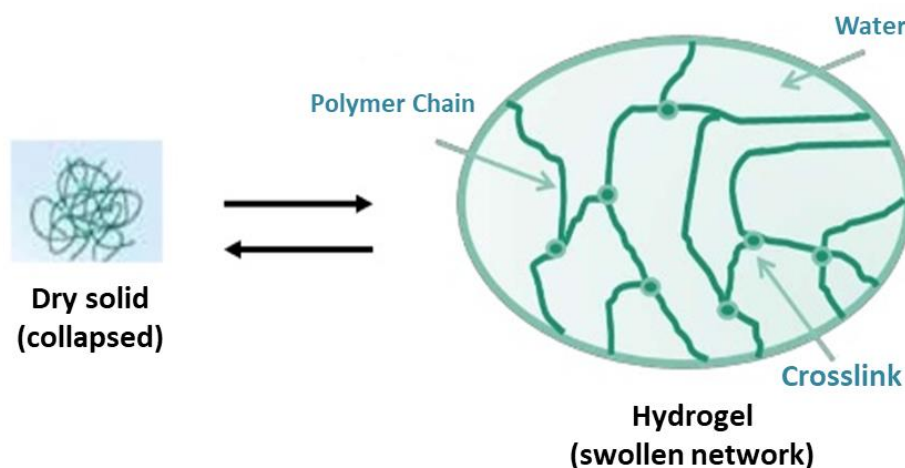


Figure 2: Reversible network swelling and shrinking with solvent

## 2. Synthesis of Gelatin Methacrylamide(GelMA):

Gelatin Methacrylamide was prepared by the reaction of gelatin with methacrylic anhydride depending on previous described methods<sup>1</sup> (Fig.3). Briefly, 5g of gelatin (Gelatin from Porcine Skin, Sigma Aldrich, 48722) was dissolved in 45ml of phosphate buffer saline (PBS, Sigma Aldrich, P4417) at 60°C. After gelatin dissolution, 1ml of Methacrylic anhydride (MA, Sigma Aldrich, 276685) was gently added to gelatin solution with a vigorous stirring for 3hrs at 60°C. Afterwards, the mixture was dialyzed for 7 days against distilled water at 40°C using dialysis bags with a molecular weight of 12-14 kDa and water was changed regularly. Finally, the product solution was stored at -20°C for overnight and then freeze-dried for 7 days.

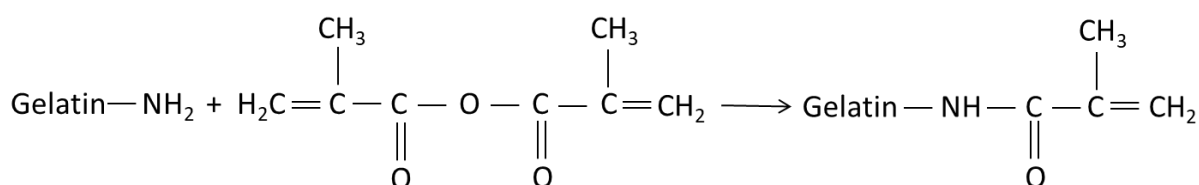


Figure 3: Synthesis of GelMA



### 3. Preparation of GelMA-AAm hydrogels:

The GelMA-acrylamide hydrogels were prepared by mixing acrylamide (AAm, Sigma Aldrich, A8887, 79-06-1, purity >99%) (5% (w/v) and 2.5% (w/v): AAm concentrations) with GelMA solutions (5% (w/v) and 3% (w/v): GelMA concentrations). This reaction was initiated using Ammonium Persulfate (APS, 25% (w/v), Sigma Aldrich, 248614, 7727-54-0, purity > 98%) and catalyzed using *N,N,N',N'* Tetramethylethylenediamine (TEMED, Sigma Aldrich, T7024, 110-18-9). The solution mixture was poured in glass molds and the polymerization will be achieved at room temperature for 3hrs. The material was washed with distilled water to ensure the unreacted elements removal.

### 4. Swelling Measurement:

After reaching the equilibrium swelling degree in DW and cell media, the swelling degree was measured. It is defined as the ratio of the network weight in the swollen state over the dry state. (Equation 1)

$$S = \frac{W_s - W_d}{W_d} \quad (1)$$

Where  $W_s$  and  $W_d$  are the weight of a fully swollen (in equilibrium with DW and cell media) and dehydrated hydrogels respectively. Measurements were repeated 3 times.

### 5. Cell Culture:

Human podocytes cell line was purchased from the Faculty of Medicine, University of Bristol, UK. Immortalized human podocytes were cultured on flasks according to the supplier protocol<sup>2</sup>. Podocytes cells were cultured in RPMI – 1640 Medium (Sigma Aldrich, R8758) supplemented with 1 % insulin-transferrin-Selenium liquid media supplement (Sigma Aldrich,

I3146), 10 % fetal bovine serum (Sigma Aldrich, F7524) and Penicillin Streptomycin solution (Sigma Aldrich, P4333). Proliferation was induced when the cells were incubated at 33°C and differentiation was induced by incubating the cells at 37°C. After proliferation, cells were plated on the hydrogel substrates having various mechanical properties. The substrates were coated with collagen type I (Sigma Aldrich, C3867, 9007-34-5) using EDC (Sigma Aldrich, E6383, 25952-53-8) and NHS (Sigma Aldrich, 130672, 6066-82-6) which crosslink with the carboxylic group.

## **6. Immunocytochemical characterization:**

Podocyte cells cultured on hydrogels for 7 days were fixed with 2% of paraformaldehyde (PFA) (Sigma Aldrich, P6148, 30525-89-4) for 15min at room temperature. Then, cell permeabilization was performed using 0.5 % Triton X-100 (Sigma Aldrich, X100, 9002-93-1) for 15 minutes into the incubator (37°C). Afterwards, the non-specific protein binding sites were blocked with 1 % of Bovine Serum Albumin (BSA) (Sigma Aldrich, A2153, 9048-46-8) and 0.5% of Triton-X in PBS during overnight at 4°C. Cells were then incubated overnight at 4°C with a primary anti-podocin antibody (Sigma Aldrich, P0372). The samples were then rinsed with PBS and incubated with secondary anti-rabbit antibody (Alexa Fluor®594, Cat: ab150080) for 1 hour in dark at room temperature. Nucleus and actin cytoskeleton staining were done with DAPI (Sigma Aldrich, D9542) and Phalloidin staining (Invitrogen, Cat: A12379), which were applied for 0.3 – 1 hours in dark at room temperature. Image acquisition was achieved using Nikon TE2000 microscope.

## **7. Cell Proliferation Assay:**

MTT (3-(4, 5-dimethylthiazol-2-yl)-2, 5-diphenyltetrazoliumbromide) test was used to evaluate podocyte cells proliferation. After 5 days of culture on hydrogels, 1mg/ml MTT solution (Sigma Aldrich, M5655, 298-93-1) was added to cells and incubated for 3h at 37°C. MTT solution was carefully descanted and replaced by Isopropanol (Sigma Aldrich, I9516, 67-63-0) to dissolve the violet formazan crystals. After 1 hour incubation at room temperature in the dark, the luminescent signals provided by MTT assay were detected and cell proliferation was determined by normalizing each luminescent signal from cells cultured on gels over cells cultured without gel (control).

## **8. Western Blot:**

Cells were lysed in 100 µL of RIPA buffer (150mM NaCl, 5mM EDTA pH8, 50mM Tris-HCl pH8, 1% IGEPAL, 0.35% Sodium deoxycholate, 0.1% SDS, 1X of protease inhibitor mix). Total protein concentration was measured using the Bradford assay with Bovine Serum Albumin (BSA) and a protein standard. Equal protein amounts were used for immunoblotting. Proteins were fractionated by gradient (7-20%) SDS-polyacrylamide gel electrophoresis, and then transferred onto PVDF membranes (Immobilon). The membranes were then blocked overnight at 4°C in PBS containing 10% non-fat dry milk and 0.1% Tween 20. Primary antibodies (podocin) were added for 2 hours at room temperature and secondary antibody (mouse anti-rabbit from Santa Cruz Biotechnology L0617) for 1 hour also at room temperature. Proteins were detected using an HRP substrate (Immobilon Forte, Millipore, WBLUF0500).

## **II. Experimental Methods:**

The experimental methods used for this purpose are described in this section.

### **1. Conventional Scanning Electron Microscopy (CSEM):**

Scanning electron microscopy (SEM) technique utility is to detect and to visualize the morphology and structure of materials with a high resolution. This technique is characterized by the application of a highly energy electron beam on the sample surface which detect the transmitted signals as secondary electrons signals indispensable to determine the morphology and the topography of the sample. For SEM images analysis, the samples must be dried and conductive or coated with a conducting material such as gold for proper analysis. Furthermore, the analysis must be performed under high vacuum conditions. Coating procedure reduces beam penetration and allows for a sharper image; however it may mask elements of interest for X-ray analysis<sup>3</sup>. The SEM images were managed with SEM ZEISS EVO HD15 (Fig. 4) using LaB6 as a microscope tip and the images resolution were taken at 10Kv. For SEM images, the samples were placed in liquid nitrogen (-197°C) for 4h and subsequently lyophilized. The freeze dried samples were processed in a vacuum system (LABCONCO®, FreeZone 4.5) at 0.02mBar and -54°C for overnight. The dried samples were gold sputter-coated to be analyzed. Furthermore, the SEM images for podocyte adherent cells were performed. Podocyte cells were fixed with 2% of paraformaldehyde (PFA) and then washed with increased concentration of ethanol (10%, 30%, 50%, 70% and 100% ethanol). Afterward, the treated samples were immersed in Hexamethyldisilasane (HDMS) and when the evaporation of HDMS is complete, the samples will be ready for sputter coating to be analyzed.



**Figure 4: Conventional Scanning Electron Microscopy**

## **2. Environmental Scanning Electron Microscopy (ESEM):**

Environmental scanning electron microscopy (ESEM) system is an imaging technique used to study the uncoated and hydrated biological or synthetic materials characterization. These materials are examined with an electron beam in a high pressure atmosphere of water vapor. For ESEM mode, the column is under high vacuum and the specimen chamber is at higher pressures of 0.1 to 30 Torr (4000 Pa). The ESEM microstructure analysis is occurred by Gaseous Secondary Electron Detector (GSED). GSED is a detection system of secondary electron which visualizes the topography images of the detected sample. The resolution provided by this technique is lower than the conventional SEM. The Quanta 200 FEG Scanning Electron Microscope is a versatile, high-performance instrument with three modes (high vacuum, low vacuum and ESEM) to accommodate the widest range of samples of any SEM system. The Quanta 200 FEGSEM system is optimized as a dedicated OIM (Orientation imaging by Electron Backscatter Diffraction) microscope<sup>4</sup>(Fig.5).

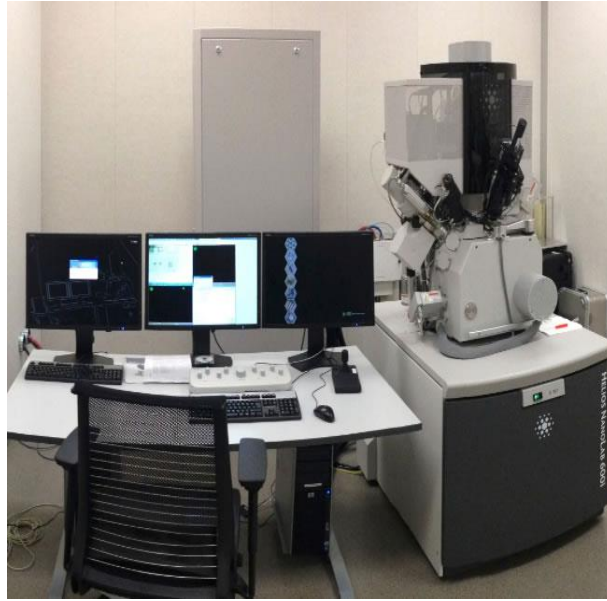
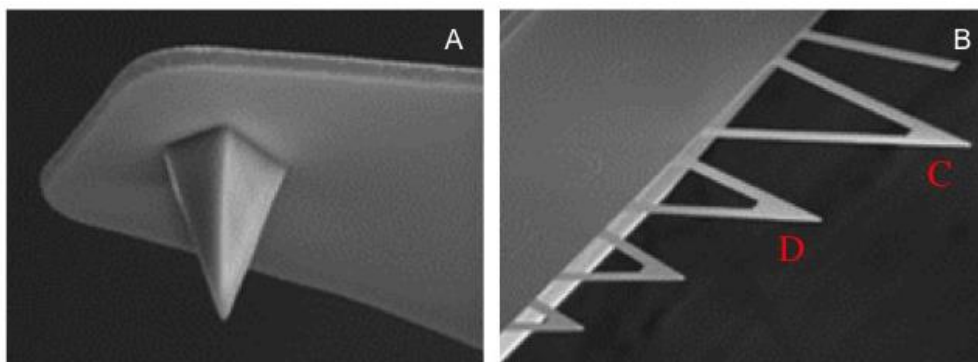


Figure 5: Environmental Scanning Electron Microscopy

### 3. Atomic Force Microscopy (AFM):

Atomic Force Microscopy, a highly resolution scanning probe microscopy type, is an indispensable tool in biological science due to its ability in recording topographic maps of sample surface (in air and liquid with sub-angstrom (in Z) and nanometer resolution (in X and Y, more than 1000 times better than the optical diffraction limit) and in measuring forces with pico-Newton precision. The information is gathered by "touching" the surface with a mechanical probe, known as tip (Fig.6). Piezoelectric elements facilitate tiny but very accurate movements enabling precise scanning.



**Figure 6: Tip (A) and cantilever (B) schematics of the MLCT tips (noted as C and D) used in our work (© Bruker AFM Probe).**

AFM has three major abilities: force measurement, imaging, and manipulation. The AFM consists of a cantilever with a sharp tip at its end that is used to scan the sample surface. The cantilever is typically made of silicon or silicon nitride with a tip radius of curvature on range of nanometers. When the tip is approached to the sample surface, forces between the tip and the sample lead to a deflection of the cantilever according to Hooke's law. The AFM can be operated in a number of modes (Fig.7). In general, possible imaging modes are divided into contact modes and "tapping" modes where the cantilever is vibrated or oscillated at a given frequency<sup>5</sup>.

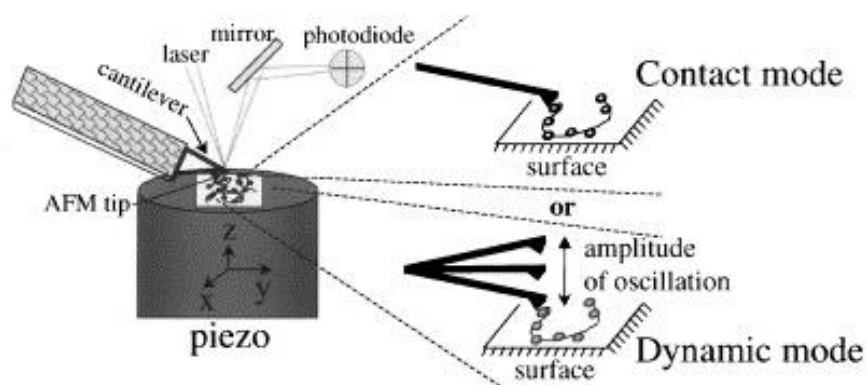


**Figure 7: Principle of the AFM imaging modes<sup>6</sup>**

The main AFM application (besides imaging) is force spectroscopy, the direct measurement of tip-sample interaction forces (known as force-distance curves). For this method, the AFM

tip is approached to and retracted from the surface as the deflection of the cantilever is controlled by the piezoelectric displacement (Fig.8). This thesis is concerned mainly with force spectroscopy, in order to measure the mechanical properties of the sample, such as the sample's Young's modulus.

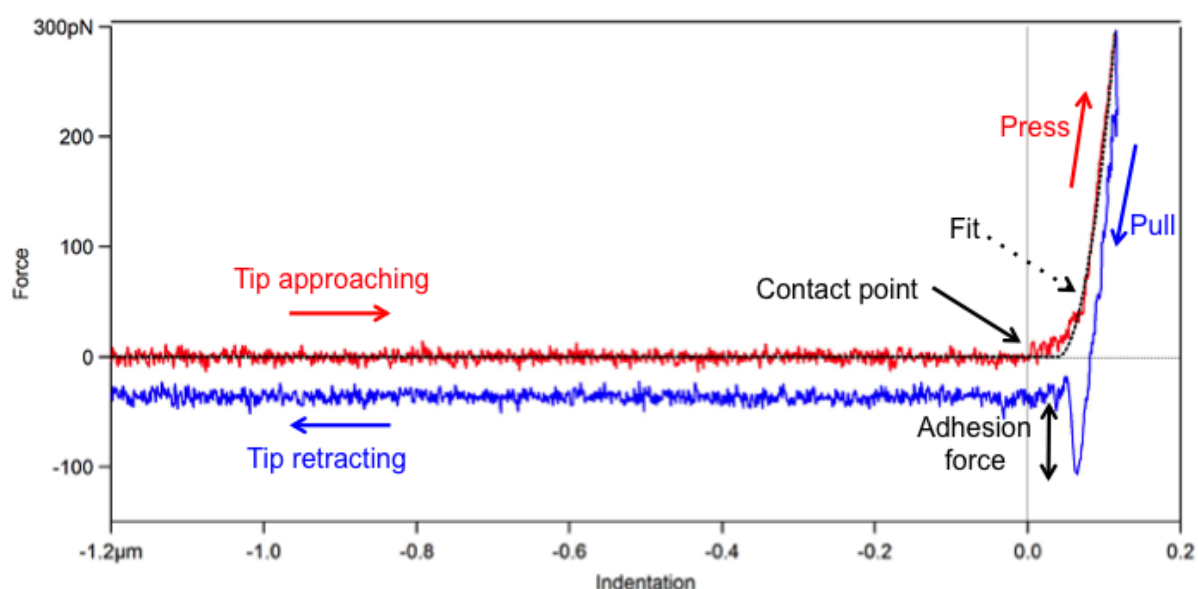


**Figure 8: Typical force-curve as a function of sample indentation showing the contact point between the tip and the sample and the fit performed to calculate the Young's modulus.**

The AFM experimental system used for force-spectroscopy measurements was an Asylum MFP-3D head coupled to a Molecular Force Probe 3D controller (Asylum Research, Santa Barbara, CA, USA). Triangular silicon nitride cantilevers C and D (MLCT, Veeco) with a nominal spring constant of 10 pN/nm, length of 310  $\mu\text{m}$ , width of 20 nm, resonance frequency of 7 kHz, and a nominal spring constant of 30 pN/nm, length of 225  $\mu\text{m}$ , width of 20 nm, resonance frequency of 15 kHz, respectively, and half-opening angle of  $\sim 19^\circ$  were used. The cantilever spring constant was determined using the thermal noise method available within the MFP-3D software.



The thermal noise procedure allows calculating either the spring constant or the inverse optical lever sensitivity (expressed in nanometers/volts), depending on the calibration option chosen. The spring constant is calculated fitting the thermal data (thermal DC, thermal Q, and thermal Frequency) after a successful fitting of the simple harmonic oscillator (SHO) equation. The thermal DC is one of the parameters that control what the SHO fit looks like, indicating how much the cantilever moves at DC from the drive that is applied to it. Thermal Q is the quality factor of the SHO peak, obtained by dividing the resonant frequency by the width of the peak at half the amplitude. Finally, the thermal frequency is the resonant frequency of the cantilever.

Hydrogel samples were glued to a Petridish with double-faced adhesive tape, and covered with 0.5 ml of deionized water. After testing a range of loading forces on the hydrogel surface, the measurements were performed in liquid at room temperature with a maximum loading force of 5nN corresponding to a maximal indentation depth of 0.3  $\mu\text{m}$ . Elastic deformation was obtained from the recorded force curves as a function of the loading force applied by the tip. Young's modulus (E) was calculated for each force from the approaching part of the curve, using the Hertz model, modified by Sneddon<sup>7</sup>.

The Hertz model was chosen to fit the force-distance curves since it has been one of the simplest and most widely used models to quantify the mechanical properties of biological samples<sup>8</sup>. This theoretical model approximates the sample as an isotropic and linear elastic solid occupying an infinitely extending half space and it assumes that the indenter is not deformable and that there are no additional interactions between indenter and sample. The Sneddon mechanical modification describes the special geometry of the indenter (conical in our case). The approach part of the force-curve is composed of two distinct processes: before tip-sample contact, it is a straight line, after reaching contact point behaves as a

second order polynomial. Preliminary analysis performed to check the order of the polynomial the curve undergoes after tip-sample contact demonstrated the behavior of second order polynomial. Assuming these features, the contact point was determined by the software where the difference between the recorded data and a theoretical curve is minimal. The latter was composed of a line and a second order polynomial, before and after the contact point, respectively. Evaluation at each piezo step along the vertical distance results in an error function, which has a local minimum at the real contact point. The error for each piezo step is calculated as a mean squared difference between the recorded data and the fitted double component curve. The correlation coefficient of theoretical and recorded data at contact point, was over  $R = 0.99$ . Smaller values than  $R = 0.95$  were not accepted, and not included in the results.

An approach velocity of  $6 \mu\text{m/s}$  was chosen, indicating a piezo-extension rate of 3 Hz to minimize hydrodynamic and viscoelastic artifacts<sup>9</sup>. The Poisson's ratio of the cells was assumed to be 0.5, as suggested for incompressible materials<sup>10</sup>. Furthermore, to investigate cells' nanomechanical properties on each sample, we repeated the force spectroscopy experiment using the same preparation's procedures and parameters.

#### **4. Fluorescence Microscopy and Immunocytochemical characterization:**

Fluorescence microscopy depends on the fluorescence or phosphorescence of components within a specimen or the addition of selective fluorescent probes (fluorophores). Both intrinsic and added fluorophores are excited with light of a specific wavelength and, if the fluorophores have been adequately chosen, their emission can be easily differentiated from the dark background.

Light emission through fluorescence is nearly simultaneous with the absorption of the excitation light due to the relatively short time delay between photon absorption and emission (less than a  $\mu\text{s}$  in duration). If emission persists longer after the excitation light has been extinguished, the phenomenon is known as phosphorescence.

Fluorescence microscopy uses a high intensity light source to excite the fluorescence specimen, which in turn emits light at longer wavelengths. Therefore, energy is absorbed by an atom that becomes excited, then the electron jumps to a higher energy level and subsequently the electron drops back to the ground state, emitting a photon of a lower energy (Fig.9).

The basic function of a fluorescence microscope is to irradiate the specimen with a desired and specific band of wavelengths, and then to separate the much weaker emitted fluorescence from the excitation light. In a properly configured microscope, only the emission light should reach the eye or detector so that the resulting fluorescent structures are superimposed with high contrast against a very dark or black background. The limits of detection are generally governed by the darkness of the background, and the excitation light is typically several hundred thousand to a million times brighter than the emitted fluorescence.

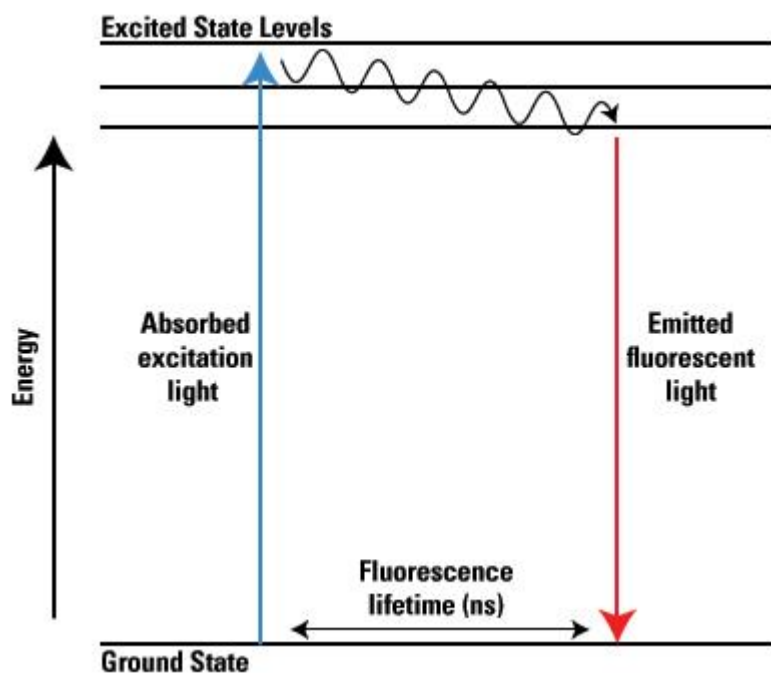


Figure 9: Energy diagram describing the excitation and emission states<sup>11</sup>

The schema presented in Fig.10 shows the main components of a fluorescence microscope. Usually, a mercury lamp is the source of excitation light. The microscope disposes of two filters: one that lets through only excitation radiation with the specific wavelength to match the fluorescing specimen and a second one that separates the specific wavelength of emission from the surrounding radiation.

In this work, a Nikon Eclipse TE 2000-E, equipped with a mercury lamp HG 100W. Images were recorded with a camera using three plan fluor (10X, 20X and 40X objectives). Two FITC filters (380-420 and 465-495 nm) were used to detect the DAPI and Phalloidin fluorophores, respectively.

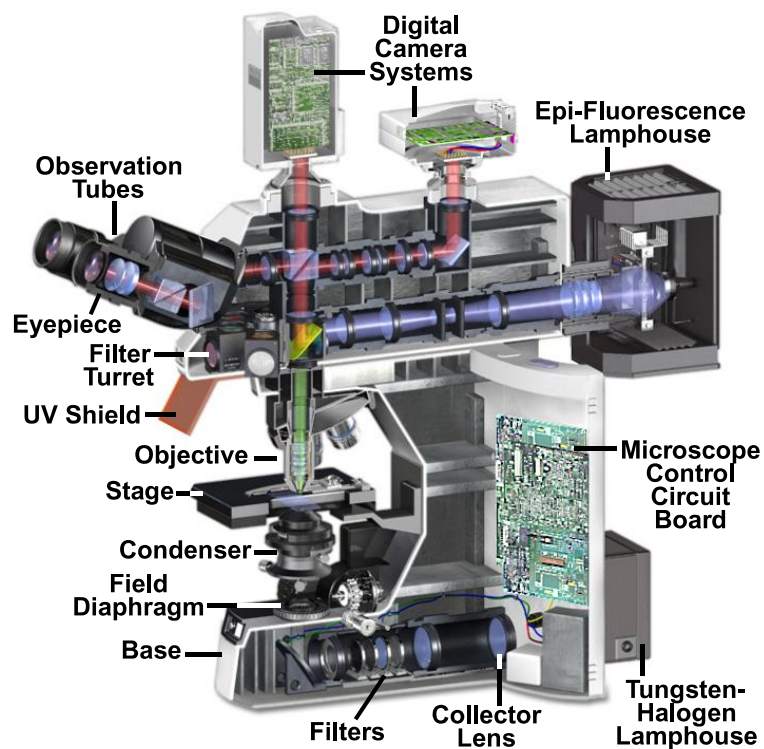


Figure 10: Epi- fluorescence microscope set-up<sup>12</sup>

## 5. Multiphoton Microscopy (MPM):

Multiphoton microscopy is an ideal method for imaging deeply into biological samples with micron resolution in three dimensions. Non-linear phenomena also can provide useful information of the structure and optical properties of a specimen.

Multiphoton excitation occurs when two (or more) photons are absorbed simultaneously leading to the emission of fluorescence (2PEF) and/or generation of second or third harmonic (SHG, THG), contrary to 1 photon excitation that results in the fluorescent excitation of a fluorescent specimen (Fig.11)

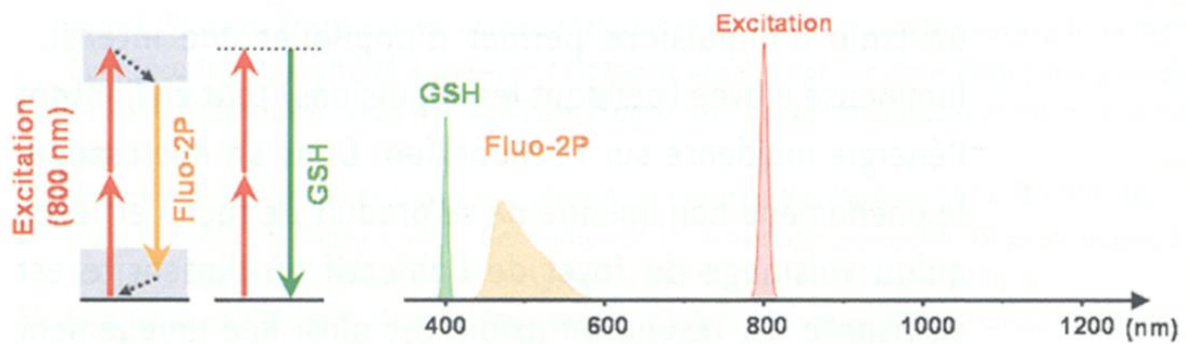


Figure 11: Mechanisms of two-photon excited fluorescence (Fluo-2P)<sup>13</sup>.

The excitation using near-infrared wavelengths allows excellent depth penetration (~400nm). The probability of 2PEF and SHG depends on the square of the light intensity, however the cross-section for excitation to take place is low and hence a high photon flux is required: the excitation is confined to a point like volume within the sample (Fig.12)

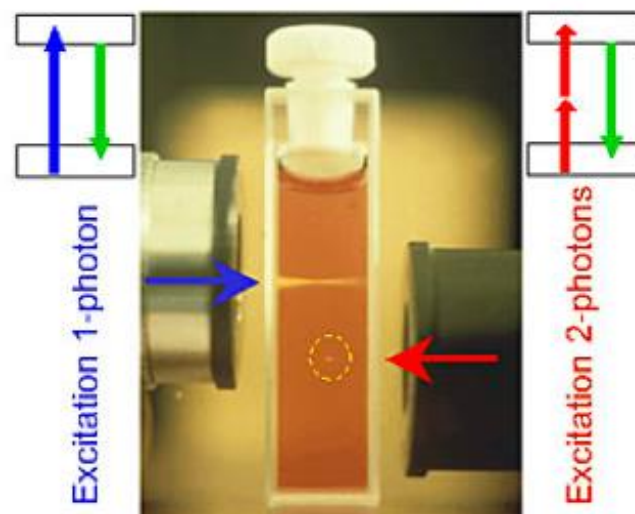


Figure 12: Confinement of the 2P excitation to a point like volume (© Cornell University)

The good light confinement in the focal point of the laser (Titanium Sapphire, 100fs) provides an excellent intrinsic optical sectioning of the sample.

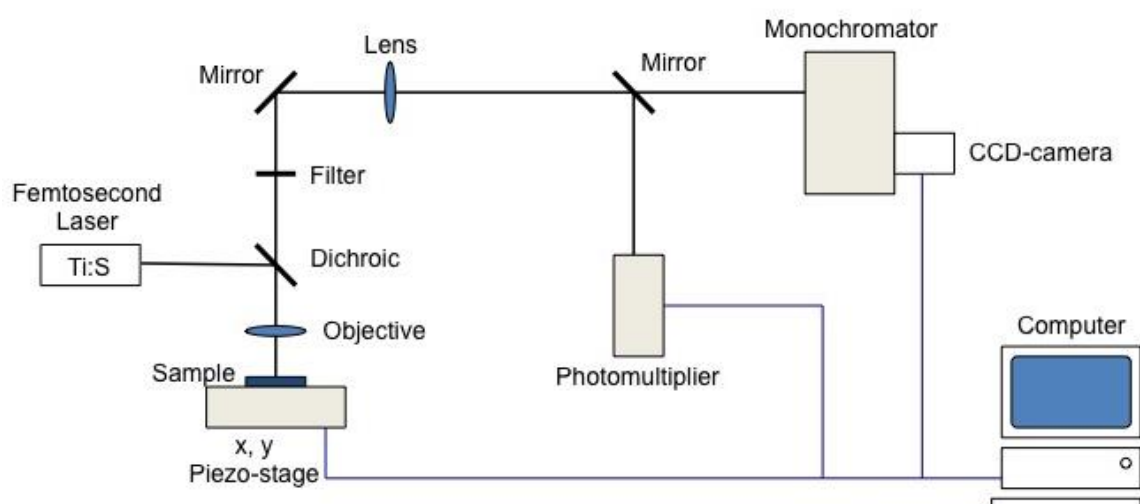


Figure 13: Basic modular components of the multiphoton microscope.

In my thesis work, and in order to record high-resolution images of cells, these were scanned with a custom-built multiphoton microscope based (Fig.13) on a SliceScope upright microscope (MPSS-1000P) equipped with a Multiphoton Scan Head (MP-2000), both from Scientifica LTD. For sample excitation, a Spectra-Physics Tsunami Ti-Sapphire laser operated in pulsed mode was used (wavelength range 760 to 900nm, typically 870 nm, repetition rate 80 MHz and pulse duration  $\sim 100$  fs). The laser beam was focused on the sample via a Nikon CFI75 LWD-16x-W objective (NA 0.8, water immersion). MPM images were created by laser raster scanning the sample. The two photon excited fluorescence signal was epi-collected through the objective.

## 6. Rheology:

Rheology is a technique using for the deformation of viscoelastic materials under stress and strain. Rheology study permits to determine the viscoelastic properties of materials by measuring the complex shear modulus. Viscoelastic materials exhibit both elastic and viscous behaviors, and have the capacity to store and lose energy when it is under small

deformations. The Rheometer applies a harmonic oscillatory torque to the polyacrylamide sample in order to measure the viscoelastic properties.

$G'$ , known as the storage modulus, represents the measurement of the storage elastic energy.  $G''$ , known as the loss modulus, determines the mechanical energy lost by the gel due to the viscous forces acting on it. Finally, the ratio  $G''/G'$  quantifies the balance between energy loss and storage, so it determines the degree of viscoelasticity of the gel.

In our study, the polyacrylamide gels were tested in 3 distinct methods in order to ensure linear viscoelastic properties of the samples. These rheometer methods were Frequency sweep, time sweep, and strain sweep.

- A strain sweep measurement was done by applying a fixed frequency of 1Hz over a range of increasing stress or strain amplitude. This test was used to detect the region of linear viscoelastic response. Using 0.1% - 100% as a range of strain amplitude shows a linear response for numerous samples. It signifies that the Rheometer is accurately characterizing the properties of the polyacrylamide gel. In addition, obtaining a non-linear region indicates that the gel was slipping or breaking down.
- A frequency sweep measurement was used to detect the response of the gels to different frequencies. This test was involved by applying low strain of 5% over a range of frequencies (0.1 – 10 Hz). The obtained results show that the complex modulus is linear at lower frequencies. At higher ones, an increase in the complex modulus was shown, which means that the machine is not able to detect the viscoelastic properties of the gel material; it is just measuring the motion of the parallel plate system. That's why all tests must be run at a lower frequency. Finally, it was indicated that all gels must be detected at a frequency of 1Hz because this value is in the middle of the linear range.



- A time sweep measurement was used to determine the stability of the polyacrylamide gels by applying a constant frequency of 1Hz and strain of 5%. The results demonstrate that the modulus remains linear for 5min before increasing. The linear range proves that the hydrogels will not be altered within the first 5min of being removed from the media. After that, the increasing of modulus indicates that the samples start to dehydrate. As the hydration plays a critical role in the mechanical properties of the polyacrylamide gels, 5min will be the ideal time to measure the modulus of a hydrogel before dehydration.

Anton Paar Physica MCR 301 rheometer was used to characterize the mechanical properties of PAAm hydrogels fully swelled in cell media. In this study, a metal plate (Anton Paar PP25, 25mm in diameter) was used to apply an oscillatory force on the surface of the hydrogel to characterize the viscoelastic properties. A frequency of 1 Hz, strain amplitude of 1 % and a fixed force of 0.5 N were applied. The rheology measurements were recorded at a temperature of 37°C.

## **7. Differential Scanning Calorimetry (DSC):**

Differential scanning calorimetry (DSC) is a technique in which the heat flux is monitored against temperature while the temperature of the sample, in a specified atmosphere, is programmed. PAAm hydrogels having different degree of crosslinking were analyzed using Differential Scanning Calorimeter DSC (TA Instruments 2920), equipped with a RCS90 cooling system. Approximately 1–3 mg of fully water swelled PAAm gel was weighed into standard aluminum TA pans with a lid. An empty aluminum sealed pan was used as a reference. The temperature is raised from 0°C to 350°C at a heating rate of 10°C/min under a nitrogen atmosphere (flow, 10 cm<sup>3</sup> /min).

## 8. Infrared Spectroscopy:

Infrared (IR) refers to that part of the electromagnetic spectrum between the visible and microwave regions. Electromagnetic spectrum refers to the seemingly diverse collection of radiant energy, from cosmic rays to X-rays to visible light to microwaves, each of which can be considered as a wave or particle traveling at the speed of light. These waves differ from each other in the length and frequency.

Infrared radiation is absorbed by organic molecules and converted into energy of molecular vibration. In IR spectroscopy, an organic molecule is exposed to infrared radiation. When the radiant energy matches the energy of a specific molecular vibration, absorption occurs. A typical IR spectrum is shown below (Fig.14). Band intensities can be expressed as absorbance.

Because there needs to be a relative scale for the absorption intensity, a background spectrum must also be measured. This is normally a measurement with no sample in the beam. This technique results in a spectrum which has all of the instrumental characteristics removed. Thus, all spectral features which are present are strictly due to the sample. A single background measurement can be used for many sample measurements because this spectrum is characteristic of the instrument itself.



Figure 14: Infrared spectrometer

## 9. Statistical Analysis:

Thorough the thesis, data are presented as mean  $\pm$  SD. Statistical significance was determined using one-way ANOVA with post hoc Tukey's Honest Significant Difference (HSD) test for multiple comparison procedures. Tukey HSD test was used to find means that are significantly different from each other, within a set of different samples by comparing the means of every data group to the means of every other data group. Therefore, it applies simultaneously to the set of all pairwise comparisons and identifies any difference between two means that is greater than the expected standard error. Tested data groups are assumed to be independent within and among the groups and are normally distributed, presenting homogeneity of variance (there is equal within-group variance across the groups associated with each mean in the test). P values of less than 0.05 were considered significant.

### **III. Conclusion:**

This chapter discusses the materials and the methods used in order to achieve the thesis work. Actually, this section shows the chemical products and the principle of the experimental methods used to determine the preparation and the mechanical properties of the hydrogels. Moreover, the materials and the methods concerning the 2D cell culture and the characteristic of podocyte cells were investigated.

The following chapters will be focused on the study of the mechanical properties of polymers based hydrogels. Furthermore, the study of the effect of hydrogels mechanical properties on cellular behaviour will be investigated such as cells attachment, proliferation, cytoskeleton reorganisation, differentiation and mechanical properties.

#### IV. References:

- (1) Van Den Bulcke, A. I.; Bogdanov, B.; De Rooze, N.; Schacht, E. H.; Cornelissen, M.; Berghmans, H. Structural and Rheological Properties of Methacrylamide Modified Gelatin Hydrogels. *Biomacromolecules* **2000**, *1* (1), 31–38.
- (2) Saleem, M. A.; O'Hare, M. J.; Reiser, J.; Coward, R. J.; Inward, C. D.; Farren, T.; Xing, C. Y.; Ni, L.; Mathieson, P. W.; Mundel, P. A Conditionally Immortalized Human Podocyte Cell Line Demonstrating Nephritin and Podocin Expression. *J. Am. Soc. Nephrol. JASN* **2002**, *13* (3), 630–638.
- (3) pubmeddev; CG, J. Scanning electron microscopy: preparation and imaging for SEM. - PubMed - NCBI <https://www.ncbi.nlm.nih.gov/pubmed/22907399> (accessed Sep 5, 2019).
- (4) pubmeddev; al, M. J., et. Environmental scanning electron microscopy in cell biology. - PubMed - NCBI <https://www.ncbi.nlm.nih.gov/pubmed/23027020> (accessed Sep 5, 2019).
- (5) Binnig, G.; Quate, C. F.; Gerber, C. Atomic Force Microscope. *Phys. Rev. Lett.* **1986**, *56* (9), 930–933.
- (6) Zlatanova, J.; Lindsay, S. M.; Leuba, S. H. Single Molecule Force Spectroscopy in Biology Using the Atomic Force Microscope. *Prog. Biophys. Mol. Biol.* **2000**, *74* (1), 37–61.
- (7) Sneddon, I. N. The Relation between Load and Penetration in the Axisymmetric Boussinesq Problem for a Punch of Arbitrary Profile. *Int. J. Eng. Sci.* **1965**, *3* (1), 47–57.
- (8) Gaboriaud, F.; Dufrêne, Y. F. Atomic Force Microscopy of Microbial Cells: Application to Nanomechanical Properties, Surface Forces and Molecular Recognition Forces. *Colloids Surf. B Biointerfaces* **2007**, *54* (1), 10–19.
- (9) Radmacher, M.; Fritz, M.; Kacher, C. M.; Cleveland, J. P.; Hansma, P. K. Measuring the Viscoelastic Properties of Human Platelets with the Atomic Force Microscope. *Biophys. J.* **1996**, *70* (1), 556–567.
- (10) Boudou, T.; Ohayon, J.; Picart, C.; Tracqui, P. An Extended Relationship for the Characterization of Young's Modulus and Poisson's Ratio of Tunable Polyacrylamide Gels. *Biorheology* **2006**, *43* (6), 721–728.
- (11) Fluorescence Microscopy | Center for Advanced Microscopy.

(12) MicroscopyU - The Source for Microscopy Education <https://www.microscopyu.com/> (accessed Sep 4, 2019).

(13) Microscopies multi-harmoniques pour l'imagerie st... – M/S : médecine sciences – Érudit <https://www.erudit.org/fr/revues/ms/2006-v22-n10-ms1424/013818ar/> (accessed Sep 16, 2019).



## **Chapter III: Influence of hydrolyzed polyacrylamide hydrogel stiffness on podocyte morphology, phenotype and mechanical properties**





### I. Abstract

Chronic kidney disease (CKD) is characterized by a gradual decline in renal function that progresses toward end-stage renal disease (ESRD). Podocytes are highly specialized glomerular epithelial cells which form with the glomerular basement membrane (GBM) and capillary endothelium the glomerular filtration barrier (GFB). GBM is an extracellular matrix (ECM) that acts as a mechanical support and provides biophysical signals that control normal podocytes behaviour in the process of glomerular filtration. Thus, the ECM stiffness represents an essential characteristic that controls podocyte function.

Hydrolyzed Polyacrylamide (PAAm) hydrogels are smart polyelectrolytes materials. Their biophysical properties can be tuned as desired to mimic the in natural ECM. Therefore, these hydrogels are investigated as new ECM-like constructs to engineer a podocyte-like basement membrane that forms with cultured human podocytes a functional glomerular-like filtration barrier. Such ECM-like PAAm hydrogel construct will provide unique opportunity to reveal podocyte cell' biological responses in an in vivo-like setting by controlling the physical properties of the PAAm membranes.

In this work, Hydrolyzed PAAm scaffolds having different stiffness ranging between 0.6 – 44 kPa are prepared. The correlation between the hydrogel structural and mechanical properties and Podocytes morphology, elasticity, cytoskeleton reorganization and podocin expression is evaluated. Results show that hydrolyzed PAAm hydrogels promote good cell adhesion and growth and are suitable materials for the development of future 3D smart scaffolds. In addition, the hydrogel properties can be easily modulated over a wide physiological range by controlling the crosslinker concentration. Finally, tuning the hydrogel properties is an effective strategy to control the cells function.

This work addressed the complexity of podocytes behaviour which will further enhance our knowledge to develop a kidney-on-chip model much needed in kidney function studies on both healthy and diseased states.

## II. Introduction:

The development of an *in vitro* model for cell differentiation and growth has a prior importance in understanding the fundamental mechanobiology as well as the medical application in damaged organs regeneration. However, different types of materials have been investigated as a support for cell culture in order to study their influence on cell behavior<sup>1</sup>. These materials permit the development of microfluidic organ-on-a-chip culturing systems. The latter can be effectively used to establish an appropriate microenvironment for cells and also mimic a functional unit of human living organ *in vitro*. Extracellular matrix (ECM) has a major effect on cellular behaviour regulation, such as, cell morphology, proliferation and differentiation. These processes can be substantially altered in response to the modification of ECM mechanical properties and chemical composition<sup>2</sup>. Damage of ECM associated with the reduction of tissue integrity is a cardinal phenomenon observed in many chronic illnesses including rheumatoid arthritis as well as chronic kidney diseases<sup>3</sup>. Therefore, engineered ECMs are useful as culture systems mimicking *in-vivo* setting that can explain how ECMs interact and control cellular processes and tissue integrity in both health and diseased states<sup>4</sup>.

Synthetic materials such as Polyacrylamide (PAAm) gel<sup>5</sup> and Polydimethylsiloxane (PDMS)<sup>6</sup> as well as natural biomaterials made of collagen and gelatin are the most commonly used in biomedical research. Collagen and gelatin represent major component of many connective tissues, they are characterized by their biocompatibility, inherent biodegradability and specific biological functions<sup>7</sup>. However, these hydrogels are limited by a low stiffness (<1 kPa) and short-term stability<sup>4</sup>. The PDMS presents an acceptable biocompatibility but does not fully mimic a soft viscoelastic matrix due to its limited scale of stiffness (> 5 kPa)<sup>7</sup>.

Therefore, these materials are not considered as a suitable GBM alternative to study glomerular filtration barrier functions<sup>8,9</sup>. PAAm gels are advantageous because their stiffness can be modulated over a wide range from 0.3 - 300 kPa<sup>10</sup>. This stiffness variation permits better understanding of the correlation between the cellular responses and the scaffolds mechanical properties<sup>11</sup>. Nevertheless PAAm gels present many disadvantages in mimicking the natural ECM. First, PAAm gel has limited capacity to interact with the physiological environment while the ECM is not just an inert scaffold but a dynamic system. Second, the presence of unreacted acrylamide residues within the PAAm network can intoxicate the cells. These important drawbacks can be tackled by using hydrolyzed PAAm hydrogels.

Hydrolyzed PAAm hydrogels are viscoelastic polymeric networks characterized by their hydrophilic structure<sup>12,13</sup>. These polymers are biocompatible polyelectrolytes capable of absorbing, holding within their interstitial space and releasing on demand large amounts of biological fluids. They are extensively used in the development of artificial muscles, sensors<sup>14,15</sup> and drug delivery carriers<sup>16</sup>. During the swelling process, unpolymerized monomers and extractable materials such as unreacted APS, TEMED and their degradation products are washed out from the polymer matrix. In addition, their swelling degree, network microstructure and stiffness<sup>17</sup> can be easily tuned as desired covering a wide range of physicochemical properties. These characteristics make them toxin free and permeable to small molecules such as oxygen, nutrients, and metabolites that are considered the main advantages allowing cells survival. Thus, hydrolyzed PAAm can be designed to simulate the *in vivo* environment<sup>13</sup> and should be regarded as a promising scaffold material.

The glomerular filtration barrier is composed of podocytes and capillary endothelial cells separated by a glomerular basement membrane (GBM). GBM is considered a soft tissue with an elasticity of 2.5 kPa<sup>3</sup>. A decrease in GBM stiffness (<2.5 kPa) is a characteristic of several

renal diseases<sup>8</sup>. Podocytes are highly differentiated glomerular epithelial cells and represent an essential component of the glomerular filtration barrier<sup>23</sup>. Podocyte structure is characterized by cytoplasmic foot processes that attach to and cover the entire endothelium. These “foot processes” interdigitate together in a zipper like structure to form molecular filtration units named “slits diaphragm”<sup>24</sup>. Podocytes are the functional element for filtering blood in the glomerulus. Their sieving function are tightly related to their differentiation and phenotype state, which are both influenced by the mechanical and chemical properties of the matrix<sup>7</sup>. Hu *et al.* have reported that the effect of gelatin-mTG substrate stiffness has a great impact on nephrin and podocin expression. These proteins are essential to form a functional slit diaphragm and are involved in the mechanosensation of human podocytes<sup>25</sup>.

Hydrolyzed PAAm hydrogels are able to hold cell medium, which together with conditionally immortalized human podocytes give the possibility to develop a 3D-model of glomerular filtration barrier. However, the optimal mechanical properties of hydrolyzed polyacrylamide hydrogels that preserve an intact “slit diaphragm” and foot processes structures remain a key question. Here, we hypothesized that modulating the crosslinker concentration will produce gels with various stiffnesses<sup>26</sup>. When the stiffness is maintained within the GBM stiffness range, we expect to reach such optimal conditions, which are crucial towards the development of a kidney-on-chip model.

This work aims at investigating the possibility of using the hydrolyzed form of PAAm hydrogel as a new scaffolding material, which is an essential step toward the development of *adaptive implant materials*, and studying the effect of matrix mechanical and structural properties on podocytes morphology and mechanical properties. Different hydrogel layers covering a wide range of properties were prepared by changing the crosslinker

concentrations. The swelling degree was measured and the mechanical properties and macromolecular microstructure were evaluated by Scanning Electron Microscopy (SEM) and Atomic Force Microscopy (AFM) respectively. Then, podocytes were cultured on the hydrolyzed PAAm scaffolds. Their morphology and mechanical properties were evaluated in order to investigate and understand how podocytes sense and respond to the mechanical properties of the substrate.

### III. Materials and Methods:

#### 1. Fabrication of Hydrolyzed Polyacrylamide Hydrogels:

##### a. Fabrication of Polyacrylamide Gels:

Acrylamide monomer (AAm, Sigma Aldrich, A8887, 79-06-1, purity >99%) and *N*, *N*'-Methylenbisacrylamide crosslinker (Bis-acrylamide, Sigma Aldrich, M7279, 110-26-9 purity >99.5%) aqueous solutions having concentrations of 30 wt % and 2 wt % respectively were prepared and used. The free radical polymerization reaction is initiated by Ammonium Persulfate (APS, 25 wt %, Sigma Aldrich, 248614, 7727-54-0, purity >98%) and catalyzed by *N*, *N*, *N*', *N*' Tetramethylethylenediamine (TEMED, Sigma Aldrich, T7024, 110-18-9).

Six PAAm gels having different crosslinking densities were prepared by mixing 1 ml of AAm, 1  $\mu$ l of APS and 1  $\mu$ l TEMED to different Bis-acrylamide concentrations (0.5, 1, 2, 5, 10 and 30  $\mu$ l). After mixing, the gel solution was poured into a rectangular rubbery mold (6 cm x 2 cm x 0.8 cm) sandwiched between 2 glass slides and left for 3 hours at room temperature to achieve polymerization.

##### b. From Gel to Hydrogel: Hydrolysis and Swelling:

After complete polymerization, PAAm gel layers were gently removed from the mold and soaked overnight in a basic solution of sodium hydroxide (1 M) (NaOH, Sigma Aldrich, S8045, 1310-73-2, purity > 98 %) to hydrolyze the PAAm gel. The hydrolysis reaction converts the

amine moieties (R-NH<sub>2</sub>) of the PAAm network chains into carboxylate (-COO<sup>-</sup>) moieties that are characterized by their high affinity for water. The hydrolyzed gel layers were then placed in deionized water (DW, MilliQ, conductivity higher than 18 MΩ) that was repeatedly changed for seven days until the equilibrium swelling was reached. The resulting fully swelled hydrogel layers were gently removed and placed in an excessive amount of complete cell medium that was repeatedly changed until reaching a new equilibrium.

### 2. Swelling Measurement:

After reaching the equilibrium swelling degree in DW and cell media, the swelling degree was measured. It is defined as the ratio of the network weight in the swollen state over the dry state. (Equation 1)

$$S = \frac{W_s - W_d}{W_d} \quad (1)$$

Where  $W_s$  and  $W_d$  are the weight of a fully swollen (in equilibrium with DW and cell media) and dehydrated hydrogels respectively. Measurements were repeated 3 times.

### 3. Rheology of PAAm Hydrogel:

Anton Paar Physica MCR 301 rheometer was used to characterize the mechanical properties of PAAm hydrogels fully swelled in cell media. In this study, a metal plate (Anton Paar PP25, 25mm in diameter) was used to apply an oscillatory force on the surface of the hydrogel to characterize the viscoelastic properties. A frequency of 1 Hz, strain amplitude of 1 % and a fixed force of 0.5 N were applied. The rheology measurements were recorded at a temperature of 37°C.

$$G = G' + G'' \quad (2)$$



$G'$  is the storage modulus that represents the elastic property meaning the capacity of membrane material to retain a recoverable elastic energy.  $G''$  is the loss modulus and determined by the loss of energy due to the viscous forces.

#### **4. Differential Scanning Calorimetry (DSC):**

Differential scanning calorimetry (DSC) is a technique in which the heat flux is monitored against temperature while the temperature of the sample, in a specified atmosphere, is programmed. PAAm hydrogels having different degree of crosslinking were analyzed using Differential Scanning Calorimeter DSC (TA Instruments 2920), equipped with a RCS90 cooling system. Approximately 1–3 mg of fully water swelled PAAm gel was weighed into standard aluminium TA pans with a lid. An empty aluminium sealed pan was used as a reference. The temperature is raised from 0°C to 350°C at a heating rate of 10°C/min under a nitrogen atmosphere (flow, 10 cm<sup>3</sup>/min).

#### **5. Scanning Electron Microscopy (SEM):**

Hydrogel microstructure was evaluated using SEM technique. The samples were placed in liquid nitrogen (-197°C) for 4 hours and subsequently lyophilized. The freeze dried samples were processed in a vacuum system (LABCONCO®, FreeZone 4.5) at 0.02 mBar and -54°C for overnight. The dried samples were gold sputter-coated to be analyzed by SEM (ZEISS, EVO I HD15).

#### **6. Atomic Force Microscopy (AFM):**

The AFM experimental system used for force-spectroscopy measurements was an Asylum MFP-3D head coupled to a Molecular Force Probe 3D controller (Asylum Research, Santa Barbara, CA, USA). Triangular silicon nitride cantilevers (MLCT, Veeco) with a nominal spring

constant of 10 pN/nm, length of 310  $\mu\text{m}$ , width of 20 nm, resonance frequency of 7 kHz, and half-opening angle of  $\sim 19^\circ$  were used. The cantilever spring constant was determined using the thermal noise method available within the MFP-3D software. Hydrogel samples were glued to a Petridish with double-faced adhesive tape, and covered with 0.5 ml of deionized water. After testing a range of loading forces on the hydrogel surface, the measurements were performed in liquid at room temperature with a maximum loading force of 1 nN corresponding to a maximal indentation depth of 0.3  $\mu\text{m}$ . Elastic deformation was obtained from the recorded force curves as a function of the loading force applied by the tip. Young's modulus ( $E$ ) was calculated for each force from the approaching part of the curve, using a modified Hertz model<sup>27</sup>, based on the work of Sneddon<sup>28</sup> and further developed for different AFM tip shapes<sup>29,30</sup>, as described elsewhere<sup>31</sup>. An approach velocity of 6  $\mu\text{m/s}$  was chosen, indicating a piezo-extension rate of 1 Hz to minimize hydrodynamic and viscoelastic artifacts<sup>32</sup>.

The Poisson's ratio of the cells was assumed to be 0.5, as suggested for incompressible materials<sup>33</sup>. Furthermore, to investigate cells' nanomechanical properties on each sample, we repeated the force spectroscopy experiment using the same parameters.

### 7. Cell Culture:

Human podocytes cell line was purchased from the Faculty of Medicine, University of Bristol, UK. Immortalized human podocytes were cultured on flasks according to the supplier protocol<sup>34</sup>. Podocytes cells were cultured in RPMI – 1640 Medium (Sigma Aldrich, R8758) supplemented with 1 % insulin-transferrin-Selenium liquid media supplement (Sigma Aldrich, I3146), 10 % fetal bovine serum (Sigma Aldrich, F7524) and Penicillin Streptomycin solution (Sigma Aldrich, P4333). Proliferation was induced when the cells were incubated at 33°C and

differentiation was induced by incubating the cells at 37°C. After proliferation, cells were plated on the hydrolyzed PAAm Hydrogel substrate having various mechanical properties. The PAAm substrates were coated with collagen type I (Sigma Aldrich, C3867, 9007-34-5) using EDC (Sigma Aldrich, E6383, 25952-53-8) and NHS (Sigma Aldrich, 130672, 6066-82-6) which crosslink with the carboxylic group.

### **8. Immunocytochemical characterization:**

Podocyte cells cultured on PAAm Hydrogels for 7 days were fixed with 2% of paraformaldehyde (PFA) (Sigma Aldrich, P6148, 30525-89-4) for 15min at room temperature. Then, cell permeabilization was performed using 0.5 % Triton X-100 (Sigma Aldrich, X100, 9002-93-1) for 15 minutes into the incubator (37°C). Afterwards, the non-specific protein binding sites were blocked with 1 % of Bovine Serum Albumin (BSA) (Sigma Aldrich, A2153, 9048-46-8) and 0.5% of Triton-X in PBS during overnight at 4°C. Cells were then incubated overnight at 4°C with a primary anti-podocin antibody (Sigma Aldrich, P0372). The samples were then rinsed with PBS and incubated with secondary anti-rabbit antibody (Alexa Fluor®594, Cat: ab150080) for 1 hour in dark at room temperature. Nucleus and actin cytoskeleton staining were done with DAPI (Sigma Aldrich, D9542) and Phalloidin staining (Invitrogen, Cat: A12379), which were applied for 0.3 – 1 hours in dark at room temperature. Image acquisition was achieved using Nikon TE2000 microscope.

### **9. Multiphoton Microscopy (MPM):**

For a high resolution images, podocyte cells were scanned with a custom-built multiphoton microscope based on a SliceScope upright microscope (MPSS-1000P) equipped with a Multiphoton Scan Head (MP-2000), both from Scientifica LTD. For sample excitation, a Spectra-Physics Tsunami Ti-Sapphire laser operated in pulsed mode was used, wavelength

range from 760 to 900 nm, typically 870 nm, repetition rate 80 MHz; pulse duration ~100 fs. The laser beam was focused on the sample via a Nikon CFI75 LWD-16x-W objective (NA 0.8, water immersion). MPM images were created by laser raster scanning the sample. The two photon excited fluorescence signal was epi-collected through the objective.

### **10. Cell Proliferation Assay:**

MTT (3-(4, 5-dimethylthiazol-2-yl)-2, 5-diphenyltetrazoliumbromide) test was used to evaluate podocyte cells proliferation. After 5 days of culture on PAAm hydrogels, 1mg/ml MTT solution (Sigma Aldrich, M5655, 298-93-1) was added to cells and incubated for 3h at 37°C. MTT solution was carefully discarded and replaced by Isopropanol (Sigma Aldrich, I9516, 67-63-0) to dissolve the violet formazan crystals. After 1 hour incubation at room temperature in the dark the luminescent signals provided by MTT assay were detected and cell proliferation was determined by normalizing each luminescent signal from cells cultured on gels over cells cultured without gel (control).

### **11. Statistical Analysis:**

Data are presented as mean  $\pm$  SD. Statistical significance was determined using one-way ANOVA with post hoc Tukey's Honest Significant Difference test for multiple comparisons. P values of less than 0.05 were considered significant.

## IV. Results and Discussion

### 1. PAAm hydrogels properties:

The mechanical properties of the hydrogel layers having increasing Bis-acrylamide crosslinker concentrations (0.5, 1, 2, 5, 10 and 30  $\mu$ l) are evaluated. The swelling is characterized by the capacity of hydrogels to absorb and retain aqueous medium. Hydrogel swelling is induced by osmotic forces generated by hydrophilic  $\text{COO}^-$  and  $\text{Na}^+$  ions entrapped inside the hydrogel matrix, while the 3D structure is maintained by the mechanical forces of the crosslinked network. The swelling degree was measured for PAAm Hydrogels fully swollen in DW and cell medium. An exponential decrease of swelling ratio from 1914 to 193 and from 54 to 26 with increasing crosslinker concentration from 0.5 to 30  $\mu$ l was determined in DW and cell medium respectively (Fig. 1A). Thus, an increase in Bis-acrylamide crosslinker concentration contributes to a significant decrease in the swelling ratio. The density of PAAm network evaluated by SEM shows that the highest concentration of Bis-acrylamide provides a highly connected structure (Fig. 1B). Consequently, the polymer network becomes more compact and thus less prone to absorb water. This indicates that the crosslinking density of polymer chain has an influence on the swelling capacity. Previous studies have investigated the effect of crosslinker concentration of PAAm hydrogel on the swelling mechanism and have showed that an increase of crosslinking density reduced the gels capacity to be swelled due to the highly crosslinked polymer network<sup>35</sup>.

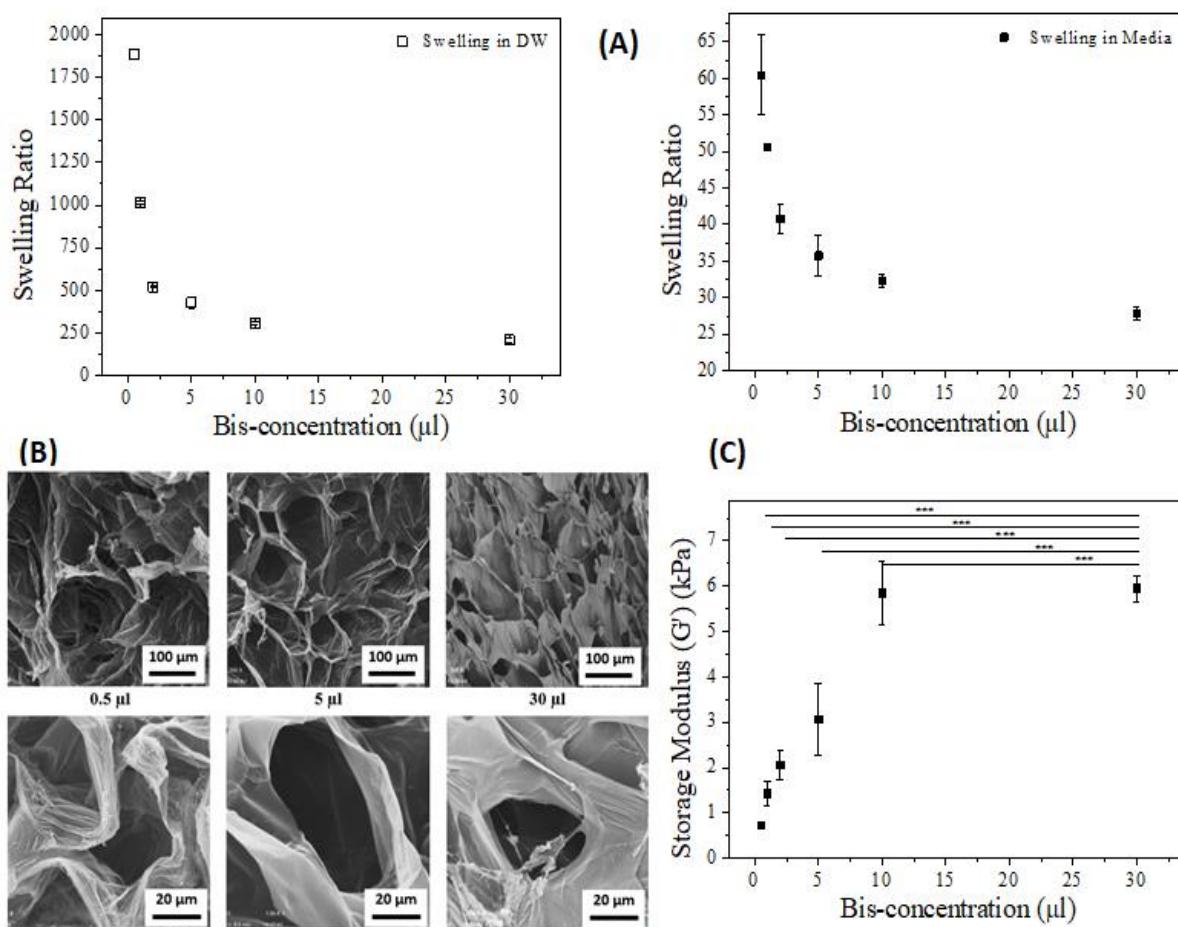


**Figure 1:** (A) Representative curve of swelling degree as a function of Bis-acrylamide concentrations (0.5, 1, 2, 5, 10 and 30 μl). (B) Scanning Electron Microscopy images of dehydrated PAAm hydrogels show the polymeric network density as a function of crosslinker concentrations. The membrane containing the highest concentration of Bis-acrylamide crosslinker (30 μl) presents a more compacted network than a membrane having a low concentration of crosslinker (0.5 μl). (Error Bar = Standard Deviation). (C) The storage modulus of PAAm membranes swelled in cell media was determined as a function of Bis-acrylamide crosslinker concentrations. (Error Bar = Standard Deviation)

Regarding the macroscopic characterization of mechanical properties, the viscoelasticity of hydrogels was determined by applying an oscillatory force on the total surface of PAAm gel fully swelled in culture medium. The elastic and viscous properties are represented by the storage modulus and the loss modulus respectively. The storage modulus is defined by the membrane capacity to hold a recoverable energy and the loss modulus is characterized by the dissipated energy. For a low concentration of crosslinker (0.5 μl), the storage modulus

was about 274 Pa and increased until 2.5 kPa for a high crosslinker concentration (30  $\mu$ l) (Fig. 1C). Many studies have worked on the characterization of PAAm hydrogels mechanical properties. Grattoni *et al.* have already analyzed PAAm hydrogels having different monomer and crosslinker concentrations. They have shown that the storage moduli of the hydrogel increased significantly with the monomer and crosslinker concentrations<sup>36</sup>. In our work, the rheology measurements showed as expected, an increase of storage modulus with the concentration of crosslinker agent. This indicates that a densely connected network requires more energy to be deformed.

Moreover, the structural characterization of PAAm hydrogels is determined by DSC. The thermograms (Fig.2) show endothermic peaks for PAAm hydrogels having the lowest and the highest Bis-acrylamide concentrations. The endothermic peak surface area permits to determine the transition enthalpies ( $\Delta H$ ). An increase of  $\Delta H$  from 1879 J/g to 1985 J/g with increasing crosslinker concentrations from 1 to 30  $\mu$ l respectively is registered. Several studies have shown that the increase of  $\Delta H$  reflects the increase of polymer strength due to the significance of intermolecular bonding<sup>37,38</sup>. Thus hydrogels containing more Bis-acrylamide present higher crosslinking densities.

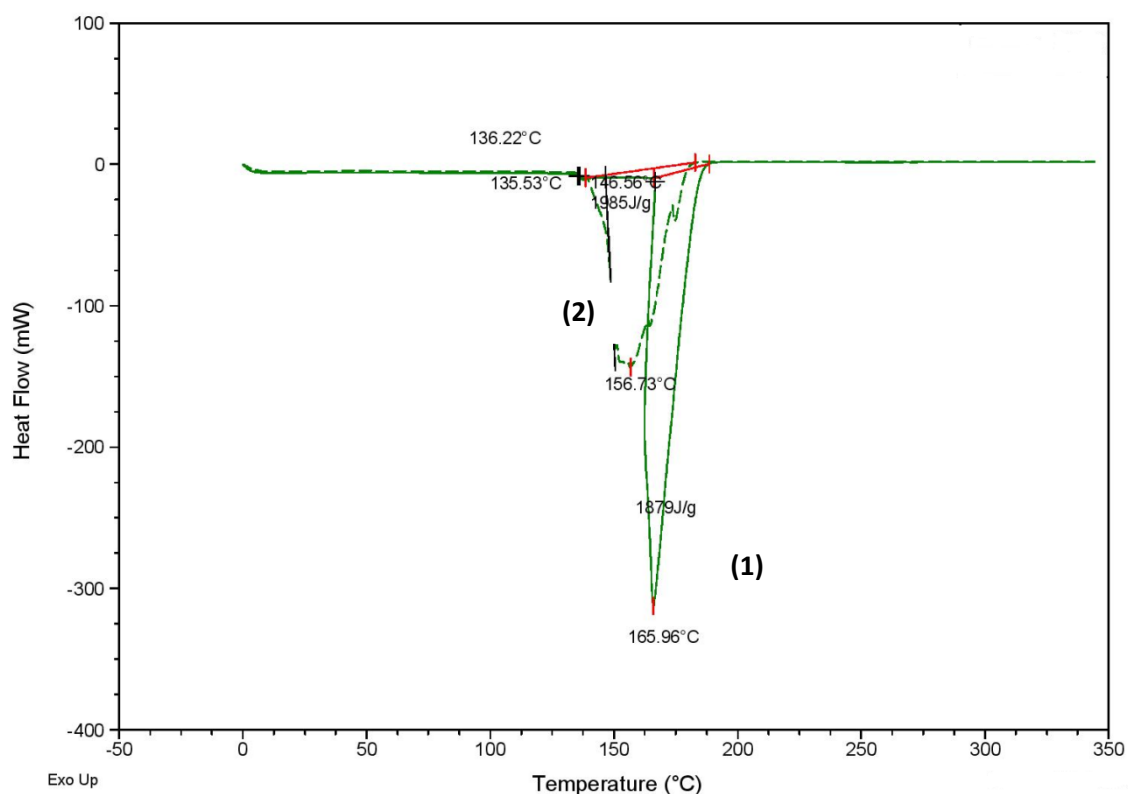


**Figure 2: DSC curves for PAAm hydrogels having different concentrations of crosslinker. Curve (1) corresponds to 1  $\mu$ l of Bis-acrylamide and curve (2) corresponds to 30  $\mu$ l of Bis-acrylamide.**

The local mechanical properties, PAAm hydrogel's elasticity was evaluated by force-spectroscopy analysis. Typical images are gathered in Fig. 3A for PAAm gels with different crosslinker concentrations. For the softest substrates (0.5, 1 and 2  $\mu$ l), the local distribution of Young's modulus is homogenous. Conversely, for the stiffest supports (10 and 30  $\mu$ l), the inhomogeneity of the surface is obvious. The maps indicate a presence of large areas having a very low elasticity comparing to the overall elasticity. For example, the stiffness map of the substrate with the highest crosslinker concentration showed areas with a stiffness ranging from 0 to 5 kPa, whereas the overall elastic modulus of this substrate is about 44 kPa.

The histograms of Fig. 3B are plotted from the local measurement of Young's modulus maps.

The average Young's modulus values of 0.5, 1, 2, 5, 10 and 30  $\mu$ l samples deduced from the



Gaussian fit are  $0.67 \pm 0.05$  kPa,  $0.90 \pm 0.06$  kPa,  $2.1 \pm 0.5$  kPa,  $9.9 \pm 4.9$  kPa,  $18.4 \pm 3.2$  kPa and  $44.3 \pm 7.1$  kPa respectively (Fig. 3C). Our data showed an exponential increase in Young's modulus with increasing crosslinker concentrations. These results are compatible with previous studies that have shown an increase in Young's modulus correlated with increasing crosslinker concentrations<sup>22</sup>.

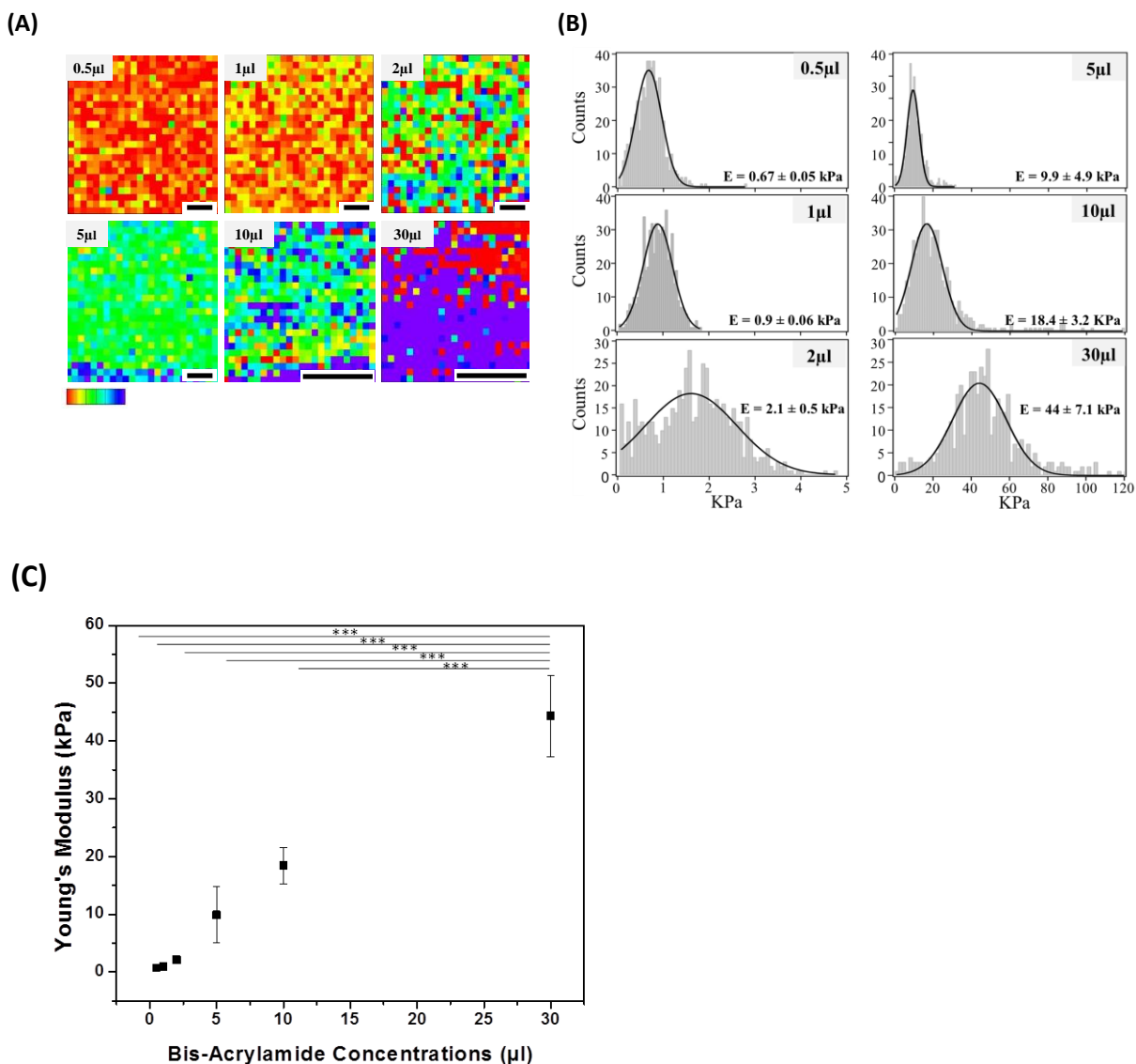


**Figure 3: (A)** Polyacrylamide hydrogels Young's modulus maps measured by AFM. White scale bar corresponds to 5μm. Dark red color depicts softer portions, while blue and purple colors show stiffer regions. Linear color scale bar for (0.5 μl), (1 μl) and (2 μl) goes from 0 to 3 kPa. Linear color scale bar for (5 μl), (10 μl) and (30 μl) goes from 0 to 30 kPa. Maps are represented by 24x24 pixels, meaning 10 minutes lag. This resolution was chosen in order to record as much maps as possible, in different sample areas, to obtain the best possible statistic (B) 1. Elasticity distribution of PAAm hydrogels. Young's moduli were best fitted with Gaussian distributions. 2. Evolution of the Young's modulus (E) as a function of bis-acrylamide crosslinker concentrations. The Young's modulus increases with increasing concentration of the crosslinker. Bars represent the obtained average of the Gaussian peaks fitted on the elasticity value distribution of individual force maps. Error bars are standard deviation of the mean. \* denotes statistical significance of  $P < 0.05$

Moreover, there is a correlation with the rheology measurements where an increase of storage modulus was observed. This can be explained by the density degree of the polymer network characterized by SEM. At this stage, the swelling degree, the polymer network density and the mechanical properties were perfectly correlated. Typically, the increase of crosslinker concentration contributes to a highly crosslinked polymer making the hydrogel stiff and less prone to the swelling. Furthermore, these PAAm hydrogels have a high Young's modulus attributed to their highly connected structure with small mesh size that contained less water. Finally, the network with high connectivity is not homogeneous since they exhibit large zones having significantly lower Young's modulus. Contrariwise, the softest hydrogel presents a more homogeneous network. Therefore, hydrogels present an inhomogeneous distribution of crosslinking density. The inhomogeneity degree increases with crosslinker concentration due to the increase of network imperfections establishing less and more crosslinked regions<sup>39</sup>.

Our study seeks to determine a substrate having elasticity close to *in vivo* state. Since the glomerular basement membrane of the kidney has an elasticity of 2.5 kPa<sup>3</sup>, the substrates with elasticity of 0.9, 2.1 and 9.9 kPa are in the range of normal GBM elasticity. Consequently, we have investigated the effect of all the hydrogels on the cellular behavior.

## **2. Influence of the scaffold mechanical properties on podocyte cells:**

### **Morphology, Elasticity, Cytoskeleton reorganization and Podocin expression**

Podocytes were cultured on PAAm hydrogels covering an elasticity range from 0.6 to 44 kPa in order to evaluate the influence of support stiffness on their morphology and mechanical properties. MTT assay was performed to confirm cell growth and survival on the PAAm hydrogels. Figure 4 showed that podocytes were able to proliferate on all hydrogels.

Accordingly, the hydrogel is non-toxic and thus all unreacted acrylamide was removed during the swelling process. However, we can notice that the proliferation rate of podocyte cells increased with gel stiffness.

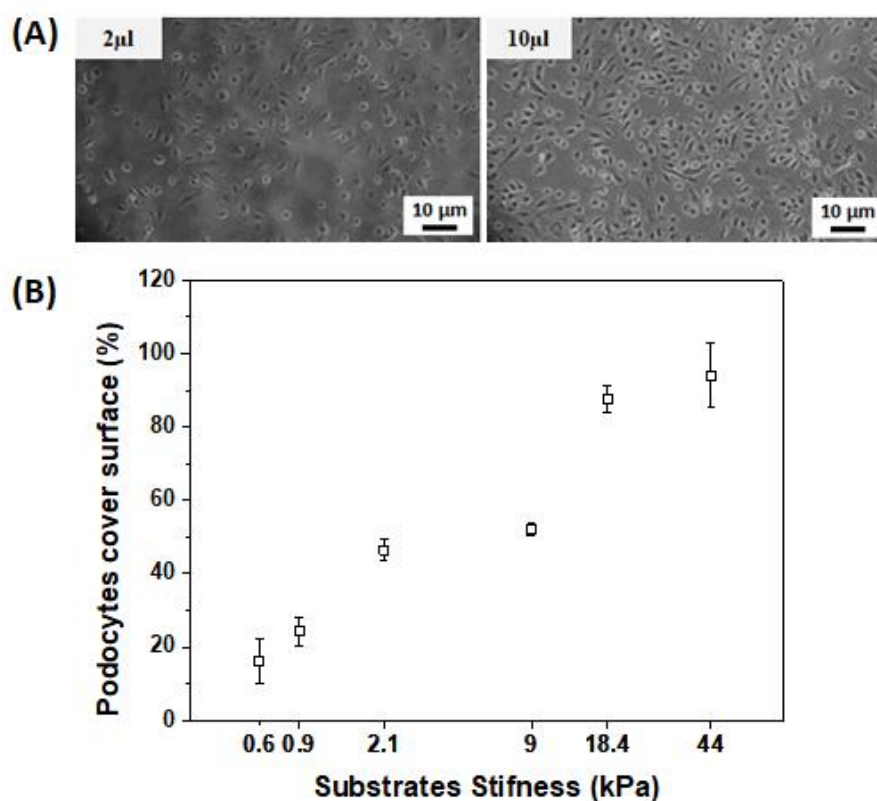


**Figure 4:** A) Human Podocyte Cells Line cultured on PAAm hydrogels substrates having different properties (2 and 10 µl Bis-acrylamide respectively). (B) Podocyte proliferation: % of podocytes cover surface as a function of substrate's elastic modulus. (Reference: 100% for podocytes seeded on the plate).

Furthermore, multiphoton microscopy and Environmental SEM (Fig. 5) showed that the morphology of conditionally immortalized human podocytes seeded on PAAm hydrogels was comparable to the previously described organoid-derived podocytes in culture<sup>40</sup> as well as the fully differentiated immortalized human podocyte previously reported<sup>34</sup>. Typically, the microscopy images showed the presence of arborized projections that can be described as “foot processes”. The latter enable possible cell-cell connections (yellow arrows in Fig. 5) mimicking the “slit diaphragm” responsible for the filtration function of the podocyte layer.

The two photon excited fluorescence images measured by MPM reveal the cytoskeletal organization of the podocytes and the interdigitating foot processes with adjacent cells (yellow arrows in Fig. 5).

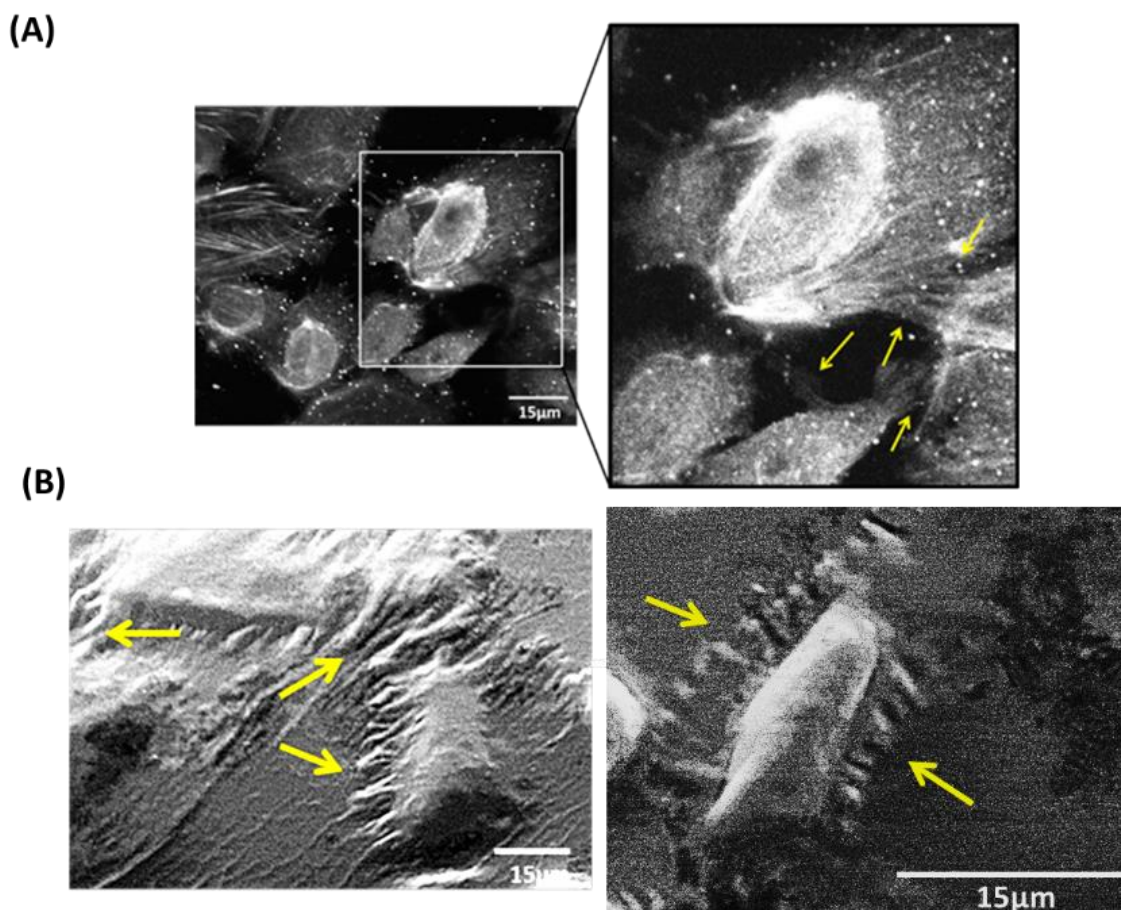


**Figure 5: Immortalized podocytes showed an arborized morphology and interdigitating foot processes with adjacent cells (yellow arrow). These images were taken using multiphoton microscopy (A) and environmental SEM (B) for substrate of 2.1 kPa.**

The mechanical properties of support have a clear effect on the morphology and the cytoskeleton reorganization of podocyte cells, which was characterized by visualizing the actin network using Phalloidin staining (Fig. 6). On the softest gel (0.67 kPa), the cells

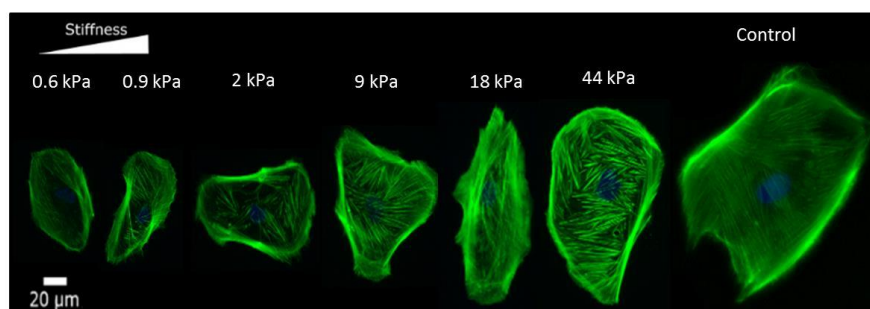
showed a small spread area. They become more and more spread as the gel Young's modulus increases.

The cells mechanosensitivity against ECM is usually explained by the activity of adhesion molecules and non-muscle myosin that produce support stiffness dependent - forces<sup>41</sup>. Cell-ECM attachment involves numerous cytoplasmic linkage proteins including integrins that connect ECM to actin filaments. Integrin play thus a crucial role in cytoskeleton reorganization and cell cycle regulation. For a matrix having high stiffness, the cells respond to mechanical strain by increasing integrin aggregation and therefore an increase in the formation of actin stress fibers. Therefore, actin cytoskeleton reorganization was analyzed in podocytes cultured on gels with different elasticity. Importantly, actin network formed a diffuse cytoskeleton with a random arrangement for soft substrates (0.67 to 2.1 kPa). In contrast, cells cultured on stiff gels reacted in response to mechanical stress by forming a dense actin cytoskeleton (Fig. 6A). The latter scenario is opposite to a random actin cytoskeleton reorganization previously reported on soft substrates<sup>18,22,41</sup>. Finally, the actin cytoskeleton is also oriented and more dense allowing to apply contractile forces that counterbalance substrate stiffness<sup>3</sup>.

Healthy podocytes integrity and phenotype are determined by their ability to express specific markers such as podocin, nephrin and CD2AP, which are responsible in the formation of the slit diaphragm<sup>42</sup>. Also, podocytes express Wilms' tumor suppressor (WT-1) which is a nuclear protein involved in the expression of major podocyte markers<sup>43,44</sup>. The expression of podocin was evaluated by immunostaining method (Fig. 6B). As expected, podocin protein is expressed in podocytes. Importantly, podocin level was found to be higher in cells cultured on substrates having an elasticity ranging from 0.9 to 9.9 kPa than on the harder substrates. The expression of podocin proteins has been also evaluated by

western blot technique. As expected, the level of podocin was higher for the cells seeded on substrates of 2.1 and 9.9 kPa (Fig.7). This result is consistent with the previously reported data by Hu *et al.* who observed the same effect on podocytes phenotype but with gelatin substrates of a Young's modulus within the range of 2–5 kPa<sup>7</sup>. This range seems to be optimal for podocin expression and, thus, it is considered compatible with the stiffness of the glomerular basement membrane. Briefly, in this range of gel stiffness, podocytes upregulated the expression of podocin and downregulated the formation of actin filaments. Conversely, the stiffest gels upregulated actin stress fibers formation and downregulated podocin expression. These results showed strong correlation between the mechanical properties of a substrate and podocyte cell morphology, actin cytoskeleton reorganization, as well as the expression of podocin. Moreover, Hydrolyzed PAAm hydrogels with an elasticity ranging from 0.9 to 9.9 kPa seems to be optimal and it is consistent with the physiological stiffness of kidney glomerular basement membrane which is 2.5 kPa.

(A)



(B)

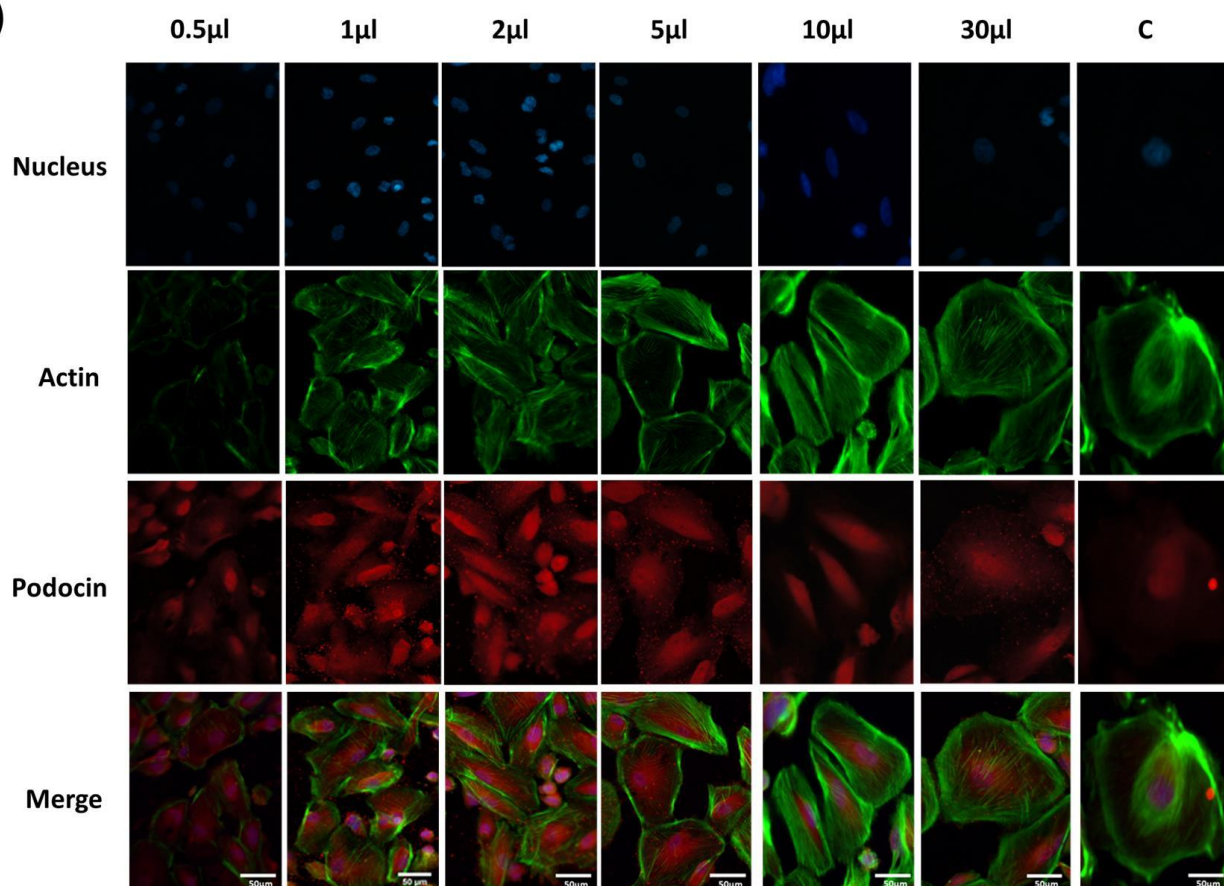


**Figure 6: (A) (B) Representative immunofluorescence images of podocytes cultured on PAAM substrates with an elasticity ranging from 0.6 to 44 kPa. The cells were detected by staining the nucleus (DAPI-blue), the actin cytoskeleton (Phalloidin-green) and Podocin protein (anti-Podocin-red). Scale bar 50  $\mu\text{m}$ . Podocyte cells sense and respond to substrates stiffness. Cell morphology was found to be elastic modulus dependent. Podocin expression is highly upregulated on PAAM membranes having elasticity of 0.9, 2 and 9.9 kPa, but decreased on the stiffest membranes.**



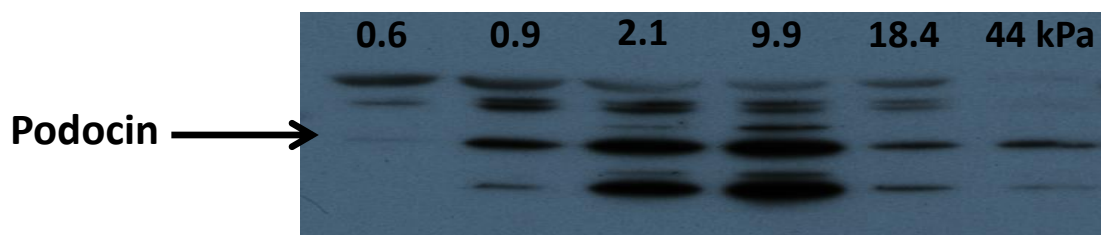


**Figure 7: Western Blot for the detection of podocin expression on PAAm hydrogels with various elasticity.**

Besides podocytes morphology, their mechanical properties can be affected by the substrate stiffness since the latter play an important role in the formation of actin filaments. AFM is a useful technique to determine the mechanical properties of living cells such as cells stiffness defined by Young's modulus measurements. AFM force spectroscopy mode has been applied to measure the Young's modulus of the whole cell and to analyze the statistical distribution of cell elasticity<sup>45,46,47</sup>.

Here, AFM was used to provide quantitative measurements of podocytes mechanical properties as a function of PAAm membranes stiffness. Typical force-volume images were gathered in Fig. 8. Panels represent the height of the contact point maps recorded during the force-volume measurement and Young's modulus maps for podocytes cultured on hydrolyzed PAAm hydrogels. The Young's modulus maps of podocytes cultured on the softest hydrogels (0.5 $\mu$ l and 1 $\mu$ l of Bis-acrylamide) showed a rather homogeneous stiffness distribution in contrast with the others. The distribution histograms of Young's modulus values for the different cases are presented in Fig. 8B.

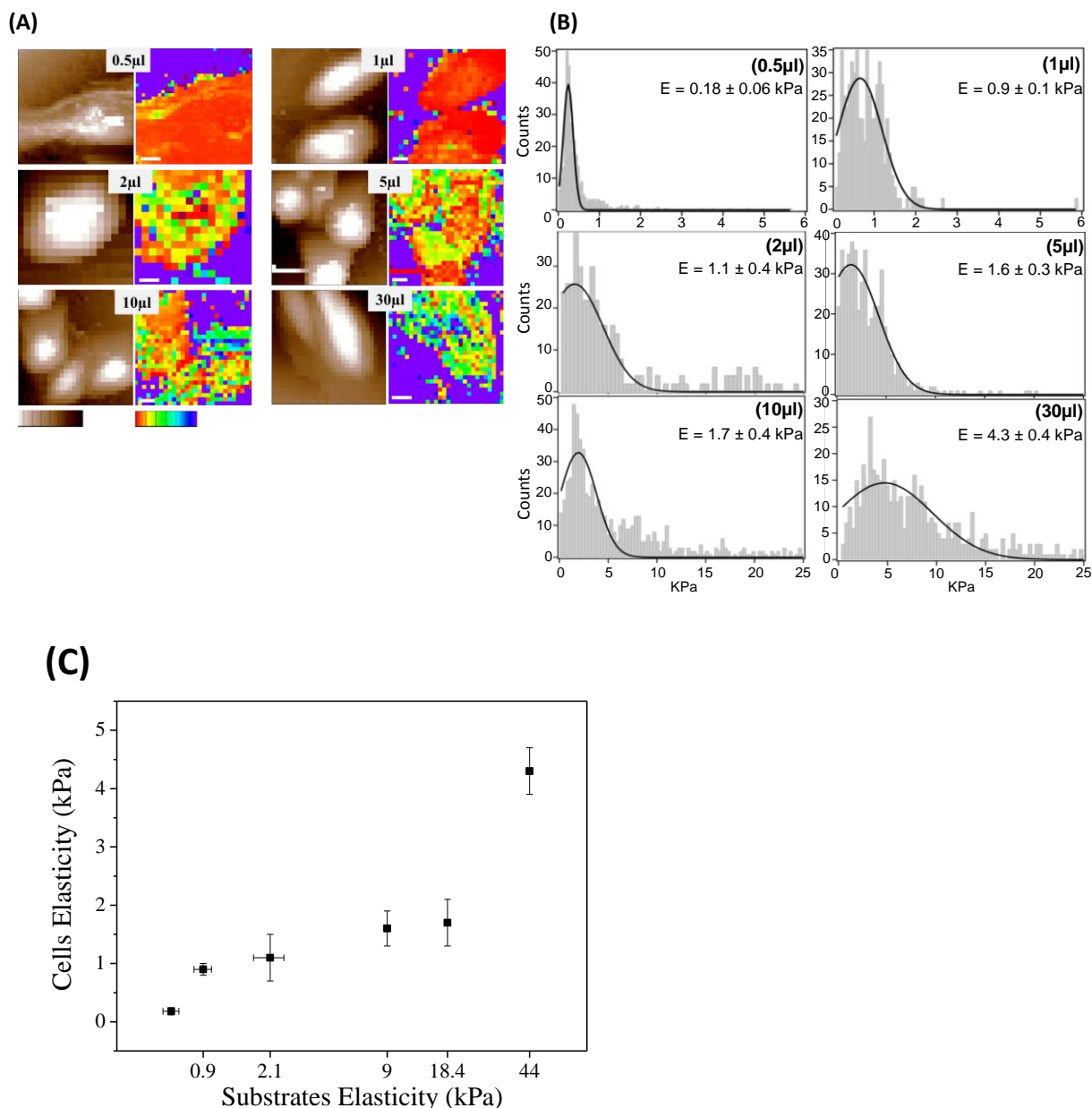


**Figure 8: Elasticity of podocytes cultured on PAAm membranes.** The diaphragms represent the height of the contact point and to the Young's modulus map. White scale bar in Young's modulus maps correspond to 10  $\mu\text{m}$ . Linear brown color bar goes from 0 to 12  $\mu\text{m}$ . Dark brown color represents deeper regions, while white depicts the higher portions of the cells. Linear scale bar goes from 0 to 16 kPa. Dark red color represents the softer portions, while blue and purple colors show the harder regions. **(B)** AFM elasticity distribution indicating podocyte elasticity for cells cultured on different samples. Young's moduli were best fitted using Gaussian distributions. **(C)** Evolution of the cells' Young's modulus ( $E$ ) as a function of hydrogel stiffness. The Young's Modulus increases significantly for podocytes cultured on M6 sample. Bars correspond to the obtained average of the Gaussian peaks fitted on the elasticity value distributions of individual force maps. Error bars are standard deviation of the mean.

The average Young's modulus values represent the evolution of the increase with hydrogel stiffness. Podocytes cultured on different substrates showed average Young's modulus of  $0.18 \pm 0.06$  kPa,  $0.9 \pm 0.1$  kPa,  $1.1 \pm 0.4$  kPa,  $1.6 \pm 0.3$  kPa,  $1.7 \pm 0.4$  kPa and  $4.3 \pm 0.4$  kPa respectively. Of note, substrates with Young's moduli ranging from 2 to 18 kPa did not cause significant variations in the cells elasticity. In contrast, the stiffest hydrogel produced an increase in podocyte stiffness. These results are consistent with the distribution of actin filaments shown in Figure 6, which corroborated the data that the actin cytoskeleton network have an essential role in determining mechanical stiffness of the cells<sup>48</sup>. Indeed for the softest substrates the low values of the Young's modulus can be assigned to the diffusive and random distribution of actin. For the stiffest substrates, the actin filaments were oriented and their sizes were moderately similar. For the substrate with the highest stiffness, the actin filament bundles were clearly larger to counterbalance the mechanical constraints exerted over the podocyte. Such increase in actin filaments size can thus explain the significantly higher Young's modulus of the podocytes.

## V. Conclusion:

In this work, the influence of PAAm hydrogel properties on podocytes was investigated. The Young's modulus of PAAm hydrogels was increased from 0.06 until 44 kPa by increasing the crosslinker concentration. The latter made the gel network more connected and thus less prone to swelling. The PAAm hydrogel is perfectly biocompatible for the podocytes in culture and did not alter their proliferation and viability. However, the substrates strongly influenced podocytes morphology and their mechanical properties. For the softest substrate having a Young's modulus of 0.6 kPa, the cells were less spread and were characterized by a

low level of podocin expression and a reduction in actin stress fiber formation. For the stiffest substrates  $E = 18$  and  $44$  kPa, podocyte cells were more spread. The mechanical stress of substrate induced the formation of actin fibers consequent to a downregulation of podocin expression. Podocytes cultured on hydrogel with stiffness ranging between  $0.9$  and  $9.9$  kPa, which is closer to the elasticity of the glomerular basement membrane provides the best conditions where normal regulation of podocytes markers e.g., podocin, occurs. According to the podocyte mechanical properties, regulation of actin stress fibers formation is optimal for substrates with stiffness ranging between  $2.1$  and  $9.9$  kPa. In addition, the presence of “foot processes” along all the above mentioned conditions makes PAAm hydrogel a worthy design to reproduce glomerular-like filtration process. In conclusion, our results present a new tool that will further contribute to better understand the behaviour of podocytes during both healthy and diseased states, and far beyond to develop a microfluidic kidney-on-chip device.

## VI. References:

- (1) Chapekar, M. S. Tissue Engineering: Challenges and Opportunities. *J. Biomed. Mater. Res.* **2000**, 53 (6), 617–620.
- (2) Korolj, A.; Laschinger, C.; James, C.; Hu, E.; Velikonja, C.; Smith, N.; Gu, I.; Ahadian, S.; Willette, R.; Radisic, M.; et al. Curvature Facilitates Podocyte Culture in a Biomimetic Platform. *Lab. Chip* **2018**, 18 (20), 3112–3128.
- (3) Janmey, P. A.; Miller, R. T. Mechanisms of Mechanical Signaling in Development and Disease. *J Cell Sci* **2011**, 124 (1), 9–18.
- (4) Caliri, S. R.; Burdick, J. A. A Practical Guide to Hydrogels for Cell Culture. *Nat. Methods* **2016**, 13 (5), 405–414.
- (5) Tse, J. R.; Engler, A. J. Preparation of Hydrogel Substrates with Tunable Mechanical Properties. *Curr. Protoc. Cell Biol.* **2010**, 47 (1), 10.16.1–10.16.16.
- (6) Palchesko, R. N.; Zhang, L.; Sun, Y.; Feinberg, A. W. Development of Polydimethylsiloxane Substrates with Tunable Elastic Modulus to Study Cell Mechanobiology in Muscle and Nerve. *PLOS ONE* **2012**, 7 (12), e51499.
- (7) Hu, M.; Azeloglu, E. U.; Ron, A.; Tran-Ba, K.-H.; Calizo, R. C.; Tavassoly, I.; Bhattacharya, S.; Jayaraman, G.; Chen, Y.; Rabinovich, V.; et al. A Biomimetic Gelatin-Based Platform Elicits a pro-Differentiation Effect on Podocytes through Mechanotransduction. *Sci. Rep.* **2017**, 7, 43934.
- (8) Wyss, H. M.; Henderson, J. M.; Byfield, F. J.; Bruggeman, L. A.; Ding, Y.; Huang, C.; Suh, J. H.; Franke, T.; Mele, E.; Pollak, M. R.; et al. Biophysical Properties of Normal and Diseased Renal Glomeruli. *Am. J. Physiol. - Cell Physiol.* **2011**, 300 (3), C397–C405.
- (9) Derieppe, M.; Delmas, Y.; Gennisson, J.-L.; Deminière, C.; Placier, S.; Tanter, M.; Combe, C.; Grenier, N. Detection of Intrarenal Microstructural Changes with Supersonic Shear Wave Elastography in Rats. *Eur. Radiol.* **2012**, 22 (1), 243–250.
- (10) Syed, S.; Karadaghy, A.; Zusiak, S. Simple Polyacrylamide-Based Multiwell Stiffness Assay for the Study of Stiffness-Dependent Cell Responses. *J. Vis. Exp. JoVE* **2015**, No. 97.

- (11) Wells, R. G. The Role of Matrix Stiffness in Regulating Cell Behavior. *Hepatology* **2008**, 47 (4), 1394–1400.
- (12) Chai, Q.; Jiao, Y.; Yu, X. Hydrogels for Biomedical Applications: Their Characteristics and the Mechanisms behind Them. *Gels* **2017**, 3 (1), 6.
- (13) Caló, E.; Khutoryanskiy, V. V. Biomedical Applications of Hydrogels: A Review of Patents and Commercial Products. *Eur. Polym. J.* **2015**, 65, 252–267.
- (14) Bassil, M.; Davenas, J.; EL Tahchi, M. Electrochemical Properties and Actuation Mechanisms of Polyacrylamide Hydrogel for Artificial Muscle Application. *Sens. Actuators B Chem.* **2008**, 134 (2), 496–501.
- (15) Bassil, M.; Ibrahim, M.; Tahchi, M. E. Artificial Muscular Microfibers: Hydrogel with High Speed Tunable Electroactivity. *Soft Matter* **2011**, 7 (10), 4833–4838.
- (16) Yahia, Lh.; Chirani, N.; Gritsch, L.; Motta, F. L.; SoumiaChirani; Fare, S. History and Applications of Hydrogels. *J. Biomed. Sci.* **2015**, 4 (2).
- (17) Bassil, M.; El Haj Moussa, G.; El Tahchi, M. Templating Polyacrylamide Hydrogel for Interconnected Microstructure and Improved Performance. *J. Appl. Polym. Sci.* **2018**, 135 (17), 46205.
- (18) Yeung, T.; Georges, P. C.; Flanagan, L. A.; Marg, B.; Ortiz, M.; Funaki, M.; Zahir, N.; Ming, W.; Weaver, V.; Janmey, P. A. Effects of Substrate Stiffness on Cell Morphology, Cytoskeletal Structure, and Adhesion. *Cell Motil.* **2005**, 60 (1), 24–34.
- (19) Flanagan, L. A.; Ju, Y.-E.; Marg, B.; Osterfield, M.; Janmey, P. A. Neurite Branching on Deformable Substrates. *Neuroreport* **2002**, 13 (18), 2411–2415.
- (20) Subramanian, A.; Lin, H.-Y. Crosslinked Chitosan: Its Physical Properties and the Effects of Matrix Stiffness on Chondrocyte Cell Morphology and Proliferation. *J. Biomed. Mater. Res. A* **2005**, 75A (3), 742–753.
- (21) Engler, A. J.; Sen, S.; Sweeney, H. L.; Discher, D. E. Matrix Elasticity Directs Stem Cell Lineage Specification. *Cell* **2006**, 126 (4), 677–689.
- (22) Solon, J.; Levental, I.; Sengupta, K.; Georges, P. C.; Janmey, P. A. Fibroblast Adaptation and Stiffness Matching to Soft Elastic Substrates. *Biophys. J.* **2007**, 93 (12), 4453–4461.

- (23) Miner, J. H. Glomerular Basement Membrane Composition and the Filtration Barrier. *Pediatr. Nephrol. Berl. Ger.* **2011**, *26* (9), 1413–1417.
- (24) Pavenstädt, H.; Kriz, W.; Kretzler, M. Cell Biology of the Glomerular Podocyte. *Physiol. Rev.* **2003**, *83* (1), 253–307.
- (25) Möller, C. C.; Flesche, J.; Reiser, J. Sensitizing the Slit Diaphragm with TRPC6 Ion Channels. *J. Am. Soc. Nephrol.* **2009**, *20* (5), 950–953.
- (26) Vining, K. H.; Mooney, D. J. Mechanical Forces Direct Stem Cell Behaviour in Development and Regeneration. *Nat. Rev. Mol. Cell Biol.* **2017**, *18* (12), 728–742.
- (27) Ueber Die Berührung Fester Elastischer Körper. *J. Für Reine Angew. Math. Crelles J.* **2009**, *1882* (92), 156–171.
- (28) Sneddon, I. N. The Relation between Load and Penetration in the Axisymmetric Boussinesq Problem for a Punch of Arbitrary Profile. *Int. J. Eng. Sci.* **1965**, *3* (1), 47–57.
- (29) Vinckier, A.; Semenza, G. Measuring Elasticity of Biological Materials by Atomic Force Microscopy. *FEBS Lett.* **1998**, *430* (1), 12–16.
- (30) Butt, H.-J.; Cappella, B.; Kappl, M. Force Measurements with the Atomic Force Microscope: Technique, Interpretation and Applications. *Surf. Sci. Rep.* **2005**, *59*, 1–152.
- (31) Martin, M.; Benzina, O.; Szabo, V.; Végh, A.-G.; Lucas, O.; Cloitre, T.; Scamps, F.; Gergely, C. Morphology and Nanomechanics of Sensory Neurons Growth Cones Following Peripheral Nerve Injury. *PLOS ONE* **2013**, *8* (2), e56286.
- (32) Radmacher, M.; Fritz, M.; Kacher, C. M.; Cleveland, J. P.; Hansma, P. K. Measuring the Viscoelastic Properties of Human Platelets with the Atomic Force Microscope. *Biophys. J.* **1996**, *70* (1), 556–567.
- (33) Boudou, T.; Ohayon, J.; Picart, C.; Tracqui, P. An Extended Relationship for the Characterization of Young's Modulus and Poisson's Ratio of Tunable Polyacrylamide Gels. *Biorheology* **2006**, *43* (6), 721–728.
- (34) Saleem, M. A.; O'Hare, M. J.; Reiser, J.; Coward, R. J.; Inward, C. D.; Farren, T.; Xing, C. Y.; Ni, L.; Mathieson, P. W.; Mundel, P. A Conditionally Immortalized Human Podocyte Cell

Line Demonstrating Nephrin and Podocin Expression. *J. Am. Soc. Nephrol. JASN* **2002**, *13* (3), 630–638.

(35) Bhadani Reena, Mitra Uttam Kumar. Studies on Water Absorbency of Polyacrylamide Hydrogels. *J. Mater. Sci. Eng. B* **2015**, *5* (11-12), 399–405.

(36) Grattoni, C. A.; Al-Sharji, H. H.; Yang, C.; Muggeridge, A. H.; Zimmerman, R. W. Rheology and Permeability of Crosslinked Polyacrylamide Gel. *J. Colloid Interface Sci.* **2001**, *240* (2), 601–607.

(37) Ferreira, L.; Vidal, M. M.; Gil, M. H. Design of a Drug-Delivery System Based On Polyacrylamide Hydrogels. Evaluation of Structural Properties. *Chem. Educ.* **2001**, *6* (2), 100–103.

(38) Zhang, X.; Yang, H.; Song, Y.; Zheng, Q. Influence of Crosslinking on Crystallization, Rheological, and Mechanical Behaviors of High Density Polyethylene/ethylene-Vinyl Acetate Copolymer Blends. *Polym. Eng. Sci.* **2014**, *54* (12), 2848–2858.

(39) Okay, O. General Properties of Hydrogels. In *Hydrogel Sensors and Actuators: Engineering and Technology*; Gerlach, G., Arndt, K.-F., Eds.; Springer Series on Chemical Sensors and Biosensors; Springer Berlin Heidelberg: Berlin, Heidelberg, 2010; pp 1–14.

(40) Hale, L. J.; Howden, S. E.; Phipson, B.; Lonsdale, A.; Er, P. X.; Ghobrial, I.; Hosawi, S.; Wilson, S.; Lawlor, K. T.; Khan, S.; et al. 3D Organoid-Derived Human Glomeruli for Personalised Podocyte Disease Modelling and Drug Screening. *Nat. Commun.* **2018**, *9* (1), 5167.

(41) Walcott, S.; Sun, S. X. A Mechanical Model of Actin Stress Fiber Formation and Substrate Elasticity Sensing in Adherent Cells. *Proc. Natl. Acad. Sci.* **2010**, *107* (17), 7757–7762.

(42) Reiser, J.; Altintas, M. M. Podocytes. *F1000Research* **2016**, *5*.

(43) Wagner, N.; Wagner, K.-D.; Xing, Y.; Scholz, H.; Schedl, A. The Major Podocyte Protein Nephlin Is Transcriptionally Activated by the Wilms' Tumor Suppressor WT1. *J. Am. Soc. Nephrol.* **2004**, *15* (12), 3044–3051.



- (44) Palmer, R. E.; Kotsianti, A.; Cadman, B.; Boyd, T.; Gerald, W.; Haber, D. A. WT1 Regulates the Expression of the Major Glomerular Podocyte Membrane Protein Podocalyxin. *Curr. Biol.* **2001**, *11* (22), 1805–1809.
- (45) Morkvėnaitė-Vilkončienė, I.; Ramanavičienė, A.; Ramanavičius, A. Atomic Force Microscopy as a Tool for the Investigation of Living Cells. *Med. Kaunas Lith.* **2013**, *49* (4), 155–164.
- (46) Suchodolskis, A.; Feiza, V.; Stirke, A.; Timonina, A.; Ramanaviciene, A.; Ramanavicius, A. Elastic Properties of Chemically Modified Baker's Yeast Cells Studied by AFM. *Surf. Interface Anal.* **2011**, *43* (13), 1636–1640.
- (47) Varga, B.; Martin-Fernandez, M.; Hilaire, C.; Sanchez-Vicente, A.; Areias, J.; Salsac, C.; Cuisinier, F. J. G.; Raoul, C.; Scamps, F.; Gergely, C. Myotube Elasticity of an Amyotrophic Lateral Sclerosis Mouse Model. *Sci. Rep.* **2018**, *8* (1), 1–10.
- (48) Thomas, G.; Burnham, N. A.; Camesano, T. A.; Wen, Q. Measuring the Mechanical Properties of Living Cells Using Atomic Force Microscopy. *J. Vis. Exp. JoVE* **2013**, No. 76.

## **Chapter IV: Enhancement of Podocyte Attachment on Polyacrylamide Hydrogel with Gelatin-based polymers**



## I. Introduction:

Recently, tissue engineering and regenerative medicine advancement are based on the development of a biomimetic extracellular matrix (ECM) providing structural support. Therefore, the main goal in this field is to design biological substitutes able to restore, maintain and enhance tissue functions<sup>1,2,3,4</sup>. ECM is defined as non-cellular bioactive component with well-organized dynamic structure network that provides biological environment and suitable mechanical support to control and modulate the cells properties such as proliferation, migration and differentiation<sup>5,6,7</sup>. Nowadays, a variety of biological (such as collagen, gelatin, chitosan and alginate) and synthetic (such as polyethylene glycol, polyacrylamide) hydrogels are widely used as suitable candidates to recapitulate the native ECM. Hydrogels are considered as biomaterials characterized by their capacity to hold a large amount of water essential for an optimal transport of both oxygen and nutrients. The mechanical properties, recapitulating cell local environment and biocompatibility of the hydrogel are tunable which can facilitate cell attachment and proliferation<sup>8,9,10,11,12,13</sup>.

Biological hydrogels derived from native ECM are recognized by the presence of biological active sites promoting the cell attachment, proliferation and differentiation. However, their limited mechanical properties are considered as a main disadvantage for tissue engineering applications<sup>14</sup>. Conversely, hydrogels based on synthetic polymers have robust mechanical properties<sup>15</sup> but the lack of biological active sites remains problem limiting the proliferation and the migration of the cells. Consequently, the combination of both biological and synthetic hydrogels, known as biosynthetic scaffolds, will be a promising way to improve the development of ECM for tissue engineering<sup>16,17,18</sup>.

Gelatin is a biocompatible, biodegradable and non-immunogenic biological polymer. According to these properties, gelatin-based hydrogels have been used in a wide range of

biomedical applications such as tissue engineering scaffolds, drug delivery systems and wound dressing. Gelatin is a natural polymer derived from collagen hydrolysis. After collagen denaturation, the bioactive properties are remained in the gelatin structure, which is determined by the presence of cell-binding sequences (Arg-Gly-Asp or RGD sequences) essential for cells attachment and matrix metalloproteinase degradable (MMP) sequences. However, these hydrogels have restrictions toward the *in vivo* applications due to the poor and limited mechanical properties and undergoes rapid degradation with enzymes like collagenase<sup>10,19,20,21</sup>. Thus, gelatin-based hydrogels are chemically crosslinked to improve their mechanical properties and to avoid their degradation. For instance, glutaraldehyde<sup>22</sup> and diisocyanate<sup>23</sup> were widely used as crosslinkers but their cytotoxicity limits their applications in tissue engineering<sup>24</sup>. The acrylate modified gelatin, widely known as gelatin methacrylate (GelMA) are chemically tunable, biocompatible and biodegradable, and provide an appropriate environment for a wide variety of cells<sup>25</sup>. GelMA-based hydrogels contain cell-binding sequence such as RGD sequence and MMP sequence implicated in cells remodeling. Due to these properties, GelMA-based hydrogels are considered as promising material that mimic the microenvironment of natural tissues<sup>26,27,28</sup>. Moreover, the modification of GelMA hydrogels mechanical properties in order to get a suitable hydrogel mimicking the target tissue can be performed by incorporating various biomaterials. For this reason, GelMA hybrid scaffolds have been used as a scaffold material in a wide variety of tissue engineering applications, including kidney, bone and cartilage tissues due to their suitable biological properties and tunable mechanical characteristics.

Synthetic polyacrylamide hydrogels have also been also widely used as scaffold matrices for cell culture with robust tunable mechanical properties. However, the deficiency in biological

active domains requires their functionalization with ECM proteins such as collagen and fibronectin<sup>29</sup>.

The biological and synthetic polymers based hydrogels limitations can be improved by the development of novel hydrogels based tissue scaffolds formed by the combination of biological and synthetic materials in order to imitate the heterogeneity of native ECM. This study aims to synthesize hybrid hydrogel using acrylamide and GelMA in order to establish a robust mechanical network with the preservation of the biological properties. The influence of the polymers concentrations on the mechanical properties of the hybrid hydrogels has been studied. Furthermore, the biocompatibility, the swelling capacity and the influence of hydrogel composition on cells behaviors has been also analyzed.

## **II. Materials and Methods:**

### **1. Synthesis of GelMA:**

Gelatin Methacrylamide was prepared by the reaction of gelatin with methacrylic anhydride (Fig. 1) depending on previous described methods<sup>30</sup>. Briefly, 5g of gelatin (Gelatin from Porcine Skin, Sigma Aldrich, 48722) was dissolved in 45ml of phosphate buffer saline (PBS, Sigma Aldrich, P4417) at 60°C. After gelatin dissolution, 1ml of methacrylic anhydride (MA, Sigma Aldrich, 276685) was gently added to gelatin solution with a vigorous stirring for 3 H at 60°C.

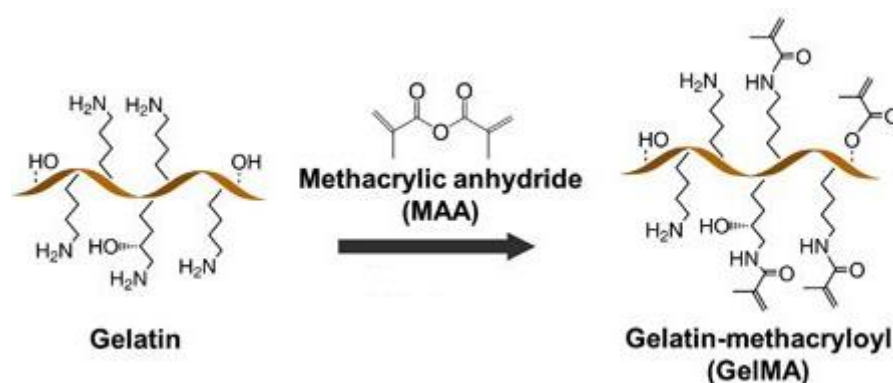


Figure 1: Synthesis of GelMA

Afterwards, the mixture was dialyzed for 7 days against distilled water at 40°C using dialysis membrane with a molecular weight cut-off of 12-14 kDa. Finally, the resultant GelMA solution was pre-freeze at -20°C for overnight and then freeze-dried for 7 days.

## 2. Preparation of GelMA-PAAm hydrogels:

The GelMA-PAA hydrogels were prepared by co-polymerized acrylamide and GelMA. The GelMA provide the biological functions needed for cell adhesion and proliferation, while the flexible polyacrylamide chains reinforced the gelatin network. Acrylamide (AAm, Sigma Aldrich, A8887, 79-06-1, purity >99%) (5% (w/v) and 2.5% (w/v): AAm concentrations) was mixed with GelMA solutions (5% (w/v) and 3% (w/v): GelMA concentrations). This reaction was initiated using ammonium persulfate (APS, 25% (w/v), Sigma Aldrich, 248614, 7727-54-0, purity > 98%) and catalyzed by *N,N,N',N'* Tetramethylethylenediamine (TEMED, Sigma Aldrich, T7024, 110-18-9). The mixture was poured in glass molds and the polymerization was achieved at room temperature for 3 H.

## 3. Swelling Measurements:

AAm-GelMA based hydrogels were incubated in water and phosphate buffer saline (PBS) at room temperature until the equilibrium is reached. The swelling degree was measured by

determining the difference between the weight of a fully swollen hydrogel and the weight of dried samples after freeze-dry for overnight.

#### **4. Fourier Transform Infrared Spectroscopy (FT-IR):**

The FT-IR spectra of freeze-dried GelMA-PAAm hydrogels were analyzed by NEXUS instrument, fitted with an attenuated total reflection (ATR) accessory. The spectra were recorded in the frequency range of 500 - 4000  $\text{cm}^{-1}$  at 4  $\text{cm}^{-1}$  resolution.

#### **5. Mechanical Characterization:**

##### **a. Atomic Force Microscopy (AFM):**

The AFM experimental system used for force-spectroscopy measurements was an Asylum MFP-3D head coupled to a Molecular Force Probe 3D controller (Asylum Research, Santa Barbara, CA, USA). Triangular silicon nitride D cantilevers (MLCT, Veeco) with a nominal spring constant of 30 pN/nm, length of 225  $\mu\text{m}$ , width of 20 nm, resonance frequency of 15 kHz, half-opening angle of  $17.5^\circ \pm 2.5^\circ$  and a nominal radius of 20 nm were used. The cantilever spring constant was determined in liquid using the thermal noise method available within the MFP-3D software. Hydrogel samples were glued to a Petri dish with double-faced adhesive tape, and covered with 0.5 ml of deionized water. After testing a range of loading forces on the hydrogel surface, the measurements were performed in liquid and at room temperature with a maximum loading force of 5 nN corresponding to a maximal indentation depth of 0.3  $\mu\text{m}$ . Elastic deformation was obtained from the recorded force curves as a function of the loading force applied by the tip. Young's modulus ( $E$ ) was calculated for each force from the approaching part of the curve, using a modified Hertz model, based on the work of Sneddon and further developed for different AFM tip shapes, as described elsewhere. An approach velocity of 6  $\mu\text{m/s}$  was chosen, indicating a piezo-



extension rate of 3 Hz to minimize hydrodynamic and viscoelastic artifacts. The Poisson's ratio of the cells was assumed to be 0.5, as suggested for incompressible materials. Furthermore, to investigate cells' nanomechanical properties on each sample, we repeated the force spectroscopy experiment using the same parameters.

### **b. Rheology:**

The mechanical properties of PAAm hydrogels fully swelled in cell media were characterized using Anton Paar Physica MCR 301 rheometer. In this study, the viscoelastic properties were investigated by applying an oscillatory force on the surface of the hydrogel using a metal plate (Anton Paar PP25, 25mm in diameter). The rheology measurements were recorded with a frequency of 1 Hz, strain amplitude of 1 % and a fixed force of 0.5 N.

$$G=G'+G'' \quad (1)$$

Where  $G'$  represents the storage modulus that corresponds to the elastic property and  $G''$  represents the loss modulus corresponding to the viscous behavior.

## **6. Cell culture:**

Human podocyte cell line was purchased from the Faculty of Medicine, University of Bristol, UK. According to the supplier protocol, immortalized human podocytes cell lines were cultured, proliferated at 33°C and then differentiated at 37°C using a RPMI – 1640 Medium (Sigma Aldrich, R8758) supplemented with 1 % insulin-transferrin-Selenium liquid media supplement (Sigma Aldrich, I3146), 10 % fetal bovine serum (Sigma Aldrich, F7524) and Penicillin Streptomycin solution (Sigma Aldrich, P4333). Cells were collected and plated on the GelMA-AAm polymer hydrogels having various mechanical properties. For immunocytochemical characterization, podocytes cells were fixed with 2% of paraformaldehyde (PFA) (Sigma Aldrich, P6148, 30525-89-4) for 15 min at RT. The

permeabilization of podocytes cells was performed by using 0.5 % Triton X-100 (Sigma Aldrich, X100, 9002-93-1) for 15 min at 37°C. Then, the blocking solution composed of 1 % of Bovine Serum Albumin (BSA) (Sigma Aldrich, A2153, 9048-46-8) and 0.5% of Triton-X in PBS was used to block the non-specific protein binding sites. Then, cells were incubated overnight at 4°C with a primary anti-podocin antibody (Sigma Aldrich, P0372) and with secondary anti-rabbit antibody (Alexa Fluor®594, Cat: ab150080) for 1h in dark at room temperature. The DAPI (Sigma Aldrich, D9542) and Phalloidin staining (Invitrogen, Cat: A12379) were used to visualize the nucleus and the actin cytoskeleton, respectively. Staining images were taken using Nikon TE2000 microscope.

### **III. Results:**

Three GelMA-PAAm hydrogels scaffolds of this study having different polymers concentrations: GelMA<sub>3%</sub>-AAm<sub>2.5%</sub>, GelMA<sub>3%</sub>-AAm<sub>5%</sub> and GelMA<sub>5%</sub>-AAm<sub>5%</sub> are prepared and their mechanical and structural properties are characterized. In addition, the interaction between the scaffolds and podocytes cells is investigated.

#### **1. H-NMR of Gelatin Methacrylamide:**

The methacrylation degree of gelatin was determined from <sup>1</sup>H NMR spectroscopy (Fig.2). Phenyl alanine signal observed between 7.2 - 7.4 ppm was integrated to 5 protons. Further, the acrylate signal observed at 5.3 and 5.7 ppm confirms the successful substitution of methacrylate on gelatin. The ratio between the area of acrylate peak and phenyl alanine was calculated to determine the degree of methacrylate substitution in gelatin. It was found to be 36%. Optimal degree of methacrylation is crucial to avoid high degree of crosslinking. High degree of methacrylation leads to higher crosslinking density which affects cell

spreading and long term survival. Sutter *et al.* showed that the degree of methacrylation in gelatin is tunable by changing the concentration of methyl methacrylate concentration<sup>31,32</sup>. In this study, 1.4 mmol of methyl methacrylate per gram of gelatin was utilized in order to obtain low degree of functionalization of methyl methacrylate on gelatin as evidenced from NMR (36%).

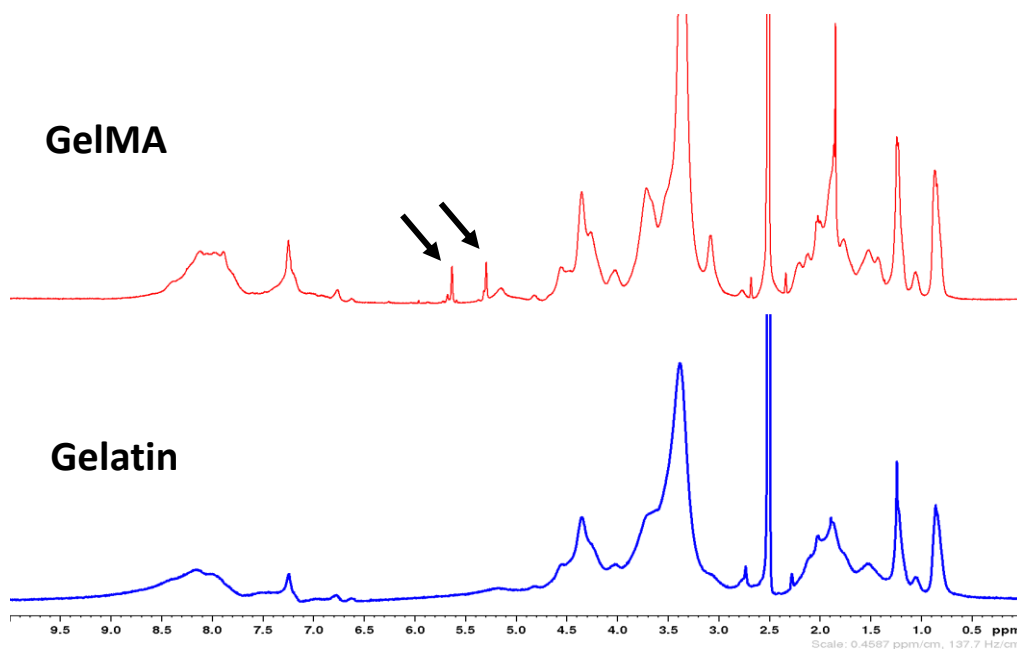


Figure 2: <sup>1</sup>H-NMR of gelatin and modified gelatin (methacrylamide gelatin GelMA).

## 2. FT-IR of hydrogel material:

FTIR spectra of gelatin and polymerized gelatin methacrylate/polyacrylamide hydrogels are shown in Fig. 3. Characteristic peaks of gelatin amide I, amide II are observed at 1630 and 1525 cm<sup>-1</sup> respectively.

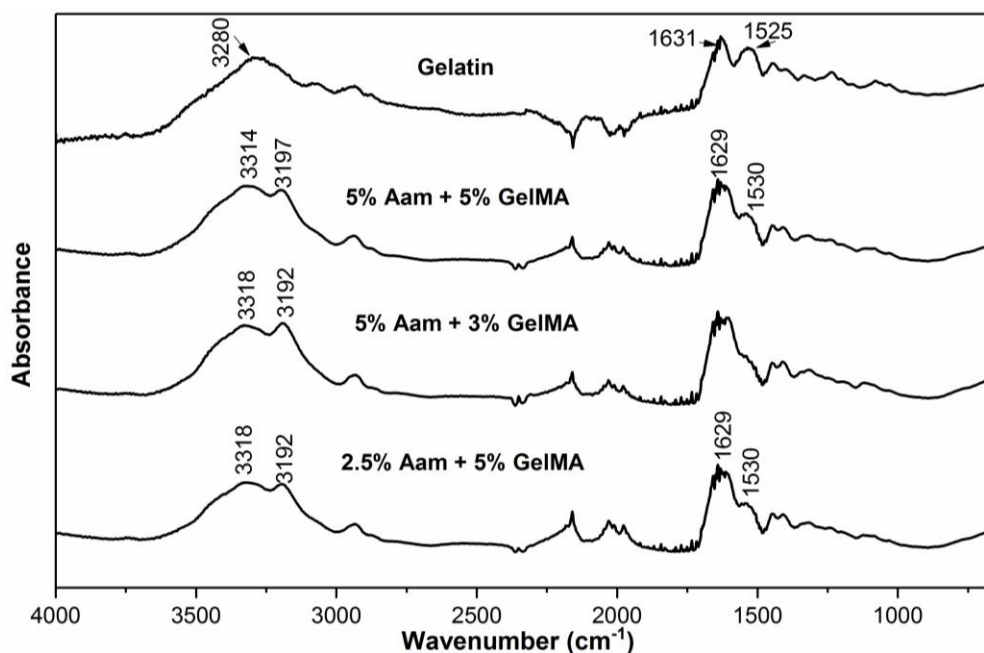


Figure 3: FT-IR of pure gelatin and GelMA-AAm interpenetrated polymer network

Broad peak observed at  $3280\text{ cm}^{-1}$  for gelatin corresponds to the O-H and N-H stretching. Peak observed at  $3070\text{ cm}^{-1}$  corresponds to N-H stretching of gelatin. GelMA/polyacrylamide hydrogel display two broad peaks at  $3197$  and  $3314\text{ cm}^{-1}$  which is also associated with the N-H stretching vibration of polyacrylamide. Generally, C-O stretching and N-H bending of polyacrylamide are observed at  $1645$  and  $1604\text{ cm}^{-1}$ . Broad peak observed between  $1500 - 1650\text{ cm}^{-1}$  for GelMA/AAm hydrogel is due to the combination of gelatin and PAAm C-O stretching vibration<sup>33</sup>.

### 3. Swelling Characterization:

Swelling property is a main characteristic of hydrogels involved in tissue engineering applications. The swelling mechanism is defined by the ability of hydrogels to absorb a large quantity of suitable solvent without dissolving. The equilibrium swelling is reached according to the osmotic and elastic forces of the material. Many factors are involved in the swelling mechanisms of polymer network such as crosslink density, molecular weight of polymers and polymer-solvent interactions. The solvent uptake is correlated with the network

structure of hydrogels which has an effect on the transport of nutrients and oxygen, through the hydrogel network. The swelling properties are highly affected by the density of hydrogels crosslinking network. The swelling ratio degree was calculated using this following equation:

$$S = \frac{W_s - W_d}{W_d} \quad (1),$$

where  $W_s$  is the weight of the fully swollen gel (in deionized water and PBS) and  $W_d$  is the weight of dry gel. Figure 4 indicates the effect of the concentration of GelMA and AAm on the swelling ratio degree. The degree of swelling for GelMA-PAAm hydrogels was influenced by the change of the GelMA and AAm concentrations.

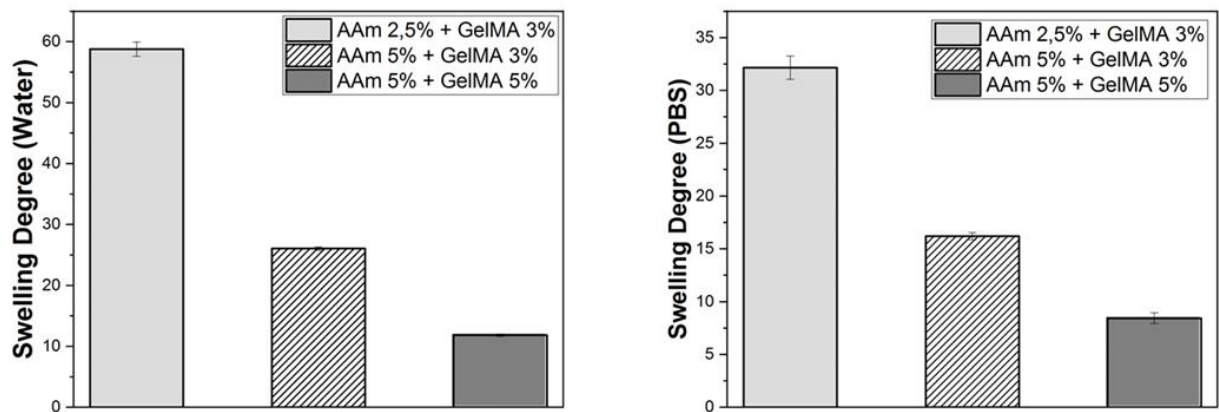


**Figure 4: Representative histogram of swelling degree as a function of acrylamide and GelMA concentrations.**

Briefly, the swelling degree increases as the concentrations AAm and/or GelMA decreases. Gelatin molecule contains multiple arms of methacrylic substitution which can acts as a crosslinker between GelMA molecules and acrylamide (Fig. 5).

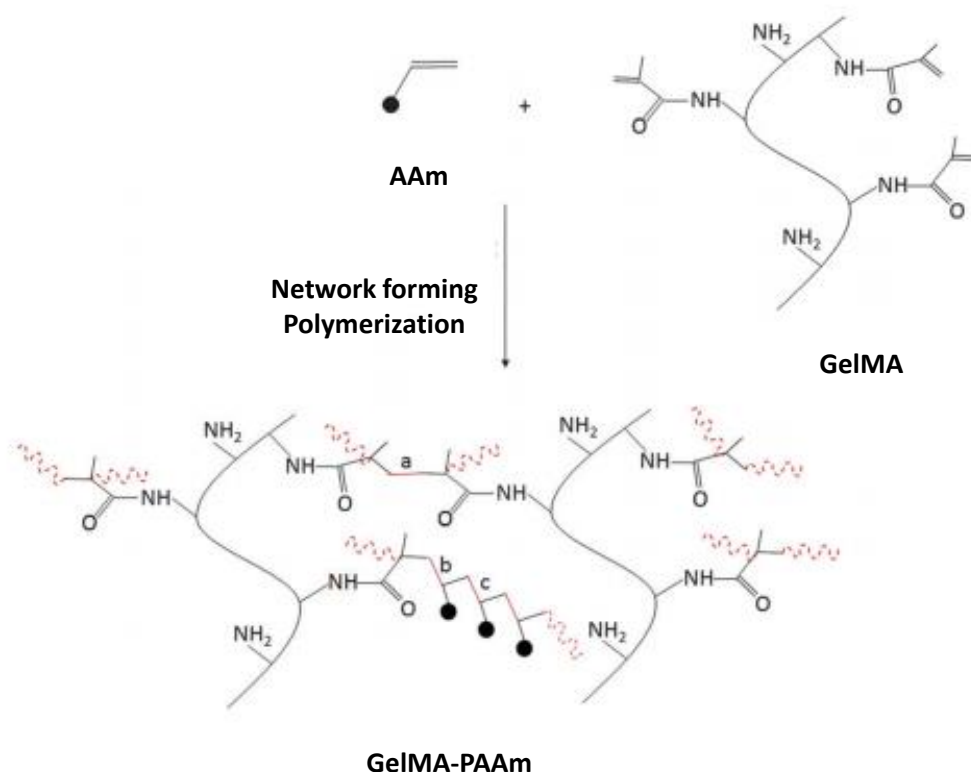


**Figure 5: Schematic simplified view of GELMA-PAAm sequences: (a) GELMA-GELMA macromolecules; (b) GELMA-AAm; (c) AAm-AAm**

The increase of AAm concentrations from 2.5% to 5% is correlated with a significantly decrease of hydrogels swelling degree. Moreover, the increase of GelMA crosslinker concentrations from 3% to 5% decreases the swelling capacity of hydrogels in both water and PBS swelling medium. Swelling test shows that the high crosslinking degree of polymer network hinders the swelling of hydrogels. This phenomenon can be explained by the effect of GelMA crosslinker on the density of polymer network; the increase of the GelMA concentrations contributes to a highly covalent crosslinked polymer network density. In addition, the swelling capacity can be restricted due to the presence of hydrogen bonds within the gelatin chains. The increase of AAm concentrations also ensures a highly connected polymer network.

The density of GelMA-PAAm hydrogels was evaluated by Scanning Electron Microscopy (SEM) (Fig.6). SEM results show that GelMA-PAAm based hydrogels exhibit highly connected and compacted network structure for the higher concentrations of AAm and GelMA crosslinker. This confirms the influence of the crosslinking network density on the swelling capacity.

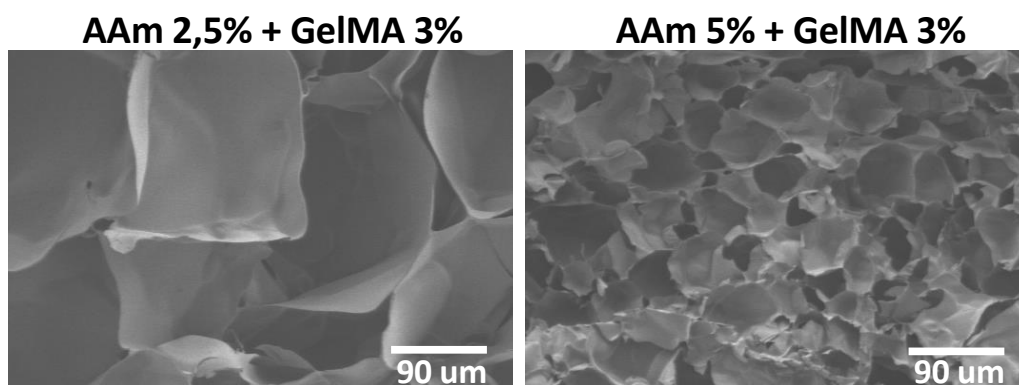


**Figure 6: Scanning Electron Microscopy for GelMA-AAm based hydrogel having different polymers concentrations**

#### **4. Mechanical Properties:**

The composition of hydrogel has an impact on their mechanical properties. Mechanical characterization of fully swollen network in cell medium was conducted using atomic force microscopy (AFM). Force curves were measured on GelMA-PAAm hydrogels having different concentrations of AAm and GelMA crosslinker corresponding to AAm<sub>2.5%</sub> + GelMA<sub>3%</sub>, AAm<sub>5%</sub> + GelMA<sub>3%</sub> and AAm<sub>5%</sub> + GelMA<sub>5%</sub>. The measurements of hydrogels elasticity were performed. For all samples, force-volume images, constructed from force curves collected at each point in a two-dimensional scan, were acquired in relative triggering mode. Typical quantitative information from these Young's modulus maps are presented in Fig. 7A, where histograms were best fitted with a Gaussian. The Young's modulus values of AAm<sub>2.5%</sub> + GelMA<sub>3%</sub>, AAm<sub>5%</sub> +

GelMA<sub>3%</sub> and AAm<sub>5%</sub> + GelMA<sub>5%</sub> are  $4.03 \pm 0.54$  kPa,  $11.82 \pm 0.49$  kPa and  $24.98 \pm 3.68$  kPa respectively (Fig. 7B). This means that the hydrogels stiffness increases as the concentrations of the GelMA crosslinker or the AAm monomer are increased.

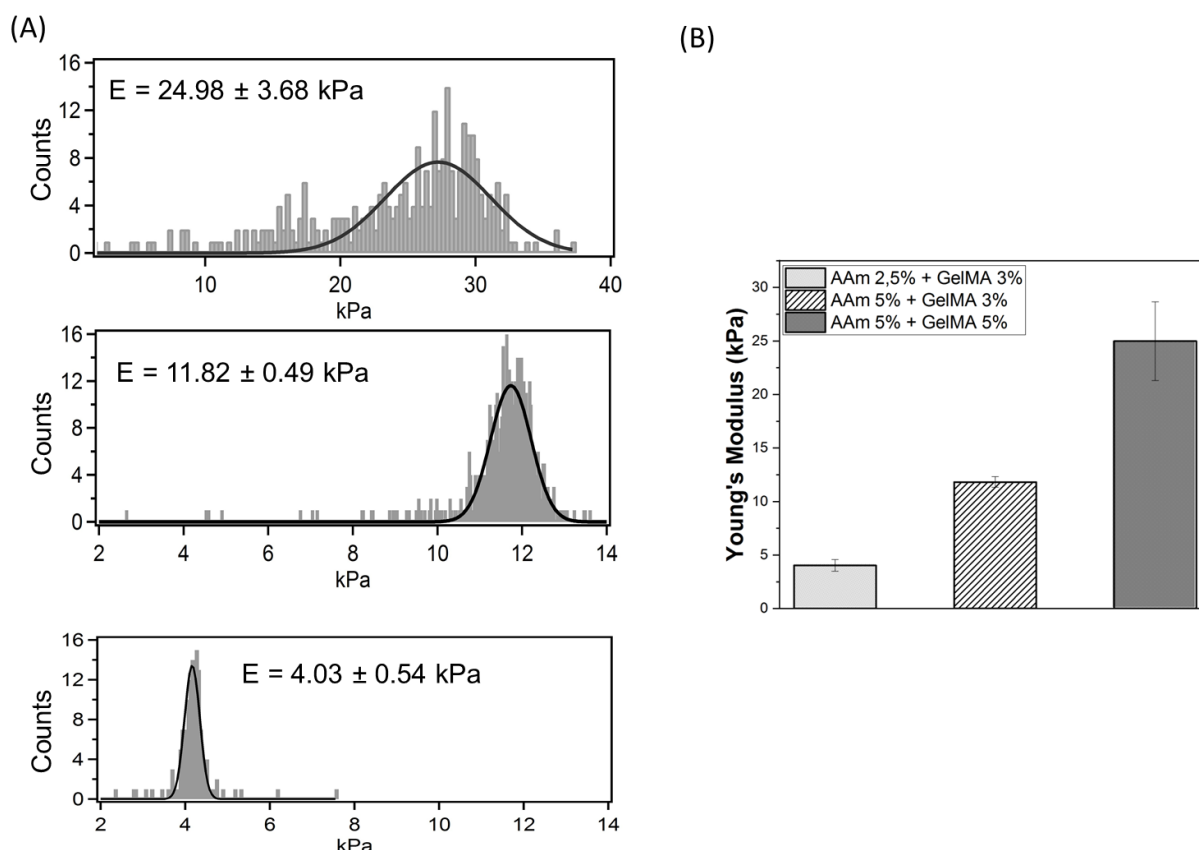


**Figure 7: (A) Elasticity distribution of GelMA-PAAm hydrogels swelled in cell medium. Young's moduli were fitted with Gaussian distributions. (B) Evolution of the Young's modulus "E" as a function of GelMA and AAm concentrations. The Young's modulus increases with the increase of the GelMA and AAm concentrations**

Moreover, dynamic shear oscillation measurements were used to characterize the viscoelastic properties of the hydrogels. The elastic modulus ( $G'$ ) of GelMA-PAAm, known as storage modulus, is characterized by the capability of hydrogels to have a recoverable energy. The storage modulus ( $G'$ ) are  $1129 \pm 53$  Pa for AAm<sub>2.5%</sub> + GelMA<sub>3%</sub>,  $1833 \pm 48$  Pa for The AAm<sub>5%</sub> + GelMA<sub>3%</sub> and  $2136 \pm 258$  Pa for AAm<sub>5%</sub> + GelMA<sub>5%</sub> (Fig. 8). Therefore, the increase of the storage modulus ( $G'$ ) is related to the crosslinker and AAm monomer concentrations. As a consequence, the high concentration of AAm and GelMA increases the



viscoelastic properties of the hydrogels. These results are consistent with the work reported by Van Den Bulcke *et al.* who's shown that the rheological properties of the gelatin based hydrogels depend on the monomer and crosslinker concentrations of the polymer network<sup>30</sup>. GelMA-PAAm mechanical properties have shown an adjustable elasticity with a broad range that permits to mimic the elasticity of glomerular basement membrane.

To sum up, our results have shown a correlation between the swelling properties and the mechanical properties of GelMA-PAAm based hydrogels. The increase of monomer and crosslinker concentrations contributes to the increase of the mechanical properties and leads to decrease the swelling activity.

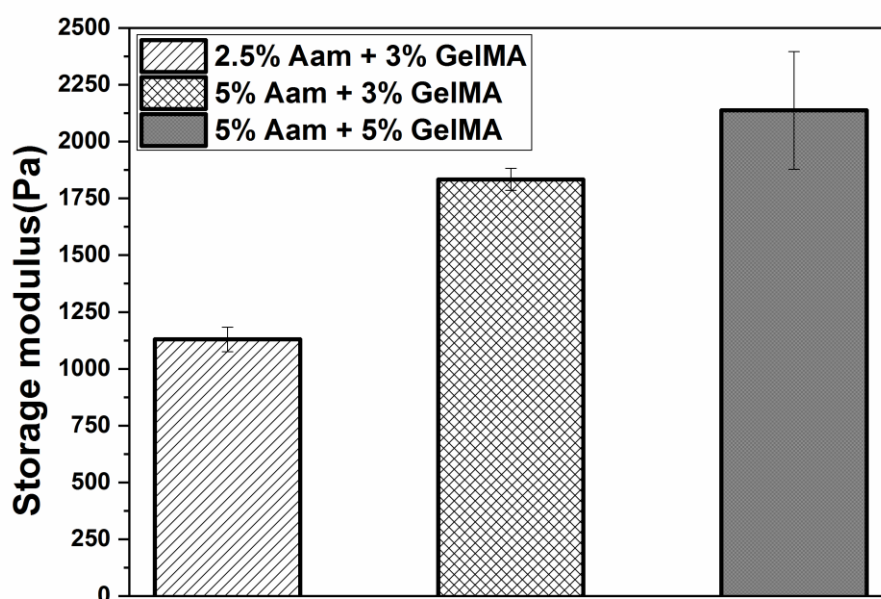


**Figure 8:** The storage modulus of GelMA-PAAm membranes fully swelled in water was determined as function GelMA and AAm concentrations. (Error Bar = Standard Deviation)

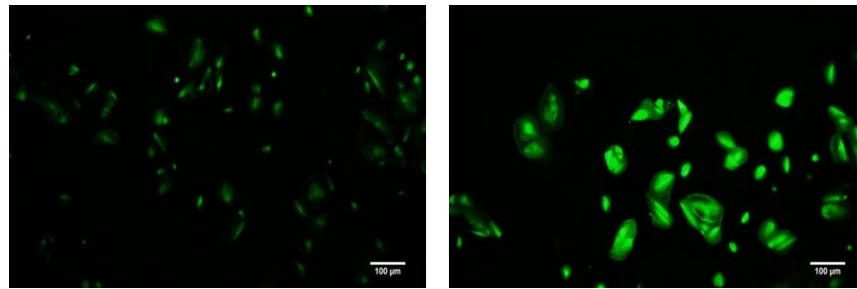
## 5. Podocytes Cells Culture:

The ECM mechanical properties induce and maintain the cells migration, proliferation and differentiation. The alteration of the elastic environment provides the development of tissue diseases<sup>34,35,36</sup>. In this study, immortalized podocyte cell line was used to investigate the effect of hydrogels mechanical properties on podocyte behavior. The podocytes are highly specialized epithelial cells of the kidney glomerulus that provide a filtration barrier preventing the passage of plasma proteins<sup>37</sup>. Research studies have shown the effect of the glomerular basement membrane (GBM) on podocytes properties. Typically, the stiffness of kidney glomerulus basement membrane measured by magnetic bead displacement is about 2.4 kPa and the change of GBM stiffness is correlated to the progression of renal diseases such as nephropathy kidney disease<sup>38</sup>. GelMA-PAAm hydrogels having various mechanical properties were developed and used as synthetic extracellular matrix supports for podocyte cells. The study of the effect of GelMA-PAAm mechanical properties on podocyte behaviors has been evaluated.

After 24hrs of seeding cells on GelMA-PAAm hydrogels and exchanging cell medium, podocyte cells viability was assessed using Live assay (Calcein). Figure 9A shows the adhesion of podocyte cells on GelMA-PAAm substrates and a homogeneous distribution of these cells. The adhesion of podocytes is related to the presence of gelatin cell-binding sequences indispensable for cells attachment. To mention that the podocytes adhesion does not occur on non-functionalized polyacrylamide based hydrogels. In addition, the cell viability test confirms the non-cytotoxicity of the GelMA-PAAm scaffolds on podocyte cells. Extracellular matrix mechanical properties have an effect on the cells morphology and cytoskeletal organization. The actin cytoskeleton of adherent podocyte cells were investigated using Phalloidin staining (Fig. 9B). Results have shown the effect of GelMA and AAm

concentrations on cells morphology and actin filaments organization. Podocyte morphology is not fully spread on the softest substrate (AAm<sub>2.5%</sub> + GelMA<sub>3%</sub>) while these cells on the stiffest substrate (AAm<sub>5%</sub> + GelMA<sub>5%</sub>) have exhibited a larger spread area with extended cytoplasm. The organization of actin cytoskeleton responds to the mechanical stress of the extracellular matrix through the transmembrane receptors called integrin. Basically, cells detect the increase of environment stiffness and react by increasing the integrin assembling which contributes to the development of stress fibers. The visualization of actin filament shows a dense actin cytoskeleton on the stiffest substrate (AAm<sub>5%</sub> + GelMA<sub>5%</sub>) compared to the softest substrate (AAm<sub>2.5%</sub> + GelMA<sub>3%</sub>) (Fig. 9B). The podocytes are characterized by the presence of several proteins implicated in the glomerular filtration barrier such as podocin and nephrin<sup>39</sup>. The results have shown a significant expression of podocin for podocytes cells on the softest substrates (AAm<sub>2.5%</sub> + GelMA<sub>3%</sub>) and (AAm<sub>5%</sub> + GelMA<sub>3%</sub>) while the podocin expression on the stiffest substrate (AAm<sub>5%</sub> + GelMA<sub>5%</sub>) decreases remarkably. Research studies have shown that podocytes cells cultured on substrates with elasticity of 3 – 5 kPa present similarities of actin fibers and focal adhesions to *in-vivo* ones. Consequently, depending on swelling characterization and mechanical properties, AAm<sub>2.5%</sub> + GelMA<sub>3%</sub> and AAm<sub>5%</sub> + GelMA<sub>3%</sub> are good candidates as matrix substrates for podocytes adhesion, proliferation and differentiation.

(A)



(B)

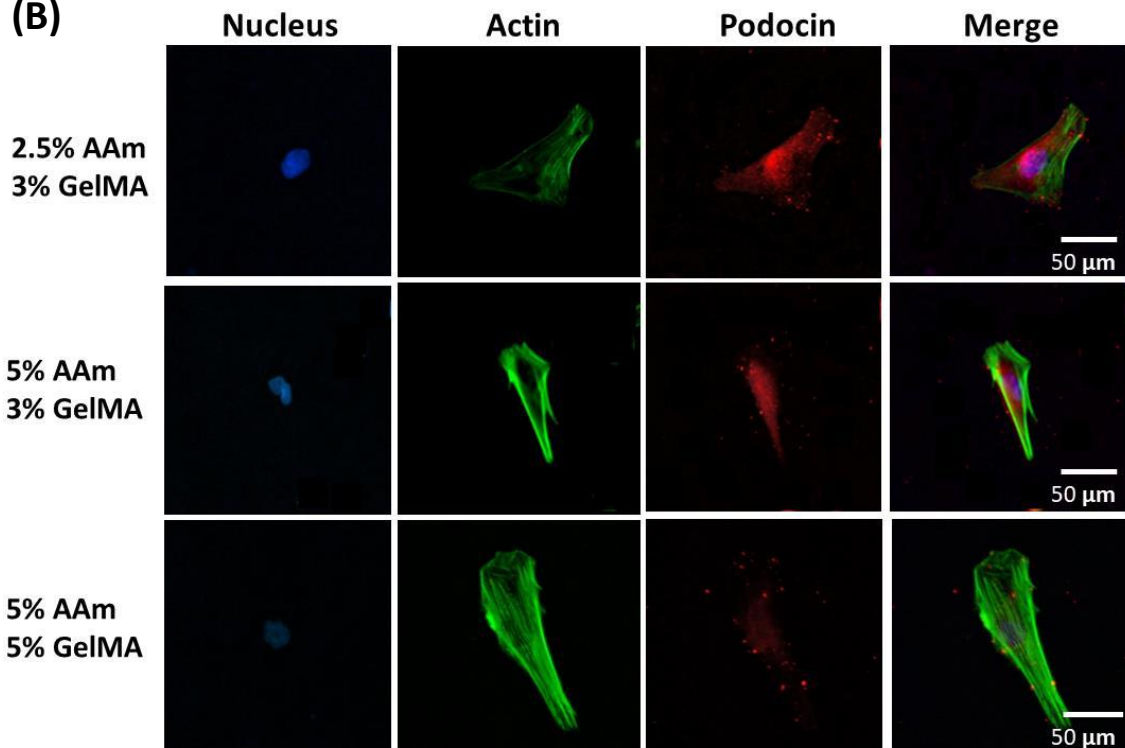


Figure 9: (A) Podocyte cells stained with calcein for the determination of cells viability. (B) Representative immunofluorescence images of podocytes cultured on GelMA-PAAm substrates having various mechanical properties. The cells were detected by staining the actin cytoskeleton, the nucleus and Podocin protein using Phalloidin (green), DAPI (blue) and anti-Podocin antibody (red) respectively.

## 6. Cells Elasticity:

AFM is a useful technique consisting to map different locations of cells and to provide quantitative measurements known by the young's modulus parameter of the local stiffness of the cell surface. Research studies have shown the effect of the cellular biological activities such as cells adhesion, proliferation, actin filaments organization and differentiation on the

mechanical properties of the cells and specifically on cells stiffness. In fact, the indentation responses of cells are mostly affected by the mechanical properties of the cell membrane and the subcellular components such as the cytoskeleton and the nucleus<sup>40</sup>. The mechanical properties of podocyte cells seeded on GelMA-PAAm hydrogels having different concentrations of AAm and GelMA were performed by AFM. The results have shown that the mechanical properties of podocyte cells can be affected by the substrates elasticity. Podocytes cultured on AAm<sub>2.5%</sub> + GelMA<sub>3%</sub>, AAm<sub>5%</sub> + GelMA<sub>3%</sub> and AAm<sub>5%</sub> + GelMA<sub>5%</sub> have shown an elasticity of  $0.46 \pm 4.35$  kPa,  $4.3 \pm$  kPa and  $11.65 \pm$  kPa respectively. Therefore, the podocyte elasticity increases with increasing the mechanical properties of GelMA-PAAm substrates. A correlation between the actin filaments and the cell stiffness was investigated and has shown a significant decrease on cells elasticity with the dissolution of actin cytoskeleton. Thus, the results of cell stiffness are correlated with the cell staining results. Podocytes have shown a dense actin cytoskeleton on the stiffest GelMA-PAAm substrate which explains the increase of the podocyte cells stiffness.

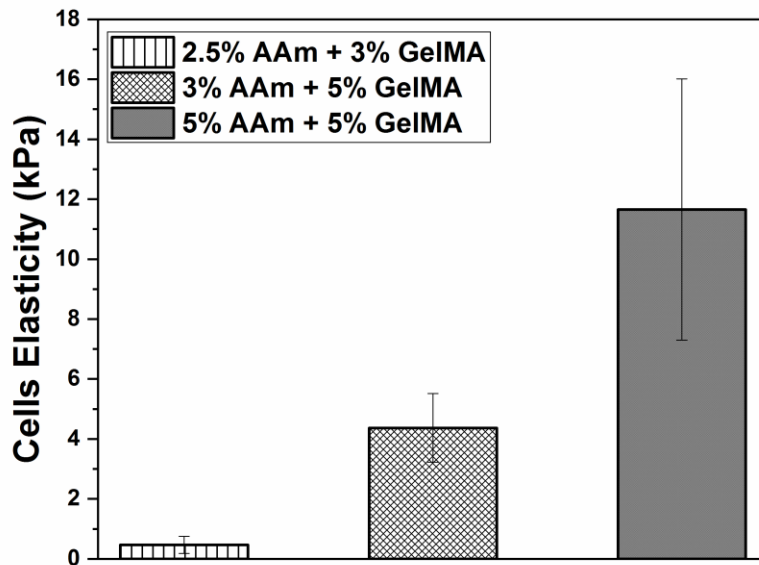


Figure 10: Evolution of the Young's modulus ( $E$ ) as a function of AAm and GelMA concentrations. Bars represent the obtained average of the Gaussian peaks fitted on the elasticity value distribution of individual force maps. Error bars are standard deviation of the mean.

#### IV. Conclusion:

The development of the polymer network based on the combination of biological and synthetic polymers improves the mechanical integrity and the cytocompatibility properties. Here, we investigated the GelMA-AAm hydrogels having different concentration. The characterization of swelling and mechanical properties of these hybrid hydrogels was determined and tunable by adjusting the concentrations of the polymers. The study of podocyte behaviors was conducted on GelMA-AAm hydrogels having different mechanical properties. The swelling study shows that an increase in the polymers concentrations contributes to a decrease in the hydrogel water uptake. Moreover, the crosslinking density of the GelMA-AAm hydrogel depends on polymers concentrations. This, in turn, also has an effect on the molecular weight amongst the crosslink points. The GelMA-AAm hydrogels are biocompatible for the podocytes culture and did not alter their proliferation as well as their

viability. However, the substrates have an effect on podocytes morphology, cytoskeleton organization and differentiation. It was determined that AAm<sub>2.5%</sub> + GelMA<sub>3%</sub> and AAm<sub>5%</sub> + GelMA<sub>3%</sub> having stiffness close to native glomerular extracellular matrix seems to be optimal for the podocyte growth. In conclusion, this work provides a new tool to combine natural and synthetic polymers mimicking the native tissue and having robust mechanical properties. Furthermore, such environment similar to *in vivo* contributes to well understand the behavior of podocytes cells in order to restore the functions of kidney diseases.

## V. References:

- (1) Fuchs, J. R.; Nasser, B. A.; Vacanti, J. P. Tissue Engineering: A 21st Century Solution to Surgical Reconstruction. *Ann. Thorac. Surg.* **2001**, 72 (2), 577–591.
- (2) Stock, U. A.; Vacanti, J. P. Tissue Engineering: Current State and Prospects. *Annu. Rev. Med.* **2001**, 52, 443–451.
- (3) Chapekar, M. S. Tissue Engineering: Challenges and Opportunities. *J. Biomed. Mater. Res.* **2000**, 53 (6), 617–620.
- (4) Furth, M. E.; Atala, A. Chapter 6 - Tissue Engineering: Future Perspectives. In *Principles of Tissue Engineering (Fourth Edition)*; Lanza, R., Langer, R., Vacanti, J., Eds.; Academic Press: Boston, 2014; pp 83–123.
- (5) Frantz, C.; Stewart, K. M.; Weaver, V. M. The Extracellular Matrix at a Glance. *J. Cell Sci.* **2010**, 123 (24), 4195–4200.
- (6) Daley, W. P.; Peters, S. B.; Larsen, M. Extracellular Matrix Dynamics in Development and Regenerative Medicine. *J. Cell Sci.* **2008**, 121 (Pt 3), 255–264.
- (7) Kular, J. K.; Basu, S.; Sharma, R. I. The Extracellular Matrix: Structure, Composition, Age-Related Differences, Tools for Analysis and Applications for Tissue Engineering. *J. Tissue Eng.* **2014**, 5, 2041731414557112.
- (8) Dhandayuthapani, B.; Yoshida, Y.; Maekawa, T.; Kumar, D. S. Polymeric Scaffolds in Tissue Engineering Application: A Review  
<https://www.hindawi.com/journals/ijps/2011/290602/> (accessed Sep 4, 2019).
- (9) Sudhakar, C. K.; Upadhyay, N.; Jain, A.; Verma, A.; Narayana Charyulu, R.; Jain, S. Chapter 5 - Hydrogels—Promising Candidates for Tissue Engineering. In *Nanotechnology Applications for Tissue Engineering*; Thomas, S., Grohens, Y., Ninan, N., Eds.; William Andrew Publishing: Oxford, 2015; pp 77–94.
- (10) Tsou, Y.-H.; Khoneisser, J.; Huang, P.-C.; Xu, X. Hydrogel as a Bioactive Material to Regulate Stem Cell Fate. *Bioact. Mater.* **2016**, 1 (1), 39–55.



- (11) Recent Advances in Hydrogels for Tissue Engineering  
/resources/publications/cep/2018/may/recent-advances-hydrogels-tissue-engineering  
(accessed Sep 4, 2019).
- (12) Geckil, H.; Xu, F.; Zhang, X.; Moon, S.; Demirci, U. Engineering Hydrogels as Extracellular Matrix Mimics. *Nanomed.* **2010**, *5* (3), 469–484.
- (13) Kim, T. G.; Shin, H.; Lim, D. W. Biomimetic Scaffolds for Tissue Engineering. *Adv. Funct. Mater.* **2012**, *22* (12), 2446–2468.
- (14) Hansen, K. C.; Kiemle, L.; Maller, O.; O'Brien, J.; Shankar, A.; Fornetti, J.; Schedin, P. An In-Solution Ultrasonication-Assisted Digestion Method for Improved Extracellular Matrix Proteome Coverage. *Mol. Cell. Proteomics MCP* **2009**, *8* (7), 1648–1657.
- (15) Fairbanks, B. D.; Schwartz, M. P.; Halevi, A. E.; Nuttelman, C. R.; Bowman, C. N.; Anseth, K. S. A Versatile Synthetic Extracellular Matrix Mimic via Thiol-Norbornene Photopolymerization. *Adv. Mater. Deerfield Beach Fla* **2009**, *21* (48), 5005–5010.
- (16) Burmania, J. A.; Stevens, K. R.; Kao, W. J. Cell Interaction with Protein-Loaded Interpenetrating Networks Containing Modified Gelatin and Poly(ethylene Glycol) Diacrylate. *Biomaterials* **2003**, *24* (22), 3921–3930.
- (17) Daniele, M. A.; Adams, A. A.; Naciri, J.; North, S. H.; Ligler, F. S. Interpenetrating Networks Based on Gelatin Methacrylamide and PEG Formed Using Concurrent Thiol Click Chemistries for Hydrogel Tissue Engineering Scaffolds. *Biomaterials* **2014**, *35* (6), 1845–1856.
- (18) Xu, K.; Fu, Y.; Chung, W.; Zheng, X.; Cui, Y.; Hsu, I. C.; Kao, W. J. Thiol-Ene-Based Biological/synthetic Hybrid Biomatrix for 3-D Living Cell Culture. *Acta Biomater.* **2012**, *8* (7), 2504–2516.
- (19) Yue, K.; Li, X.; Schrobback, K.; Sheikhi, A.; Annabi, N.; Leijten, J.; Zhang, W.; Zhang, Y. S.; Hutmacher, D. W.; Klein, T. J.; et al. Structural Analysis of Photocrosslinkable Methacryloyl-Modified Protein Derivatives. *Biomaterials* **2017**, *139*, 163–171.
- (20) Djagny, V. B.; Wang, Z.; Xu, S. Gelatin: A Valuable Protein for Food and Pharmaceutical Industries: Review. *Crit. Rev. Food Sci. Nutr.* **2001**, *41* (6), 481–492.

- (21) Chang, K.-H.; Liao, H.-T.; Chen, J.-P. Preparation and Characterization of Gelatin/hyaluronic Acid Cryogels for Adipose Tissue Engineering: In Vitro and in Vivo Studies. *Acta Biomater.* **2013**, *9* (11), 9012–9026.
- (22) Jayakrishnan, A.; Jameela, S. R. Glutaraldehyde as a Fixative in Bioprotheses and Drug Delivery Matrices. *Biomaterials* **1996**, *17* (5), 471–484. (23) Olde Damink, L. H. H.; Dijkstra, P. J.; Van Luyn, M. J. A.; Van Wachem, P. B.; Nieuwenhuis, P.; Feijen, J. Crosslinking of Dermal Sheep Collagen Using Hexamethylene Diisocyanate. *J. Mater. Sci. Mater. Med.* **1995**, *6* (7), 429–434.
- (24) Speer, D. P.; Chvapil, M.; Eskelson, C. D.; Ulreich, J. Biological Effects of Residual Glutaraldehyde in Glutaraldehyde-Tanned Collagen Biomaterials. *J. Biomed. Mater. Res.* **1980**, *14* (6), 753–764.
- (25) Xiao, S.; Zhao, T.; Wang, J.; Wang, C.; Du, J.; Ying, L.; Lin, J.; Zhang, C.; Hu, W.; Wang, L.; et al. Gelatin Methacrylate (GelMA)-Based Hydrogels for Cell Transplantation: An Effective Strategy for Tissue Engineering. *Stem Cell Rev. Rep.* **2019**, *15* (5), 664–679.
- (26) Yue, K.; Trujillo-de Santiago, G.; Alvarez, M. M.; Tamayol, A.; Annabi, N.; Khademhosseini, A. Synthesis, Properties, and Biomedical Applications of Gelatin Methacryloyl (GelMA) Hydrogels. *Biomaterials* **2015**, *73*, 254–271.
- (27) Nichol, J. W.; Koshy, S.; Bae, H.; Hwang, C. M.; Yamanlar, S.; Khademhosseini, A. Cell-Laden Microengineered Gelatin Methacrylate Hydrogels. *Biomaterials* **2010**, *31* (21), 5536–5544.
- (28) Chen, Y.-C.; Lin, R.-Z.; Qi, H.; Yang, Y.; Bae, H.; Melero-Martin, J. M.; Khademhosseini, A. Functional Human Vascular Network Generated in Photocrosslinkable Gelatin Methacrylate Hydrogels. *Adv. Funct. Mater.* **2012**, *22* (10), 2027–2039.
- (29) Kandow, C. E.; Georges, P. C.; Janmey, P. A.; Beningo, K. A. Polyacrylamide Hydrogels for Cell Mechanics: Steps Toward Optimization and Alternative Uses. In *Methods in Cell Biology*; Cell Mechanics; Academic Press, 2007; Vol. 83, pp 29–46.
- (30) Van Den Bulcke, A. I.; Bogdanov, B.; De Rooze, N.; Schacht, E. H.; Cornelissen, M.; Berghmans, H. Structural and Rheological Properties of Methacrylamide Modified Gelatin Hydrogels. *Biomacromolecules* **2000**, *1* (1), 31–38.

- (31) Sutter, M.; Siepmann, J.; Hennink, W. E.; Jiskoot, W. Recombinant Gelatin Hydrogels for the Sustained Release of Proteins. *J. Controlled Release* **2007**, *119* (3), 301–312.
- (32) Pepelanova, I.; Kruppa, K.; Scheper, T.; Lavrentieva, A. Gelatin-Methacryloyl (GelMA) Hydrogels with Defined Degree of Functionalization as a Versatile Toolkit for 3D Cell Culture and Extrusion Bioprinting. *Bioeng. Basel Switz.* **2018**, *5* (3).
- (33) Serafim, A.; Tucureanu, C.; Petre, D.-G.; Dragusin, D.-M.; Salageanu, A.; Vlierberghe, S. V.; Dubruel, P.; Stancu, I.-C. One-Pot Synthesis of Superabsorbent Hybrid Hydrogels Based on Methacrylamide Gelatin and Polyacrylamide. Effortless Control of Hydrogel Properties through Composition Design. *New J. Chem.* **2014**, *38* (7), 3112–3126.
- (34) Miller, R. T.; Janmey, P. A. Relationship of and Cross-Talk between Physical and Biologic Properties of the Glomerulus. *Curr. Opin. Nephrol. Hypertens.* **2015**, *24* (4), 393–400.
- (35) Janmey, P. A.; Miller, R. T. Mechanisms of Mechanical Signaling in Development and Disease. *J Cell Sci* **2011**, *124* (1), 9–18.
- (36) Wells, R. G. The Role of Matrix Stiffness in Regulating Cell Behavior. *Hepatology* **2008**, *47* (4), 1394–1400.
- (37) Reiser, J.; Altintas, M. M. Podocytes. *F1000Research* **2016**, *5*.
- (38) Embry, A. E.; Mohammadi, H.; Niu, X.; Liu, L.; Moe, B.; Miller-Little, W. A.; Lu, C. Y.; Bruggeman, L. A.; McCulloch, C. A.; Janmey, P. A.; et al. Biochemical and Cellular Determinants of Renal Glomerular Elasticity. *PLOS ONE* **2016**, *11* (12), e0167924.
- (39) Fukasawa, H.; Bornheimer, S.; Kudlicka, K.; Farquhar, M. G. Slit Diaphragms Contain Tight Junction Proteins. *J. Am. Soc. Nephrol. JASN* **2009**, *20* (7), 1491–1503.
- (40) Luo, Q.; Kuang, D.; Zhang, B.; Song, G. Cell Stiffness Determined by Atomic Force Microscopy and Its Correlation with Cell Motility. *Biochim. Biophys. Acta* **2016**, *1860* (9), 1953–1960.

## General Conclusion



The challenge of tissue engineering is to create an artificial scaffold material mimicking the extracellular matrix (ECM) in order to regenerate the functions of damaged tissue *in vivo*. The ECM properties have shown an importance in the regulation of cellular activities such as proliferation, migration and differentiation. They provide a mechanical support for cells adhesion and their physical properties such as stiffness induce the cells to respond and to react in a various way. Moreover, the cells interact with the extracellular environment and sense the biochemical cues provided by ECM components such as collagen and growth factors.

The aim of this work was to design suitable scaffolds materials based on polymers having the functional similarities of ECM. This involves investigating the role and the impact of ECM on cellular behavior. Hydrolyzed PAAm and GelMA-AAm based hydrogels were considered as scaffolds for the glomerular kidney cells known as podocytes.

Hydrolyzed PAAm based hydrogels are biocompatible and characterized by their tunable mechanical properties. Hydrolyzed PAAm based hydrogels having different mechanical properties have shown an influence on podocyte behaviors including morphology, cytoskeleton organization and differentiation. The elasticity of PAAm substrates in the range of 0.9 – 9.9 kPa close to the *in vivo* glomerular basement membrane stiffness has shown an effect on podocyte behaviors similar to those *in vivo*. For these stiffnesses, the podocyte cells were less spread with no stress fibers and have exhibited an upregulation of podocin, the protein marker of differentiated podocytes. While, the podocyte cells on PAAm substrates having a high stiffness were more completely spread and expressed stress fibers. Moreover, the expression of podocin marker was downregulated. Hydrolyzed PAAm based hydrogel is a synthetic material characterized by the lack of biological properties. This limitation is regulated by the functionalization of the PAAm surface with adhesion proteins

such as fibronectin and collagen. Therefore, the synthesis of hybrid hydrogels based on natural and synthetic polymers is a promising approach to combine the biological properties such as cell-binding motif and the robust mechanical properties.

The hybrid hydrogel composed of gelatin methacrylate (GelMA) and acrylamide (AAm) was the choice of study for a suitable scaffold imitating the complexity of natural ECM. The mechanical properties of GelMA-AAm were studied and tuned by adjusting the concentrations of the polymers. It was shown that increasing the concentrations of the polymers contributes to the increase of the polymer network density and substrate elasticity. Moreover, the effect of the mechanical properties of GelMA-AAm scaffolds on podocyte behaviors was investigated. A significant effect was shown on cell adhesion and proliferation comparing to the non-functionalized polyacrylamide hydrogels with an adhesion protein. Even, the cytoskeleton organization and the expression of podocin were detected and have shown that the substrate having elasticity close to the kidney glomerular basement membrane seems to be optimal for the podocyte adhesion, proliferation and differentiation.

These scaffolds hydrogels are considered as promising candidates to mimic the glomerular basement membrane as they offer optimal conditions for podocyte adhesion, proliferation and differentiation. They represent robust mechanical properties due the presence of synthetic polymer (PAAm) characterized by its synthesis in a wide range of elasticity. The drawback of these synthetic polymers is their lack of biological properties. The combination of a natural polymer with a synthetic polymer leads to a scaffold polymer having both biological and mechanical properties.

Organs-on-chips are microfluidic devices for culturing living cells in order to synthesize minimal functional units recapitulating the physiological functions of tissues and organs. This

*in vitro* model provides an *in vivo* microenvironment by incorporating physical forces such a physiological level of fluid shear stress, cyclic strain and mechanical compression. The advantage of organ-on-chip is the ability to develop a disease model for the establishment of new therapies and to better understand the mechanisms of tissue functions. Kidney dysfunction is correlated with the leakage of albumin into urine. The selection of albumin is achieved by the glomerular filtration barrier (GFB). Therefore, the perspective of this study will be to develop kidney glomerulus-on-a-chip providing an *in vitro* model to mimic the complex structure and the function of the GFB. The scaffold materials worked on seeded with podocytes will be use as the glomerular basement membrane. Then, the selectivity of glomerulus-on-chip will be tested by adding a physiological concentration of FITC-conjugated albumin to the media to follow the efficiency of the function of this system by preventing the leakage of albumin. Furthermore, the hyperglycemia has shown a significant impact on the progression of kidney disease. Therefore, the *in vitro* model mimicking the *in vivo* microenvironment permits to study the effect of the glomerular filtration barrier in such diseased environment. This *in vitro* system will be exhibited to a medium containing a high concentration of glucose and then their effect on podocyte behaviors will be investigated.





## **Abstract**

Extracellular matrix (ECM), non-cellular component, regulates and maintains the main biological activities of cells such as cellular survival, proliferation and differentiation. Recently, hydrogels scaffolds have shown a remarkable advancement as candidates for tissue engineering and regenerative medicine. Hydrogels are defined as hydrophilic polymer network having the ability to hold a large amount of water and biological fluid. Various natural and synthetic hydrogels have been studied and developed in many tissue regeneration purposes. They provide an appropriate mechanical support, chemical and biological cues mimicking the native extracellular matrix (ECM). These artificial matrices characteristics contribute to induce the cellular functions as adhesion, proliferation and differentiation. The thesis aim was to develop polymers based hydrogels and to study the effect of their physical properties on podocyte kidney cells. Synthetic hydrolyzed polyacrylamide based hydrogel (PAAm) was the choice of study where the physical properties can be tailored and tuned over a wide range. These scaffolds have provided elasticity similar to the *in vivo* glomerular basement membrane (GBM) and have shown a suitable candidate for the regulation of podocyte functions. Moreover, the development of synthetic and biologic hybrid hydrogels was able to mimic the biological and mechanical properties of native ECM. The combination of gelatin methacrylate and acrylamide (GelMA-AAm) based hydrogels have been investigated and has shown tunable mechanical properties mimicking the native kidney GBM elasticity and a significant attachment of podocytes without any surface functionalization with adhesion proteins. This work permits to investigate the cellular physiology and to develop kidney-on-chip in order to study the functions of kidney on both healthy and diseased states.

## **Résumé**

La matrice extracellulaire (MEC) contrôle et maintient les principales activités biologiques telles que la survie, la prolifération et la différenciation cellulaire. Récemment, les hydrogels ont marqué une progression remarquable en tant que candidats dans le domaine de l'ingénierie tissulaire et de la médecine régénérative. Les hydrogels sont des réseaux polymériques hydrophiles ayant la capacité d'absorber une grande quantité d'eau et de fluide biologique. Les hydrogels présentent un support mécanique approprié pour les cellules tissulaires et fournissent des signaux chimiques et biologiques imitant la MEC native. Par conséquent, de nombreux hydrogels de nature biologique et chimique ont été développés dans le domaine de régénération tissulaire. Les propriétés mécaniques des hydrogels sont nécessaires pour induire les fonctions biologiques telles que l'adhésion, la prolifération et la différenciation cellulaire. L'objectif de la thèse était de développer des hydrogels à base de polymères et d'étudier l'effet de leurs propriétés physiques sur les activités biologiques des cellules podocytaires. Cette étude consiste de synthétiser et de développer des hydrogels à base de polyacrylamide hydrolysé (PAAm) où les propriétés physiques peuvent être adaptées et réglées sur une large gamme d'élasticité. Ces matériaux ont fourni une élasticité similaire à celle de la membrane basale glomérulaire (GBM) *in vivo* et ont représenté un candidat approprié pour la régulation des fonctions des cellules podocytaires. De même, la synthèse des hydrogels à la fois synthétiques et biologiques a pu imiter les propriétés biologiques et mécaniques de la MEC native. La combinaison des polymères à base de méthacrylate de gélatine et d'acrylamide (GelMA-AAm) a été synthétisée et analysée. Ces hydrogels ont montré des propriétés mécaniques ajustables imitant l'élasticité native du GBM du rein et une fixation significative des podocytes sans modification de surface par des protéines d'adhésion. Ce travail consiste à étudier la physiologie cellulaire et à développer un système microfluidique afin de suivre les fonctions rénales dans les états normales et défectés.



